# Recent progress in the application of Ni-based catalysts for the dry reforming of methane

J.J. Torrez-Herrera, S.A. Korili, A. Gil*

INAMAT^2-Departamento de Ciencias, Edificio de los Acebos, Universidad Pública de
Navarra, Campus de Arrosadía E-31006 Pamplona, Spain.
Email: andoni@unavarra.es

## Abstract

Ni-based catalysts are highly efficient in methane-reforming processes. In the particular case of methane reforming in the presence of carbon dioxide, or dry reforming of methane (DRM), it is necessary to modify and control the initial properties of the catalyst to confer on it resistance to carbon deposition in particular, and to sintering of the Ni metal particles. In this regard, catalytic supports and promoters of different natures have been proposed. Likewise, the addition of small amounts of noble metals to avoid oxidation of the Ni active phase during the reforming reaction has been proposed. Catalyst preparation methods have also been identified as being of particular interest, since they can affect the structure of the Ni metal particles. In this review, the thermodynamic and kinetic aspects of the dry reforming of methane reaction are presented first. The most recent developments in synthetic methods (impregnation, sol-gel, co-precipitation, equilibrium deposition filtration, atomic layer deposition, non-thermal glow discharge plasma, multi-bubble sonoluminescence, "core-shell" structure) aimed at maximizing the dispersion and thermal resistance of Ni particles are then discussed and compared. The catalytic supports used to promote dispersion of the active metallic phase, the oxygen-storage capacity, and the metal/support interaction are also described. The review then addresses the fact that both the nature of the support and the addition of promoters and other metallic phases that modify the surface properties can control the interaction between the metal and the support, the electronic density of the active phase, and the degree of Ni reduction. Finally, new lines of research focused on the DRM process to make the reaction conditions milder and favor the process at low temperatures are also summarized.

**Keywords:** $CO_2$ utilization, $CH_4$ valorization, greenhouse gases, heterogeneous catalysts, Ni-based catalyst, bimetallic catalyst, noble metal catalyst, catalytic promoter.

## 1. Introduction

The current dependence on fossil fuels to meet energy demand has led to environmental problems due to emissions of greenhouse gases. $CH_4$ and $CO_2$ are the most abundant—along with $H_2O$ vapor, $NO_x$ and $O_3$—and, as such, are the main contributors to recent climate change problems.[1] Although the concentration of $CH_4$ in the atmosphere is lower than that of $CO_2$,[2] it has been reported to be responsible for about 25-35% of overall global warming.[3,4] $CH_4$ is produced from natural sources—such as grasslands, wildfires, lakes, and wetlands—and from human activities—such as agriculture and coal mining, oil, and gas processing.[5] According to the US Environmental Protection Agency (USEPA),[6] $CH_4$ production from landfills contributes to about one-third of all $CH_4$ emitted in the US alone.[7] Similarly, although $CH_4$ is also the major component of natural gas, most natural gas reservoirs are located far from industrial areas and are often found offshore, thus resulting in limitations in terms of both technology and the cost of transporting the gas from the oceans to processing plants.[8] This results in a significant source of wasted hydrocarbons and a major contribution to global warming when this greenhouse gas is released into the atmosphere.[9] Along these lines, $CO_2$ capture and storage (CCS) has been favored around the world with the aim of reducing emissions of $CO_2$ and of other gases contributing to the greenhouse effect.[10] Renewable energy sources are also needed urgently to replace petroleum-derived sources.[11]

One of the strategies to reduce the amount of $CH_4$ and $CO_2$ reaching the atmosphere is to try to convert these two gases into other valuable products. The best proposal to date is the conversion of $CH_4$ and $CO_2$ into syngas using a relatively well-established and low-cost technology.[12] The syngas produced can be transformed into hydrocarbons, thus making it possible to expand the raw materials that can be obtained.[13] Syngas is considered a basic component that can be used as a reagent for other applications, such as the Fischer–Tropsch (FT) process and the production of methanol and other valuable liquid fuels and chemicals.[14] Reforming is the most commonly used method in industry to produce syngas via one of three main reforming processes: steam reforming of methane (SRM), partial oxidation of methane (POM), and dry reforming of methane (DRM).[15] SRM is the most widely used conventional technology for the production of hydrogen from hydrocarbons as it produces a higher hydrogen yield compared to the other two reforming methods.[16] Indeed, approximately 75% of the hydrogen produced worldwide is derived from the SRM process.[17] In addition to its carbon-neutral nature, recent advances in SRM have focused on bio-alcohols such as methanol, ethanol, propanol, propanediol, butanol, ethylene glycol and glycerol.[18-24] The differences between SRM, POM and DRM are based on the oxidant used, the kinetics and energy requirements of the reaction and the ratio of the syngas produced ($H_2/CO$).

$$\text{SRM:} \quad CH_4 + H_2O \rightleftharpoons CO + 3H_2 \tag{1}$$

$$\text{POM:} \quad CH_4 + 1/2O_2 \rightleftharpoons CO + 2H_2 \tag{2}$$

$$\text{DRM:} \quad CH_4 + CO_2 \rightleftharpoons 2CO + 2H_2 \tag{3}$$

The SRM reaction (Eq. 1) is characterized by producing the highest $H_2/CO$ ratio (3:1)[25] (the ratio required for the FT synthesis is 2:1).[26] However, SRM is a very expensive process as it requires a high energy input due to its endothermic nature.[27] Similarly, a high $H_2O/CH_4$ ratio is required to achieve a higher $H_2$ yield, which makes the SRM process unfavorable in terms of energy and favors catalyst deactivation.[28] POM, in turn, is a suitable process for the production of heavier hydrocarbons and naphtha.[29] The POM process has a very short residence time, high conversion rates, and high selectivity.[30] However, it has been reported that the exothermic nature of the reaction favors the appearance of hot spots in the catalyst and makes it difficult to control the operation.[15] Considering the remaining processes, DRM is the most promising, since it uses two abundant greenhouse gases ($CO_2$ and $CH_4$) to produce syngas and, at the same time, can reduce the net emission of these gases into the environment.[31] The DRM process is also cheaper than the other processes described, since it allows simple separation of the gases produced as products.[32] Moreover, the $H_2/CO$ ratio produced by DRM can be used for the synthesis of oxygenated chemicals[33] and higher hydrocarbons via the FT process.[27] DRM can also be used with biogas ($CO_2$, CO and $CH_4$) as raw material to produce clean and environmentally friendly fuels.[34] Finally, the synthesis gas obtained from DRM can also be considered for energy storage.[35]

The use of catalysts in the DRM reaction allows the production of syngas to be maximized as this helps to alter and improve the reaction rate without being depleted in the process. Although DRM requires a high temperature to function due to its endothermic nature, the presence of catalysts can significantly reduce the reaction temperature required. All these factors have led to a significant increase in research into DRM in the last 10 years,[36-44] including the study of catalysts based on noble and non-noble metals.[45] Noble metals such as Ir, Rh, Ru, Pt, and Pd have a higher resistance to coke deposition than non-noble metals.

Given that the cost of noble metals is higher than that of non-noble metals, an inexpensive way to prevent coke formation consists in using multi-metal formulations of non-noble metals such as Ni, Co and Fe with noble metals. These formulations facilitate metallic dispersion and generate more active metallic centers.[46] Ni is the only transition metal that exhibits catalytic properties comparable to precious metals. However, Ni-based catalysts tend to generate carbon deposits on the catalyst surface, thus resulting in a loss of catalyst activity. The resulting poor stability limits the commercial use of Ni-based catalysts for DRM reactions and means that Ni-based catalysts must be modified to improve their performance and resistance to carbon deposition.

In addition to the active metallic phase, optimization of the active catalyst requires a study of properties such as dispersion of the active metallic phase on the catalytic support, the metal–support interaction, and the active surface that allows dispersion of the metallic phase and the acid-base centers, as well as modification of the properties of the catalytic support to reduce the deposition of coke, improve initial activation of the active phase, etc. As such, optimization of the catalyst synthesis method can lead to better catalytic performance, greater stability, and inhibition of coke formation during the reaction. A thorough study of all these variables can increase the performance of the catalyst and allow it to operate at higher temperatures than those initially foreseen, taking into account its thermal stability and metallic dispersion.[45]

This review article covers recent developments in synthetic methods and the catalytic application of Ni-based catalysts for DRM. Conventional and new synthetic methods for Ni catalysts are introduced and discussed, with special emphasis on the new formulations that allow better metal dispersion and greater catalytic stability by reducing coke formation. In addition to the preparation method, the nature of the support is crucial to provide adequate Ni dispersion, with the incorporation of promoters making it possible to reduce catalyst deactivation due to carbon deposition. The purpose of the study is to present how all the variables involved in the preparation of Ni-based catalysts affect catalytic behavior during the dry reforming of $CH_4$. At the end of the review, the main conclusions and perspectives regarding some of the main scientific challenges remaining in the field of the DRM reaction are also analyzed.

## 2. Reaction thermodynamics

In order to determine the reaction temperature, the working pressure, and the most suitable feed ratio to produce a high yield of synthesis gas, the thermodynamic behavior of DRM must be studied. As it is a highly endothermic reversible reaction, DRM requires a large amount of energy for it to occur.[47] As such, a very high temperature is necessary for the reaction to occur in the forward direction and to obtain a high conversion of syngas.[48-50]

Various reactions can occur during the DRM process, (see **Table 1**). The main reaction (Eq. 4) shows that DRM produces a $H_2$/CO ratio of 1; it is highly endothermic, thermodynamically feasible above 640 °C, and favored at low pressures. However, DRM typically gives a $H_2$/CO ratio of less than 1 due to the simultaneous production of CO via the reverse-water-gas-shift (RWGS) reaction (see Eq. 5), which results in a higher amount of CO compared to $H_2$.[51] Although $H_2$/CO ratios of less than 1 may seem undesirable, this syngas ratio can, in fact, be used in FT synthesis to produce higher hydrocarbons.[52] In addition to the RWGS reaction, other side reactions can also occur depending on the $CH_4$/$CO_2$ feed ratio and operating temperature and pressure, including the formation of carbon (coke; see **Table 1**). Coke is an unwanted product, since it inhibits the activity of the catalyst by poisoning the active metallic centers and blocking the porous structure.[53] Numerous authors agree that coke is formed by the decomposition of $CH_4$ (Eq. 6) and the disproportion of CO (Boudouard reaction, Eq. 7).[54] However, it has also been proposed that two other reactions, namely hydrogenation of $CO_2$ (Eq. 8) and hydrogenation of CO (Eq. 9),[51] contribute to coke formation.

DRM typically involves carbon deposition, which can reduce catalyst performance. Three types of carbon are generally formed: pyrolytic, encapsulating, and whisker carbon (see **Figure 1**). Pyrolytic carbon forms when long-chain hydrocarbons are exposed to high temperatures, generally above 600 °C, and the critical parameters are high temperature, high pressure, and the presence of acid centers in the catalyst.[55] Carbon encapsulation can occur during reforming of heavy hydrocarbon feeds with a higher content of aromatic compounds (see **Figure 1**). The high final boiling point and low temperatures of the hydrocarbon mixture increase the rate of encapsulating carbon formation.[56] Encapsulating carbon comprises a thin CHx film covering the metal active particles, which can lead to catalyst deactivation. Generally, encapsulating carbon forms at temperatures below 500 °C.[55] The last type of carbon formed is whisker carbon, which is considered to be the most critical type formed in the DRM reaction.[56] This type of carbon formation leads to breakdown of the catalyst, a higher pressure decrease, and significant deactivation of the metal surface. Whisker carbon is usually formed at temperatures above 450 °C.[55]

**Table 1.** Main reactions in the dry reforming of methane (DRM).

| | **Reaction equation** | **ΔH25 ºC (kJ/mol)** | **Comments** |
|---|---|---|---|
| **(4)** Dry Reforming of Methane (DRM) | $CH_4 + CO_2 \rightleftharpoons 2CO + 2H_2$ | 247 | |
| **(5)** Reverse Water-Gas-Shift (RWGS) | $CO_2 + H_2 \rightleftharpoons CO + H_2O$ | 41.0 | Side reaction that leads to the decrease in $H_2/CO$ ratio to < 1 |
| **(6)** Decomposition of methane | $CH_4 \rightleftharpoons C + 2H_2$ | 75.0 | Side reaction that lead to formation of carbon (coke) |
| **(7)** Disproportionation of CO (Boudouard) | $2CO \rightleftharpoons C + CO_2$ | - 173.0 | Side reaction that lead to formation of carbon (coke) |
| **(8)** Hydrogenation of $CO_2$ | $CO_2 + 2H_2 \rightleftharpoons C + 2H_2O$ | - 90.0 | Side reaction that lead to formation of carbon (coke) |
| **(9)** Hydrogenation of CO | $H_2 + CO \rightleftharpoons C + H_2O$ | - 131.3 | Side reaction that lead to formation of carbon (coke) |

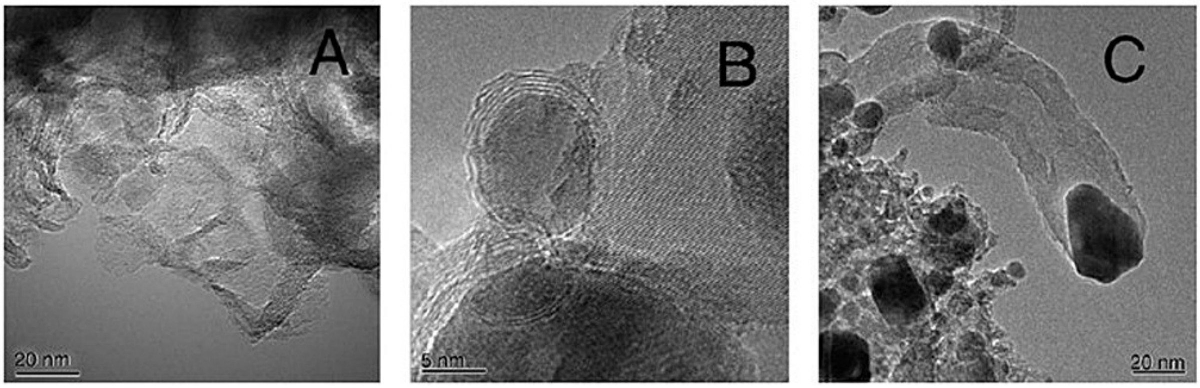

**Figure 1**. TEM images of pyrolytic carbon on a $MgAl_2O_4$ carrier (A), encapsulating carbon (B), and whisker carbon (C) on $Ni/MgAl_2O_4$ catalysts (Reproduced with permission from[39]).

If the quantities and conversions at equilibrium, calculated as a function of temperature and at a pressure of 1 atm and 2 moles of feed ($CO_2/CH_4$ = 1), are predicted thermodynamically, $CO_2$ and $CH_4$ consumption decreases as CO and $H_2$ production increases at temperatures above 300 ºC ($H_2/CO$ = 1), while reagent conversions and production reach a constant maximum at 850 °C, which is the optimum temperature during DRM (see **Figure 2-a**). Water formation is noticeable at temperatures below 800 °C and coke formation is reduced at temperatures above 800 °C (see **Figure 2-b**). Higher pressures require higher reaction temperatures and $CO_2/CH_4$ ratios to minimize carbon formation.[57] In order to produce syngas for FT applications, Nikoo and Amin[51] found that the reaction temperature must be higher than 900 °C for a $CO_2/CH_4$ ratio of 1. Under these conditions, coke formation is reduced and $CO_2$ conversions are greater than 98%.

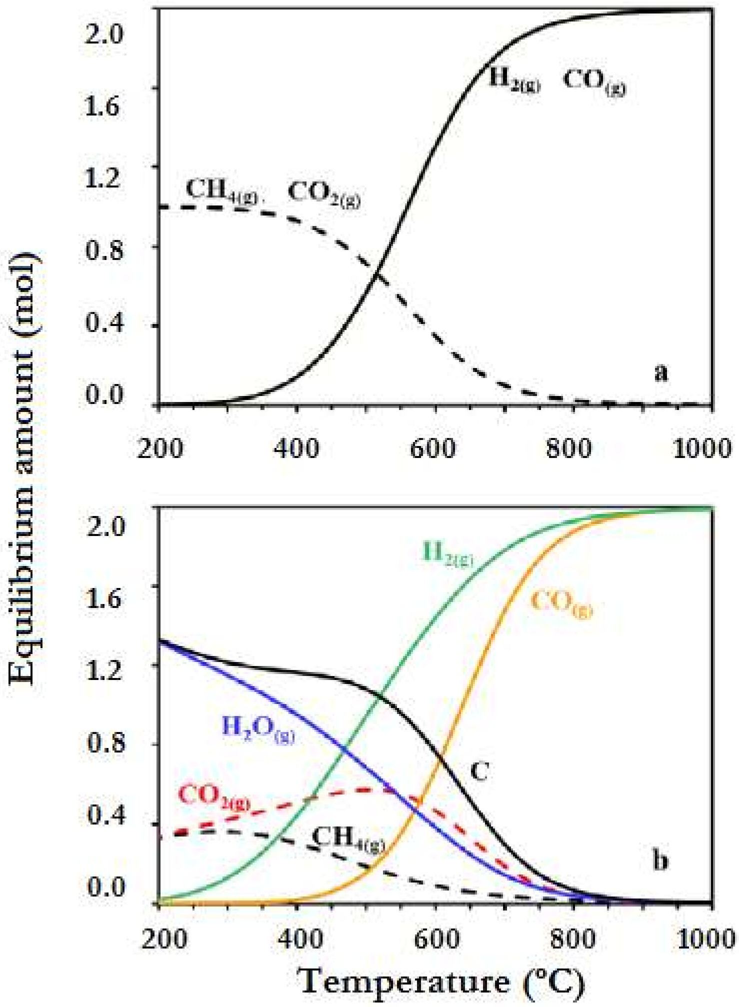

**Figure 2.** Thermodynamic prediction of quantities and conversions at equilibrium calculated as a function of temperature. 1 atm and 2 moles of feed ($CO_2/CH_4$ = 1).

## 3. Kinetics and mechanistics

Kinetic studies are used to fit experimental results from an empirical or theoretical reaction rate model and to describe the reaction rate and define the chemical process.[58] Additionally, they can further optimize catalyst and reactor design, thereby improving overall DRM development.[59] The SRM process has been developed to a greater extent from a mechanistic point of view. However, the recent interest in DRM due to the characteristics of the products obtained has led to optimization of the catalysts used and, therefore, the need for studies of the reaction mechanism.

The DRM reaction process is complex and comprises different reaction mechanisms for different catalysts and reaction conditions. Several authors have proposed that the key step in DRM is the adsorption and dissociation of $CH_4$ on the catalyst surface. At low temperatures, the dissociation of $CH_4$ proceeds gradually, with marked dissociation being observed at high temperatures. The DRM reaction mechanism on a Ni-based catalyst was studied by Aldana et al.[60] (see **Figure 3**), who proposed that the $H_2$ molecule dissociates at the metallic Ni centers at the same time as $CO_2$ is activated on the ceria-zirconia support to produce carbonate species, which could be hydrogenated into formate species and, finally, methoxy species. This proposed mechanism includes weak basic support centers for $CO_2$ adsorption and involves a stable metal-support interface. This type of catalyst makes it possible to better explain their behavior than in the case of $Ni/SiO_2$ catalysts, in which both $CO_2$ and $H_2$ are activated by the NiO particles. This proposed reaction mechanism has been corroborated by other authors using catalysts of a different nature.[61-67]

The effect of process variables on the performance of the catalyst in the DRM reaction has been studied intensively. These studies are required because changes in various process variables can result in different catalyst performance. If the activation energy (*Ea*) is taken into account, most studies confirm that the activation energy of $CH_4$ is greater than that of $CO_2$, since $CH_4$ molecules are more stable than those of $CO_2$. As such, more energy is required to activate these stable molecules [68]. Kathiraser et al.[69] proposed that the activation energy in the DRM reaction depends, to a marked extent, on the type of catalyst support, the promoter, and the bimetallic interactions in the catalyst. Thus, Cui et al.[70] conducted an exhaustive study of the DRM mechanism in $Ni/\alpha\text{-}Al_2O_3$ catalysts at temperatures between 550 and 750 $^{o}$C and observed that the *Ea* values for $CH_4$ dissociation and $CO_2$ conversion can be divided into temperature regions: 550-575 $^{o}$C, 575-650 $^{o}$C, and 650-750 $^{o}$C. The authors suggested that, at temperatures above 650 $^{o}$C, the dissociation of $CH_4$ into $CH_x$ and hydrogen species at the active Ni centers reached the equilibrium state. In order to accurately formulate intrinsic kinetic models for the catalyst, it is necessary to reduce other effects, such as the mass transport of the reactants. The reduction of this effect is possible if different gas hourly space velocities (GHSVs) are studied to confirm that the conversions have reached a steady-state value, so that an additional change in GHSV does not affect reactant conversions. Along the same lines, to reduce resistance to internal mass transport, the particle size of a catalyst should be as small as possible, so that a further decrease in size does not affect conversions.[69] Contact times also play an important role in $CO_2$ and $CH_4$ conversions. Thus, for a high value of contact time, $CO_2$ or $CH_4$ conversions are not affected. In general, a high GHSV value and a low amount of catalyst with a small particle size can minimize the amount of external and internal mass-transfer limitations.

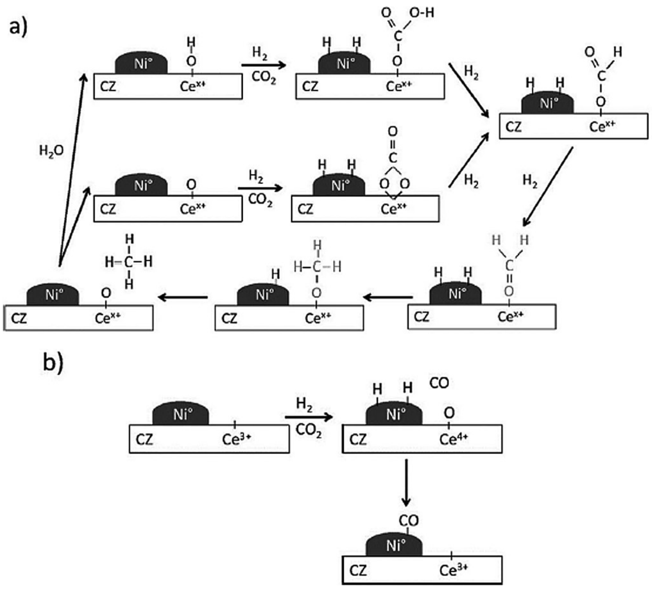

**Figure 3.** Reaction mechanism proposed on a Ni-CeZr sol-gel sample for: (a) $CO_2$ methanation and (b) CO formation. (Reproduced with permission from[60]).

Three types of kinetic models have been used to study the DRM reaction: the Power Law model, the Eley Rideal (ER) model, and the Langmuir Hinshelwood-Hougen-Watson (LHHW) model. The most widely used is the Power Law model, probably due to its simplicity as regards the application and estimation of parameters. Although this model is useful to make initial estimates and obtain information to solve more complex models that require a greater amount of data, it is not applicable to the reaction kinetics of the various catalysts as a whole. Power Law models can be expressed as:

$$Reaction\,rate\ (r) = k \cdot \left[p_{CH_4}\right]^m \cdot \left[p_{CO_2}\right]^n \tag{4}$$

Power law-based models have a limitation as regards explaining the various steps in the reaction mechanism that take place on the surface of the catalyst. Thus, based on the ER model, Akpan et al.[71] developed a kinetic model for a Ni/$CeO_2$-$ZrO_2$ catalyst. These authors assumed that the rate-determining step is the dissociative adsorption of $CH_4$. The proposed model was validated by fitting the experimental results obtained. The steps of the mechanism, as well as the reaction rate, are included in **Table 2**, where * and Ox represent the unoccupied active centers and the $O_2$ network on the support surface, respectively.

Verykios[72] conducted a study with a Ni/$La_2O_3$ catalyst for the DRM reaction, using various methods to explain the reaction mechanism based on previous results from the literature. Based on the characterization results obtained by XRD and FTIR, this author reported the formation of relatively stable $La_2O_2CO_3$ species from $CO_2$ and the $La_2O_3$ support.[73] In another work, the same author indicated that either the $La_2O_3$ support or the $La_2O_2CO_3$ species is responsible for CO formation by acting as an efficient source of oxygen.[74] The dissociation rate of $CO_2$ on the surface of metallic Ni was found to be very low, thus suggesting to the authors that the coke that accumulates on the metal surface comes mainly from $CH_4$.[75] Based on these previous findings, Verykios[72] proposed a mechanism for DRM on the Ni/$La_2O_3$ catalyst. Thus, this author stated that $CH_4$ is adsorbed on the surface of the active metal centers of the Ni catalyst, followed by the deposition of coke and the formation of hydrogen as a result of the cracking of the adsorbed $CH_4$. Subsequently, once the reversible adsorption of $CH_4$ reaches a steady state, the coke deposited on the active metal center could react with the $La_2O_2CO_3$ species. As such, the performance of the catalyst is not affected by $CH_4$ cracking, since the catalyst is very stable. The reaction rate was also determined taking into account the proposed kinetic mechanism (see **Table 2**), and the author showed that the kinetic model fits well with the experimental kinetic results found. $K_1$ and $K_3$ are the equilibrium constants for $CH_4$ adsorption and the reaction between $CO_2$ and $La_2O_3$, respectively, as a function of temperature, and $k_2$ and $k_4$ are rate constants, as a function of temperature and their respective activation energies.

**Table 2.** Reaction mechanisms for the dry reforming of methane (DRM) proposed by several authors.

| **Mechanism** | |
|---|---|
| *Akpan el at.*[71] | |
| Adsorption | $CH_4 + 2^* \rightleftharpoons CH_{3(*)} + H_{(*)}$<br>$CH_{3(*)} + * \rightleftharpoons CH_{2(*)} + H_{(*)}$<br>$CH_{2(*)} + * \rightleftharpoons CH_{(*)} + H_{(*)}$<br>$CH_{(*)} + * \rightleftharpoons C_{(*)} + H_{(*)}$ |
| Surface reaction | $C_{(*)} + O_x \rightleftharpoons CO + HO_{x-1} + *$ |
| Surface reaction | $CO_2 + O_{x-1} \rightleftharpoons O_x + CO$ |
| Surface reaction | $4H_{(*)} \rightleftharpoons 2H_2 + 4^*$<br>$H_2 + O_x \rightleftharpoons O_{x-1} + H_2O$ |
| Rate of reaction | $-r_A = \dfrac{2.1x10^{17} e^{\frac{222800}{RT}} \left(N_A - \frac{N_C^2 N_D^2}{K_p N_B}\right)}{\left(1 + 34.3N_D^{1/2}\right)}$ |
| *Verykios*[72] | |
| Adsorption | $CH_4 + M_{(as)} \overset{K_1}{\leftrightarrow} M_{(as)} - CH_3 + H_2$ |
| Surface reaction | $Ni_{(as)} - CH_4 \overset{k_2}{\rightarrow} Ni_{(as)} - C + 2H_2$ |
| Adsorption | $CO_2 + La_2O_3 \overset{K_3}{\leftrightarrow} La_2O_2CO_3$ |
| Surface reaction | $La_2O_2CO_3 + Ni_{(as)} - C \overset{k_4}{\rightarrow} La_2O_3 + 2CO + Ni_{(as)}$ |
| Rate of reaction | $R_{CH4} = \dfrac{K_1k_2K_3k_4P_{CH4}P_{CO2}}{K_1k_2K_3k_4P_{CH4}P_{CO2} + K_1k_2P_{CH4} + K_3k_4P_{CO2}}$ |
| *Quiroga and Luna*[76] | |
| Adsorption | $CH_4 + M_{(as)} \overset{K_{CH4}}{\longleftrightarrow} M_{(as)} - CH_3 + H_2$ |
| Adsorption | $CO_2 + Sup_{(as)} \overset{K_{CO2}}{\longleftrightarrow} CO_2 - Sup_{(as)}$ |
| Surface reaction | $M_{(as)} - CH_3 + CO_2 - Sup_{(as)} \overset{k_1}{\rightarrow} 2CO_{(g)} + 2H_{2(g)} + M_{(as)} + Sup_{(as)}$ |
| Rate of reaction | $R_{CH4} = \dfrac{k_1K_{CH4}K_{CO} \left(\frac{P_{CH4}P_{CO2}}{p_{H2}^{0.5}} - \frac{p_{H2}^{0.5}p_{CO2}^2}{b}\right)}{\left(1 + \frac{p_{CH}}{p_{H2}^{0.5}K_{CH4}} + P_{CO2}K_{CO2}\right)}$ |

*Sup*$_{(as)}$: active site of catalyst support. Rate of reaction[71] :r$_A$ (kg$_{methane}$/kg$_{cat}$ h); Nx (mol/h).

Quiroga and Luna[76] proposed another kinetic model for the DRM reaction based on the assumption that the adsorption and decomposition of $CH_4$ are followed by the non-dissociative adsorption of $CO_2$ at the active center of the catalyst support. The reaction proposed as the determining step in this mechanism is the surface reaction between the adsorbed species (see **Table 2**).

Comparison of the two reaction mechanisms proposed for DRM reveals that, in both of them, $CH_4$ adsorption occurs on the surface of the metallic active center (as already proposed by other authors[77-82]) as a stage prior to the cracking of $CH_4$, the deposition of coke, and hydrogen formation. The difference between the mechanisms proposed by Verykios[72] and Quiroga and Luna[76] is the stage that determines the reaction rate. Thus, in the mechanism proposed by Verykios,[72] this stage is $CH_4$ cracking, while Quiroga and Luna[76] suggest that the $CH_4$ cracking and adsorption stages are in a steady state. It can therefore be concluded that the different catalyst formulations exhibit different activities, and that they have different control stages, which results in a certain difference in the mathematical kinetic model. Despite this, a study of the kinetics and the mechanism of the DRM reaction can allow the design and optimization of the catalyst, thus promoting industrialization of the reforming catalyst.

## 4. Metal-based catalysts

The development of catalysts has focused on new formulations that result in a better performance and greater catalytic stability by reducing coke formation, prevent sintering of the active metallic phases, control the formation of active chemical species and avoid oxidation of the active metallic phases.[79,83] In this sense, the active centers of the catalysts can be modified by adding catalyst promoters, as well as by using supports that favor anchoring of the active phase to their surface. This typically results in higher conversions and selectivities in the DRM reaction.

The main interest of researchers regarding the DRM reaction is the development of cheap and cost-effective catalysts with high activity and resistance to carbon deposition. Various researchers have conducted studies on the type of catalytic support used[84] and the effect of the presence of promoters to try to improve resistance to carbon deposition. Similarly, studies have been carried out to improve catalytic activity and inhibit carbon formation by combining two or three metals as active centers.[85] The preparation method and the catalyst pretreatment processes[86] also play an important role in the change of structural properties, reduction behavior, and catalytic performance. The main methods reported for the preparation of catalysts used in the DRM reaction are wet impregnation, the sol-gel method, and the co-precipitation method. Catalyst preparation methods have a marked effect on performance and physicochemical properties.[87,88] Indeed, preparation of the catalysts affects the size and dispersion of the metallic particles, thereby affecting the catalytic properties.[89]

A large number of studies concerning the development of catalysts that are active and resistant to carbon deposition have been published.[12,31] The most commonly used catalysts are supported catalysts containing noble metals such as Ir, Rh, Ru, Pt, and Pd or transition metals such as Ni, Co, Cu, and Fe.[90] Although noble metals are very active and more resistant to coke deposition during the DRM reaction than transition metals, their low resistance at high temperature, as well as their greater tendency to be deactivated by the presence of S and Cl, amongst others, are major disadvantages.[91] Ni-based catalysts are currently the most widely used catalysts on an industrial scale.[92]

Goula et al.[93] prepared a series of $Ni/Al_2O_3$ catalysts with low and high metal loadings (8 and 16 wt.%) and found that the synthetic method plays a decisive role in the reducibility and particle size of the catalyst. These authors used standard impregnation preparation methods (incipient wetness and wet impregnation methods) as well as the slightly modified equilibrium deposition filtration (EDF) technique to synthesize their catalysts. They obtained results showing that the EDF method creates Ni with better stability and enhanced activity. Use of the impregnation and sol-gel methods in the synthesis of $Ni/Al_2O_3$-$CeO_2$ and $Ni/Al_2O_3$-MgO catalysts was compared by Rad et al.[94] (see **Figure 4**). The results of the characterization carried out by these authors show the formation of $NiAl_2O_4$ spinels in the catalysts prepared using the sol-gel method. Furthermore, the presence of $CeO_2$ favors the formation of smaller and more uniform NiO nanoparticles, which results in a $H_2/CO$ molar ratio of almost 1, a hydrogen yield of 94% and greater stability after a reaction time of 24 h. Zhang et al.[95] published a study comparing the properties and catalytic behavior of Ni catalysts prepared by impregnation (Ni-IM) and by homogeneous precipitation (Ni-HP). These authors reported that the preparation method affected the metal-support interaction and, therefore, the degree of metal dispersion. In the case of the DRM reaction, as the reforming reaction proceeds, the conversion of $CH_4$ over the Ni-HP catalyst decreased slightly from 74.5% to 73.8%, whereas the conversion of $CH_4$ over the Ni-IM catalyst decreased from 61.7% to 37.3%. Albarazi et al.[88]

discussed the properties of ceria-zirconia catalysts mixed with Ni/SBA-15 using various methods (one-step impregnation, two-step impregnation, co-precipitation) and reported that the synthesis process strongly affects the structure and chemical properties of the catalyst. Due to the strong interaction between the active metal centers and SBA-15, the co-precipitation method results in the formation of Ni silicate species. The presence of these metal species leads to lower catalytic performance but higher catalytic stability compared to impregnated catalysts. These authors also indicated that the catalyst obtained by co-precipitation does not cause direct decomposition of $CH_4$, thus inhibiting carbon formation. Hao et al.[96] found that $Ni/Al_2O_3$ catalysts prepared using the sol-gel method have a larger specific surface area, stronger metal-support interaction, excellent Ni dispersion, and smaller Ni nanoparticles, which results in higher catalytic performance and stability compared to catalysts prepared using the impregnation method. Similarly, Shang et al.[97] proposed a method, known as atomic layer deposition (ALD), to synthesize a catalyst with high catalytic activity and stability. The resulting catalyst showed a stable conversion of 93% at 850 $^oC$. The high catalytic performance is related to reduction of the $NiAl_2O_4$ spinel to Ni and to the high dispersion of the Ni nanoparticles deposited using the ALD method (see **Figure 5**).

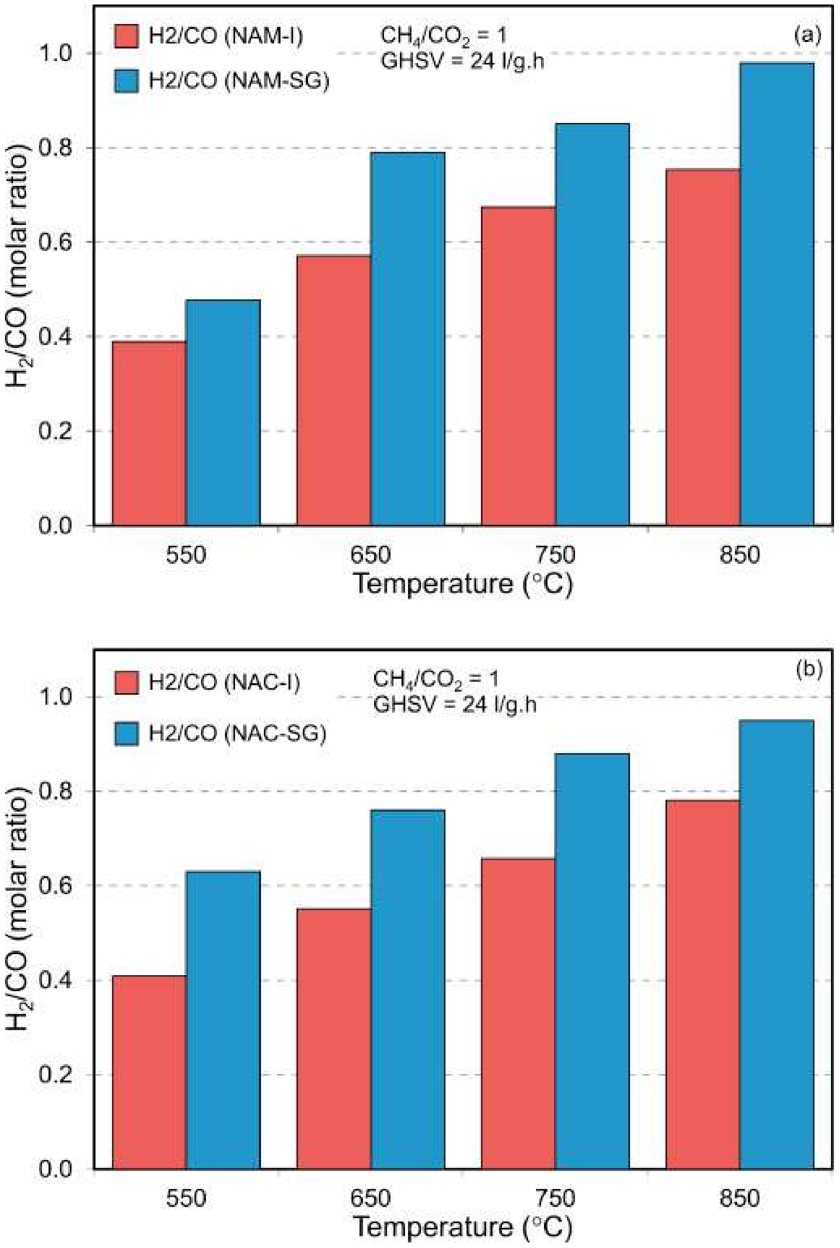

**Figure 4.** Effect of synthesis method (impregnation (I) and sol-gel (SG)) on $H_2/CO$ molar ratio in the product at various temperatures: (a) Ni/$Al_2O_3$-MgO (NAM) and (b) Ni/$Al_2O_3$-$CeO_2$ (NAC) (Reproduced with permission from[94]).

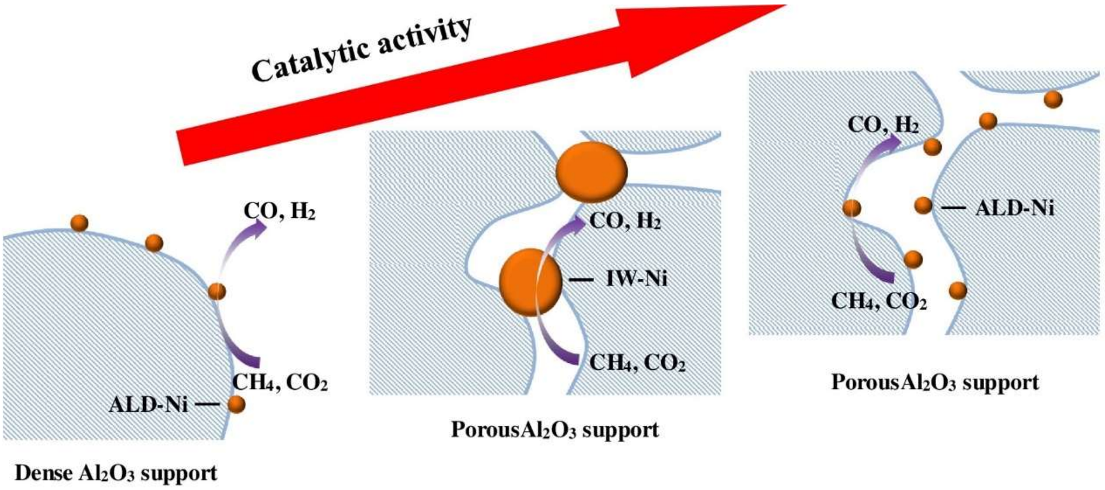

**Figure 5.** Schematic representation of the atomic layer deposition method for the synthesis of a Ni catalyst (Reproduced with permission from[97]).

Catalysts synthesized using several preparation methods can affect the formation of intermediates in the reaction process and thus affect the activation of $CH_4$ and $CO_2$. In this regard, Yao et al.[98] studied the effect of the impregnation method (joint impregnation and step-by-step impregnation) and the degree of excitation of $CH_4$ and $CO_2$ using DRIFTS in situ. These authors observed that the adsorbed carbonate completely disappeared at 300 $^oC$ in the Ni-ZrOxMnOx/$SiO_2$ and MnOx/Ni-ZrOx/$SiO_2$ catalysts but noticed new carbonate absorption bands at 350 $^oC$ for the ZrOx/Ni-MnOx/$SiO_2$ catalysts, thus favoring the activation of $CO_2$ and $CH_4$. Furthermore, formate species begin to appear in the Ni-ZrOx-MnOx/$SiO_2$ and MnOx/Ni-ZrOx/$SiO_2$ catalysts at 300 and 400 $^oC$, respectively, whereas formate formation started at 250 $^oC$ on the ZrOx/Ni-MnOx/$SiO_2$ catalyst. These results demonstrate that ZrOx/Ni-MnOx/$SiO_2$ catalysts can promote intermediate formation at relatively low temperatures. All these effects result in good catalytic performance for the DRM reaction at a relatively low temperature. Albarazi et al[88] proposed the synthesis of doped ceria-zirconia catalysts using two methods: co-precipitation and impregnation. They noted that the catalyst prepared by co-precipitation gave a slightly lower conversion of $CH_4$ and $CO_2$ but exhibited greater stability than the catalyst synthesized by impregnation. These authors attempted to explain these results by proposing that the catalyst synthesized by co-precipitation could effectively restrict the direct decomposition of $CH_4$ to carbon on the catalyst surface, whereas decomposition is the main cause of deactivation of the impregnated catalyst. Furthermore, Aw et al.[99] deposited $CeZrO_2$

on γ-$Al_2O_3$ and *β*-SiC, respectively, using different synthetic routes, and subsequently used these systems as Ni-Co-based catalyst supports. In these catalysts, Al reacts to form a spinel structure with Ni and Co, while $CeZrO_2$ remains as a solid mixed-oxide solution. Compared to the impregnated catalysts, those prepared by deposition-precipitation maintain the highest yield of $H_2$ and CO, as well as the lowest content of deposited carbon (7.7 and 0.6 wt.%, respectively). It has been reported that an $Al_2O_3$ surface coating plays an important role in the sintering resistance of Ni nanoparticles at high temperature. In this sense, Luisetto et al.[100] compared a Ni/$CeO_2$-$Al_2O_3$ catalyst prepared using the citric acid method with others prepared using the traditional co-precipitation method, the impregnation method, and the sol-gel method (see **Figure 6**). The authors reported that the citric acid method provides a relatively small Ni nanoparticle size and a large number of $CeAlO_3$ species, which may be advantageous for increasing catalytic activities and reducing graphitic-like carbon deposition. Furthermore, despite the formation of carbon deposits for the co-precipitated catalyst in the DRM reaction, these mainly comprise filamentous carbon, which does not encapsulate the active Ni centers. The authors also indicated that the catalyst prepared using the citric acid method shows comparable catalytic activity while also providing good catalytic stability due to reduced carbon deposition. Another study that investigates the effect of the support and the method for incorporating the metal was conducted by Chen et al.,[101] who found that the Ni/$Ce_{0.75}Zr_{0.25}O_2$ catalyst in which the support was synthesized by co-precipitation with the help of a surfactant exhibited higher catalytic activities than catalysts prepared by co-precipitation, without the use of a surfactant, and impregnation. They proposed that the higher catalytic activities observed in the catalysts prepared by the co-precipitation/surfactant method may be due to the incorporation of Ni in a solid solution ($Ce_{0.75}Zr_{0.25}O_2$), which produces a greater dispersion and a strong interaction with the metallic support. These authors also noted that the appropriate choice of preparation method implies certain textural properties, support activity and improved interaction of the metal support, which result in a higher catalytic activity and less carbon deposition.

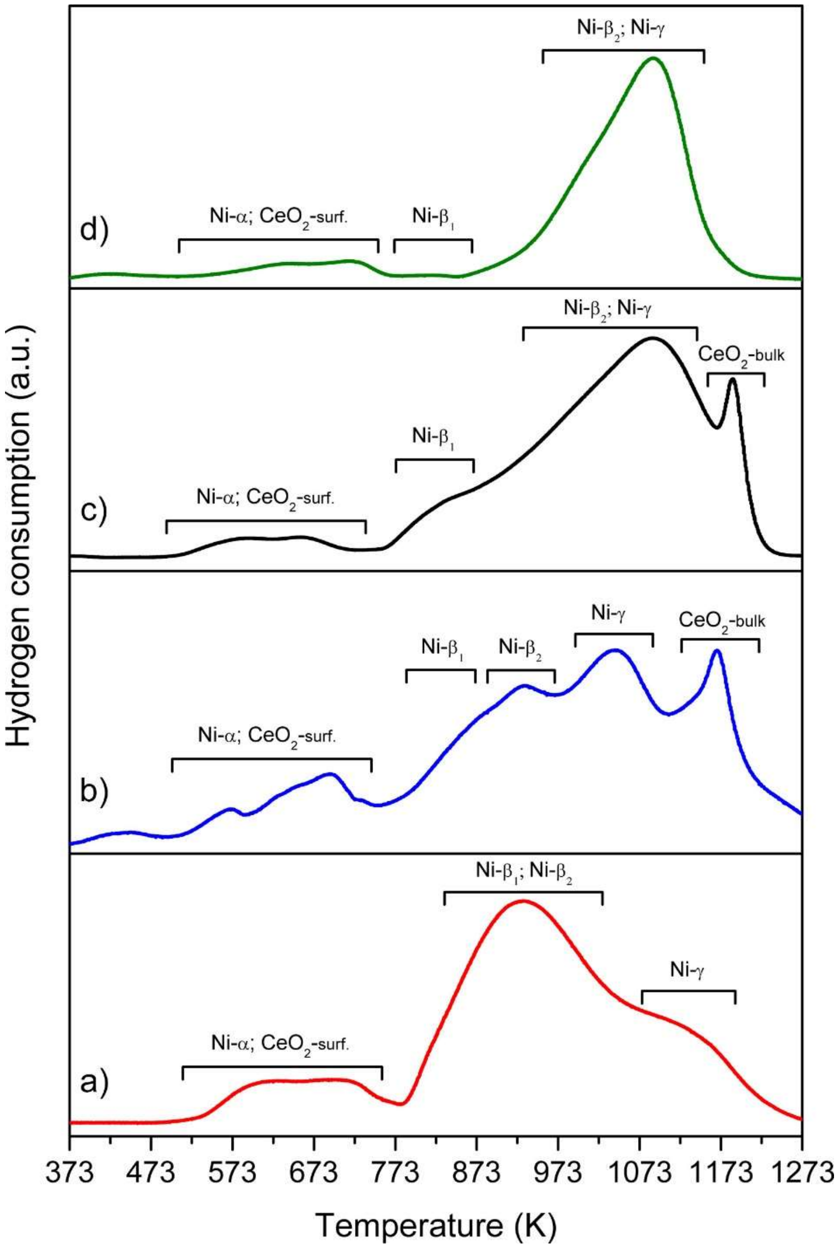

**Figure 6.** $H_2$-TPR profiles for catalysts calcined at 100 °C: citric acid method (CA) (a); sol-gel method (SG) (b); wet impregnation method (WI) (c); co-precipitation method (CP) (d) (Reproduced with permission from[100]).

Several novel methods for catalyst synthesis have been developed recently. Thus, non-thermal glow discharge plasma treatment has been used to improve the interaction with the metallic support and produce highly dispersed Ni particles, thereby improving stability and catalytic activity.[102] The XRD and XPS results obtained by the authors indicated the presence of a strong interaction of the metal with the support in plasma-treated catalysts, which was not the case in impregnated catalysts. Another explanation provided by the authors for the higher catalytic activity of the plasma-treated catalysts is the lower mass-transfer limitations due to the presence of a large quantity of nanoparticles on the surface of the support, which leads to a greater adsorption of reactants on the surface of plasma-treated catalysts. Odedairo et al.[103] prepared a $Ni/CeO_2$ catalyst by impregnation and subsequently treated it with microwave plasma, omitting the thermal calcination step. They reported higher conversions compared to the thermally calcined catalyst. These findings are related to the smaller Ni particle size and the metal-support interface generated during the plasma treatment. Another method that has been proposed is the synthesis of a so-called reverse catalyst.[104] In this method, metal oxides are deposited on bulk metal surfaces instead of the active metal being supported on the metal oxides. Thus, the authors prepared a reverse $TiO_2/Ni$ catalyst by performing five deposition cycles. This method achieves greater catalyst stability and activity due to the formation of smaller $TiO_2$ particles and the greater number of active centers. The deposition of $TiO_2$ on Ni significantly reduced the size of the pool and increased the resistance to carbon deposition. A $Ni/Al_2O_3$ catalyst prepared using various methods (sol-gel and supercritical drying,[96] impregnation,[105] precipitation,[106] and multi-bubble sonoluminescence (MBSL)[106]) showed higher catalytic activity, stability and lower carbon deposition for the catalyst prepared by MBSL. The authors attributed these results to the formation of smaller particles by sonoluminescence. The MBSL method is considered to allow the formation of tens of thousands of transient bubbles upon the application of high intensity ultrasound. The TPR profile reported by the authors indicated the presence of well-dispersed NiO and NiOx species and also the presence of Ni ions, thus leading to a strong metal/support interaction.

As a general summary of this section, it should be noted that impregnation, sol-gel, and co-precipitation are the most widely reported methods for catalyst preparation. Impregnation is the conventional method; however, it has been reported that it has low reproducibility and Ni as an active component is not homogeneously distributed on the surface of the support. In contrast, the sol-gel method makes it possible to achieve uniformity of the active centers at the molecular level. This may be because the reagents mix uniformly at the molecular level when the gel forms. At the same time, it is easy to incorporate some of the active ingredients uniformly at the molecular level to achieve homogeneous doping. The main disadvantages of this method include the time required for the preparation and the production of a network of micropores, which complicates both preparation of the catalyst and the DRM reaction. In the DRM reaction, it is difficult for the reactants to access the active centers and carbon deposition can quickly hinder this access by blocking the active metal centers. The co-precipitation method has become the most widely studied preparation method. The main drawback of this method is that addition of the precipitating agent can make the partial concentration too high, thus resulting in a non-homogeneous composition. As such, catalyst synthesis operations still need to be improved by using unconventional preparation methods. In this regard, core-shell catalysts opened up a new horizon for the synthesis of novel catalysts that may be able to overcome the issues of carbon deposition and sintering in DRM. The synthesis of such catalysts faces the challenge of having to develop high-throughput methods with enhanced control over the catalyst composition, particle size, shapes and uniformity and, more importantly, at low cost.[107]

Catalysts with a core-shell structure have recently been developed.[108] The core-layer structure is based on coating of the active metal with a catalytic support layer that has a high specific surface area, thereby effectively dispersing the active metal phase.[109-111] The encapsulation of Ni within the porous structure of the support protects the active metallic phase from the deposition of coke and also reduces the agglomeration of Ni particles.[112] The final structure is obtained by way of an initial reaction to form metallic particles that act as a "core" and the subsequent addition of reagents that allow formation of the "shell" that covers the nucleus[113] (see **Figure 7**). In this way, it is possible to synthesize Ni catalysts with inherent control of their size and particle distribution to achieve resistance to sintering and carbon deposition.[114,115] The results obtained by Jabbour et al.[116] using catalysts synthesized according to the core-shell method can be explained by the strong Ni-support interaction facilitated by encapsulation and the uniformly dispersed Ni particles, thus reducing coke formation.

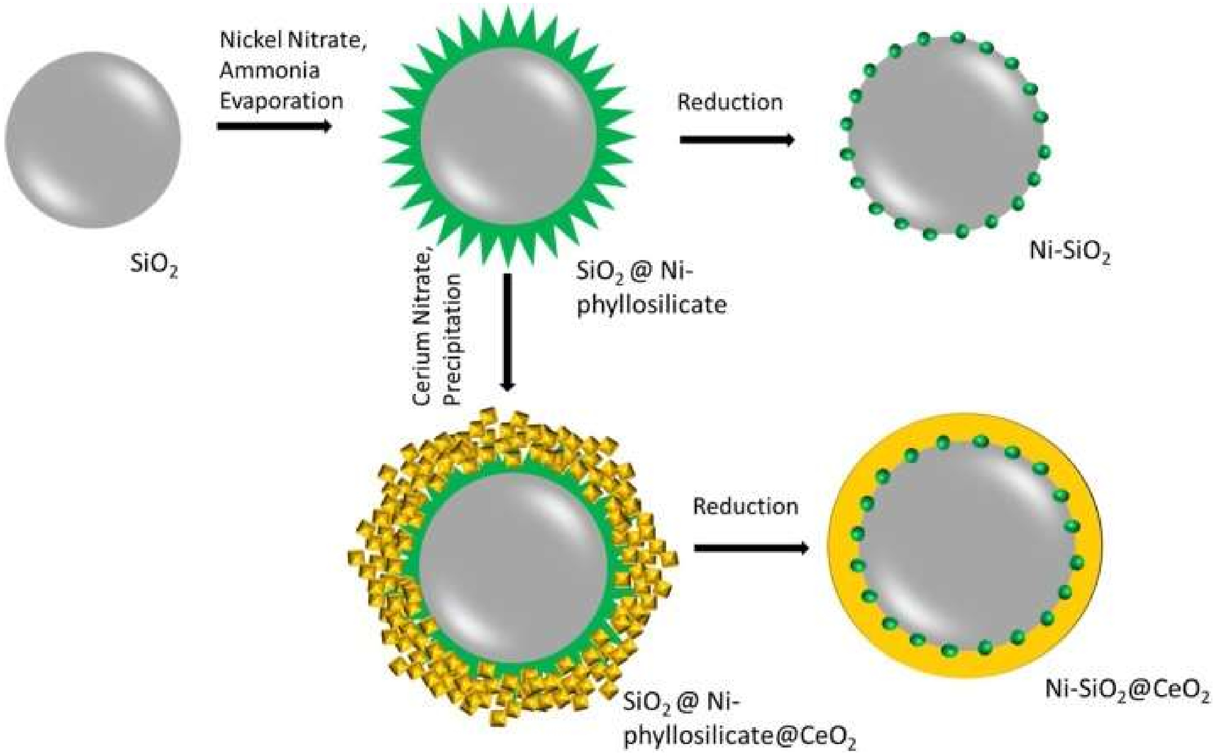

**Figure 7.** Schematic representation of the synthesis of Ni-SiO$_2$ and Ni-SiO$_2$@CeO$_2$ catalysts. (Reproduced with permission from[113]).

### 4.1 Catalytic supports

In general, a catalytic support is not active in a reaction by itself but can modify the properties of the catalyst as a whole. Many authors have reported that the catalytic behavior of metallic catalysts improves with dispersion of the active metallic species, the oxygen storage capacity, and the interaction between the support and the metal.[117,118] The support must also provide strong mechanical strength and high thermal stability. All these aspects must be taken into account in the selection of the catalytic support, with special emphasis on the stability of the active metallic phase and the low rate of carbon deposited.

A broad spectrum of oxides have been used as catalytic supports. For example, Sokolov et al.[119] prepared a series of supported Ni catalysts to observe the effect of the nature of the support on the performance of the catalysts. The study was conducted using Ni/Al$_2$O$_3$, Ni/MgO, Ni/TiO$_2$, Ni/SiO$_2$, Ni/ZrO$_2$, Ni/La$_2$O$_3$-ZrO$_2$, and Ni supported on mixed metal oxides (Ni/Siral 10 and Ni/PuralMG30) as supported catalysts at low temperature (400 °C). The results showed that those catalysts containing Zr showed the highest initial activities. Thus, the authors observed that Ni/La$_2$O$_3$-ZrO$_2$ produced CO and H$_2$ at close to equilibrium, and presented the highest stability, followed by Ni/$ZrO_2$. Although the Ni/$SiO_2$ catalyst had the highest specific surface area, the initial $H_2$ yield was the lowest, followed by Ni/$Al_2O_3$, Ni/MgO, and Ni/$TiO_2$. These authors also noted as remarkable that the Ni/MgO catalyst achieves an initial $H_2$ yield of 2.5%, considering that the catalyst has a low specific surface area. Catalyst performance (based on $H_2$ yield) can be represented as Ni/$La_2O_3$-$ZrO_2$ > Ni/$ZrO_2$ > Ni/PuralMG30 > Ni/Siral 10 > Ni/$TiO_2$ > Ni/MgO > Ni/$Al_2O_3$ > Ni/$SiO_2$. In order to obtain a better understanding of the catalyst resistance to deactivation, the authors compared the $H_2$ yield at run times of 0 and 100 h. The Ni/$La_2O_3$-$ZrO_2$ catalyst was found to have the highest stability with only a 9% loss of $H_2$ yield from the initial state. The lowest catalyst stability, with the 20% loss of $H_2$ yield, was found for Ni/$ZrO_2$, whereas 89% of the $H_2$ yield was maintained for Ni/$TiO_2$. Han et al.[120] studied the effect of Ni particle size and the nature of the support using $SiO_2$, $Al_2O_3$, MgO, $ZrO_2$ and $TiO_2$ as supports. The catalytic behavior evolved as follows: NiO/$Al_2O_3$ ≥ Ni/MgO > Ni/$SiO_2$ > Ni/$ZrO_2$ > Ni/$TiO_2$. This evolution was attributed to the effect of the supports on the reaction. Zhang et al.[121] also observed the following evolution in the catalytic behavior: $Al_2O_3$ modified with NiO/MgO > Ni/MgO > Ni/$SiO_2$ > Ni/$Al_2O_3$ > Ni/$ZrO_2$ > Ni/$TiO_2$. The higher activity of $Al_2O_3$ modified with NiO/MgO was related to the textural properties, the strong metal-support interaction (SMSI) effect, and the size of the well-dispersed Ni particles. $TiO_2$ showed lower catalytic activity due to the low specific surface area, the weak metal-support interaction (WMSI) effect, and the limited dispersion of Ni. Goula et al.[117] also investigated the catalytic behavior of Ni/$La_2O_3$-$ZrO_2$ and Ni/$CeO_2$-$ZrO_2$, finding an improved catalytic behavior with respect to the individual oxides. Kim et al.[122] also used double oxides, especially $TiO_2$ and $CeO_2$, to synthesize Ni catalysts. As in the case of the previous authors, the mixed oxide catalyst showed the best performance and stability, along with a higher resistance to coking due to its redox properties. Among the reported supports, MgO has a high Lewis basicity, which increases the chemisorption of $CO_2$. As such, MgO may be an interesting catalytic support for use in the DRM reaction. In this regard, Usman et al.[123] prepared a Ni/MgO catalyst and found that the catalyst exhibited better catalytic performance and stability when calcined at 800 ºC and reduced at 550 °C. The explanation proposed by the authors is that Ni forms a solid solution with the MgO support, which makes the Ni active center more stable. To explain this behavior, Zanganeh et al.[124] proposed the formation of a reduced solid solution of $Ni_{0.03}Mg_{0.97}O$ that presents an excellent anti-carbon capacity. These properties are related to the excellent dispersion of Ni species, the alkaline properties of the support surface, and the Ni-support interaction. The behavior of the Ni/MgO-γ-$Al_2O_3$ and Ni/$MgAl_2O_4$ catalysts was compared with a Ni/γ-$Al_2O_3$ catalyst, with the former exhibiting better stability and higher activity.[125] The stability presented by the catalyst was attributed to $MgAl_2O_4$ spinel layer formation in the Ni/MgO-γ-$Al_2O_3$ catalyst, which reduces the tendency to form the $NiAl_2O_4$ spinel. The authors attributed the high activity of the catalysts, as well as the high resistance to carbon deposition and sintering compared to γ-$Al_2O_3$, to the characteristics of $MgAl_2O_4$, which has higher basic properties due to the presence of Mg. At the same time, the interaction between Ni and $MgAl_2O_4$ allows a higher dispersion of Ni on the support. As described above, $ZrO_2$ is widely used in the DRM reaction as a catalytic support due to its acid-base surface properties and high thermal stability. Zhang et al.[126] found that a Ni-ZrO2-CR-15 catalyst exhibited interesting catalytic performance and stability properties. In addition, Ni/$La_2O_3$-$ZrO_2$ catalysts prepared using the sol-gel method[127] were also studied. These authors indicated that, due to the formation of a strong interaction between the $La_2O_3$-$ZrO_2$ support and Ni, the dispersion of Ni is improved and coke formation is strongly inhibited. The catalyst with a Ni content of 10 wt.% was found to have the best catalytic performance and anti-coking performance.

$CeO_2$ has been selected as a promising candidate due to its remarkable oxygen storage capacities, carbon resistance property, acid-base centers, and unique redox properties. Indeed, it can release and store $O_2$ under reducing and oxidizing atmospheres by filling the oxygen vacancy defects associated with the $Ce^{4+}/Ce^{3+}$ redox cycles. It also improves the inhibition of coke formation and stable catalytic activity. Therefore, $CeO_2$ may be an attractive carrier for the DRM reaction.[118] In this regard, Dong et al.[128] prepared NiO/$CeO_2$ catalysts and reported the excellent performance thereof in POM. Similarly, Wang et al.[129] found that the strong interaction between NiO and $CeO_2$ significantly reduced carbon deposition on their catalysts. Löfberg et al.[130] prepared a Ni/$CeO_2$ catalyst by wet impregnation and found that the resulting Ni species performed two necessary functions: activating reactants and supplying oxygen. These studies can be included within the research efforts that have been carried out to find and study supports that maximize oxygen vacancies and thus allow the dissociation and activation of $CO_2$ to produce CO to be increased. The search for catalytic supports with unique redox properties and with $O_2$ storage capacity (OSC) is one of the main challenges in DRM. The storage of $O_2$ favors oxidation of the carbon deposits and the creation of vacancies in the catalytic supports for the activation of $CO_2$[131] (see **Figure 8**).

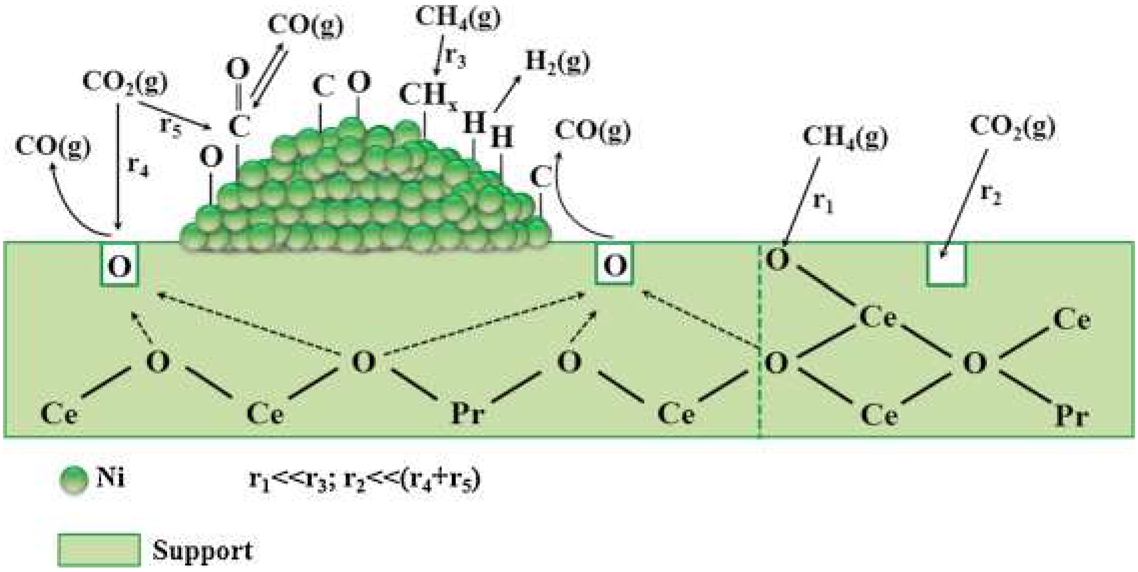

**Figure 8.** Schematic representation of the main chemical reaction steps in the $CH_4$ and $CO_2$ activation routes on 5 wt.% Ni/$Ce_{0.8}Pr_{0.2}O_{2-\delta}$ catalyst (Reproduced with permission from[131]).

Given their textural properties, ordered mesoporous and microporous silicas have also been used as catalytic supports. The incorporation of Ni particles inside mesoporous supports has been proposed to increase the conversion of reactants and product yield, thus avoiding the sintering of metallic particles and strengthening the metal-support interaction.[132] To achieve these objectives, catalytic supports must be mesoporous and have high specific surfaces so that they can improve the dispersion of Ni particles on the supported catalyst.[126] A strong metal-support interaction stabilizes the Ni particles that are incorporated into the mesoporous matrix. As examples, the incorporation of Ni into mesoporous supports such as MCM-41, SBA-16, TUD-1, meso-$Al_2O_3$, and meso-$ZrO_2$ has been proposed, with the resulting catalysts exhibiting high catalytic activity and high resistance to coke deposition in the DRM reaction.[126] Thus, Drobna et al.[133] synthesized Ni catalysts supported on MFI and FAU zeolites, Al-MCM-41, SBA-15, and $Al_2O_3$. The catalytic behavior observed depended on the support used and the authors found the following catalytic order: Ni/SBA-15 ≈ Ni/Al-MCM-41 > Ni/$Al_2O_3$ > Ni/MFI > Ni/FAU. The properties that explain the observed trend were a high specific surface area, the reducibility of Ni, and good dispersion of the Ni particles. In light of their basic properties, mesoporous silica nanoparticles have been used as supports by Sidik et al.[134] and found to show better catalytic behavior than when MCM-41 is used as support.

Similarly, Donphai et al.[135] successfully synthesized compounds comprising Ni and carbon nanotubes on a mesoporous silica support (Ni-CNT/MS). These authors found that Ni-CNT/MS catalysts show $CO_2$ and $CH_4$ conversions similar to those that can be obtained initially when using Ni/MS catalysts. When comparing the results obtained after reaction for 24 h, the conversions of $CO_2$ and $CH_4$ were found to increase with the Ni-CNT/MS catalysts and to decrease with the Ni/MS catalysts (see **Figure 9**). Natural mineral clays are considered alternatives to traditional supports due to their easy availability, low cost, and desirable physical and chemical properties. Akri et al.,[136] Liu et al.[137,138] and Che et al.[139] have used natural mineral clays as a support for the preparation of Ni-based catalysts for DRM. Synthetic clays allow the physicochemical properties to be adjusted to meet the specific needs of the reaction. Thus, anionic clays, hydrotalcites (HTC) or laminar double hydroxides (LDH) have also been used as supports in this application due to their ability to improve the dispersion and reducibility of Ni.[140] Feng et al.[141] used a Ni-Mg-Al catalyst made from a hydrotalcite precursor. This catalyst exhibited superior and more stable catalytic behavior than its NiO-MgO and Ni/$\gamma$-$Al_2O_3$ counterparts. Activated carbon has also received attention as a catalytic support due to its neutral surface properties and excellent textural properties, with some authors using activated carbon derived from biomass as a catalytic support.[142,143] Oxides with a perovskite-like structure have been evaluated as catalysts for DRM.[144-147] Thus, Valderrama et al.[148-150] synthesized catalysts with a structure based on the perovskites $La_{1-X}Sr_XNi_{0.4}Co_{0.6}O_3$ and $La_{0.8}Sr_{0.2}Ni_{1-Y}Co_YO_3$ using a sol-gel method, and Lima et al.[151] analyzed the effects of Ce on the catalytic properties of $La_{1-X}Ce_XNiO_3$. These latter authors reported that the presence of Ce prevented coke deposition.

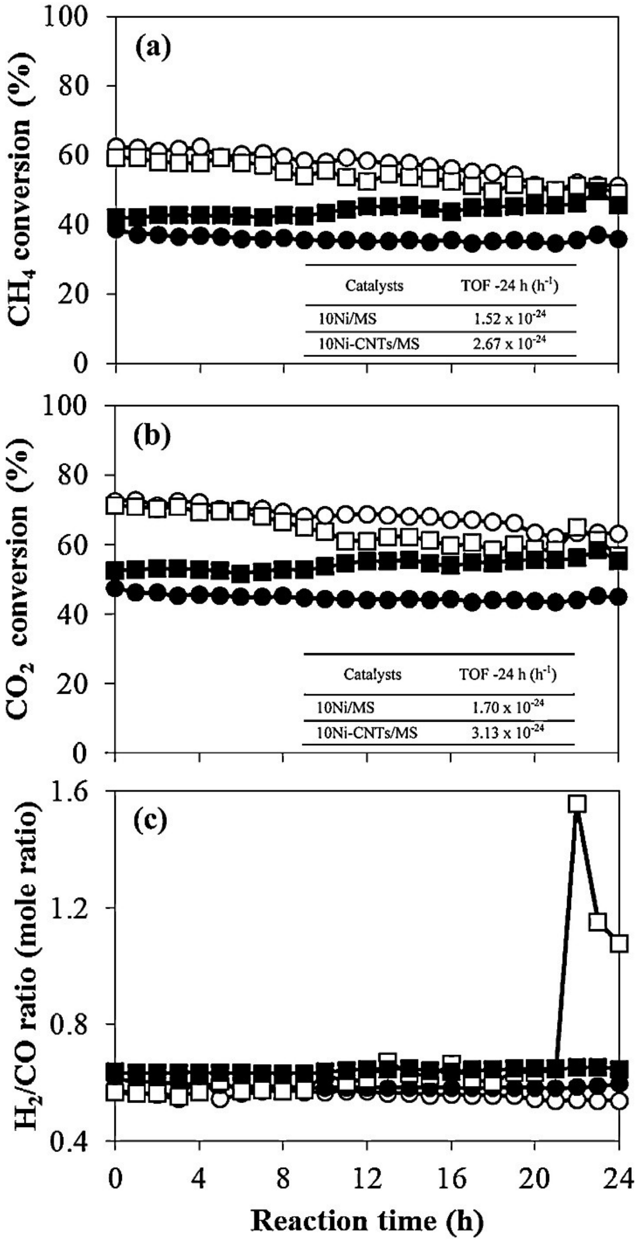

**Figure 9.** Performances of catalysts with and without carbon nanotube (CNT) composites on mesoporous silica (MS) with time on-stream during the dry reforming reaction at 650 °C for 24 h. (a) $CH_4$ conversion, (b) $CO_2$ conversion, (c) $H_2$/CO molar ratio. (○) 5Ni/MS, (□) 10 Ni/MS, (●) 5Ni-CNT/MS, (■) 10Ni-CNT/MS (Reproduced with permission from[135]).

The catalytic support can react with the active metallic phase and thereby affect the reaction. In the case of DRM, two types of interactions can be distinguished: an interaction between the active metal and the support, or the combined interaction of bimetals and the support. The SMSI effect results in a better dispersion of the active metal and resistance to sintering. This interaction makes it possible to maintain a small size for the active metal species. In contrast, the synergistic effect of bimetals improves dispersion and provides complementary active metal centers. Wang and Ruckenstein[152] studied the SMSI effect using Rh catalysts with reducible ($CeO_2$, $Ta_2O_5$, $TiO_2$, $Nb_2O_5$ and $ZrO_2$) and non-reducible (γ-$Al_2O_3$, $La_2O_3$, MgO, $SiO_2$ and $Y_2O_3$) oxide supports. In their experiments, the authors found that Rh/γ-$Al_2O_3$ and Rh/MgO exhibited better catalytic behavior and were more stable than other supported non-reducible catalysts. Using TPR and XRD analyses, the authors attributed the improved catalytic activity to the SMSI effect as a result of the formation of a homogeneous solid solution. Oxides that could be reducible showed lower activity and required considerably longer activation. The authors characterize MgO and γ-$Al_2O_3$ as the supports that can confer a greater SMSI effect when the active metallic phase is Ni.[153-158] In the case of the NiO-MgO-based catalyst, in addition to presenting high conversions of $CH_4$ and $CO_2$, it showed adequate resistance to coke deposition.

Oxides with a structure similar to $NiAl_2O_4$ spinels were prepared by Sahli et al.[159] to study the SMSI effect. The authors found that for a Ni to Al molar ratio of exactly 0.5, the crystalline spinel phase formed above a temperature of 725 $^{o}$C. When the ratio was greater than 0.5, the excess Ni gave rise to the formation of NiO particles deposited in the spinel phase. This situation was achieved at temperatures lower than 750 $^{o}$C, but it had the disadvantage of carbon deposition. Noble metal-based catalysts suffer from a weak metal-support interaction (WMSI) effect. As such, their performance is strongly affected by the sintering and agglomeration of the metallic particles under the reaction conditions. Beltran et al.[160] compared the activity of Rh/$Al_2O_3$, and Rh and $ZrO_2$ deposited on $Al_2O_3$ and found that the addition of zirconia promotes the SMSI effect and further enhances the metal-support interaction. Li et al.[161] modified the Ni/$Al_2O_3$ catalyst by adding $La_2O_2CO_3$ (see **Figure 10**), and observed that the incorporation of $La_2O_2CO_3$ inhibits the formation of $NiAl_2O_4$ by preventing Ni diffusion on the alumina support during the reaction and improving the dispersion of the Ni particles in comparison to the Ni/$La_2O_3$ catalyst.[162]

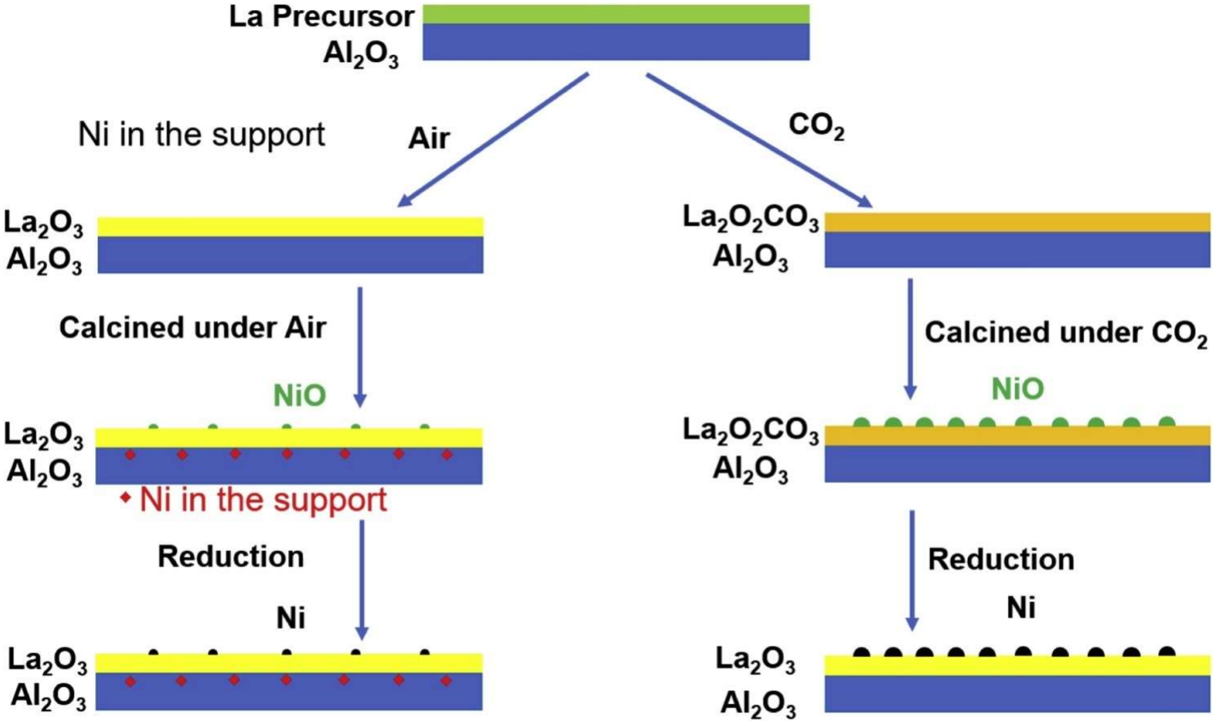

**Figure 10.** Schematic representation of the effect of air or $CO_2$ on Ni dispersion in the Ni/$La_2O_3$ catalyst (Reproduced with permission from[161]).

## 4.2 Catalytic promoters

The nature of the catalytic support as well as the addition of species that modify its surface properties can provide good catalyst activity affecting, for example, carbon deposition. The addition of promoters can improve both the acidity and alkalinity of the catalyst surface and the interaction between the metal and the support, regulate the electronic density of the active metal phase, and improve the dispersion of the metal. It can also affect the adsorption, dissociation and activation capacity of $CH_4$ and $CO_2$ in the catalyst, thus improving the reaction efficiency of the catalyst or improving the resistance to carbon deposition.

Carbon deposition on the catalyst surface can be reduced if the acid-base properties of the catalyst are modified. One way to achieve this is by adding alkali and alkaline-earth metals to act as modifiers.[163] These modifiers can also have the effect of preventing sintering of the active metal particles in the catalyst, thereby reducing deactivation of the catalyst.[164] With this in mind, the promoters used in DRM have been grouped into three categories: **a.** alkali and alkaline-earth metals such as K, Li, Na, Mg, Ba, and Ca; **b.** rare-earth metals such as Ce, La, Zr, Pr, and Sm; and **c.** others, such as Ag, As, Au, Bi, Cu, and Sn.[165] When used as a promoter, CaO reacts with the support at a structural level and increases the resistance of the Ni species to sintering. The competition between Ca and Ni during this interaction helps the formation of reducible Ni species. The authors observed that the Ca concentration in the catalyst affected the conversion of $CO_2$ and $CH_4$ in the DRM reaction. Thus, low Ca concentrations resulted in an increase in $CO_2$ conversion. This behavior is explained by the authors as being due to an increase in the interaction of $CO_2$ on the catalyst surface, which also increases the conversion of $CH_4$. However, an increase in the amount of Ca leads to higher electron density of Ni, which results in a decrease in $CH_4$ and $CO_2$ conversions.[164] Similar findings were also reported by Choudary el al. using NiO/CaO and Ni/$Al_2O_3$ catalysts precoated with MgO, CaO and rare-earth metals and Ni/CaO/γ-$Al_2O_3$ catalysts with various CaO contents.[166,167] Alipour et al.[168] also used basic oxide promoters such as MgO, BaO and CaO supported on $Al_2O_3$ to increase the basicity of a Ni catalyst. These authors observed that the presence of these modifiers also helped reduce coking and improved catalyst performance due to increased $CO_2$ adsorption.

The presence of K in NiO-$Al_2O_3$ catalysts modifies the interaction of NiO with the support and improves the reducibility of the Ni species. Furthermore, K can also act as a catalyst for gasification of the coke formed during the reaction without changing its structure. The size and structure of the Ni particles were not modified by the presence of K. Castro Luna and Iriarte[169] also reported similar findings whereby the formation of coke on the catalyst surface is prevented when the catalyst is promoted with K. Generally speaking, the reducibility of the catalyst increases when K modifies the interaction between the metal and the support. To explain this behavior, it has been suggested that the transfer of K from the support to the Ni surface in a promoted K catalyst decreases the conversion of $CH_4$ because a portion of the most active centers for DRM reactions are neutralized.[169] Ngaraja et al.[170] investigated the effect of K on Ni/MgO-$ZrO_2$ and also highlighted the importance of the appropriate weight percentage for the promoter. Thus, they reported that 0.5 wt.% K had a significant effect on the catalytic activity and stability, and also observed an increase in surface area with an increase in the weight percentage of the promoter, although this led to a lower catalytic activity (see **Figure 11**). Jeong et al.[171] studied the effect of Mg, Mn, K and Ca (5 wt.%) on the Ni/HY catalyst and found that its performance, in decreasing order, was as follows: Ni-Mg/HY > Ni-Mn/HY > Ni-Ca/HY > Ni/HY > Ni-K/HY. The highest $CH_4$ conversion (85%) and stability

(96%) was obtained for the Ni-Mg/HY catalyst as a consequence of decoration of the Ni surface with the partially reduced metal oxide MgOx (see **Figure 12**). These authors noted that the presence of the modifiers reduces the size of the Ni particles (from 23.7 to 14.9 nm) and favors the metal-support interaction.

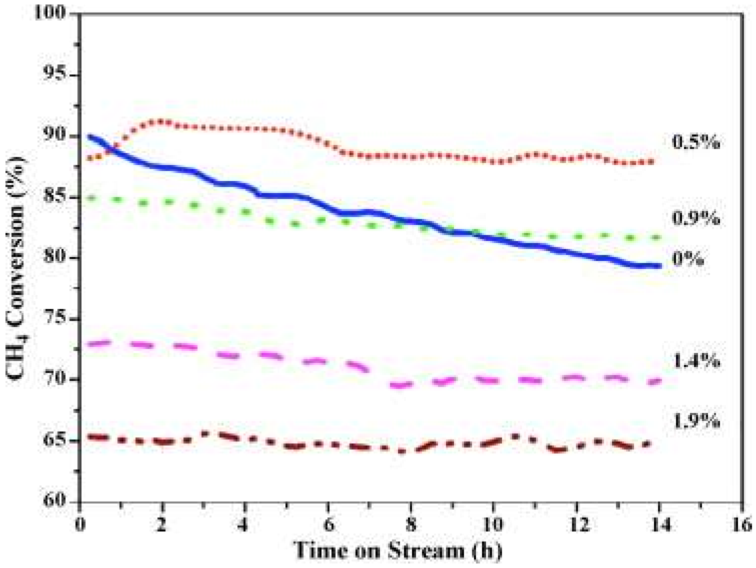

**Figure 11.** $CH_4$ conversion vs. time on-stream at 250 °C over the Ni/MgO-$ZrO_2$ catalyst (NM5Z2) with various K loadings (Reproduced with permission from[170]). (Reaction conditions: catalyst weight: 20 mg, reduction conditions: 250 °C/2h; $CH_4/CO_2$/Ar ratio: 1:1:8; total flow rate: 50 ml/min.).

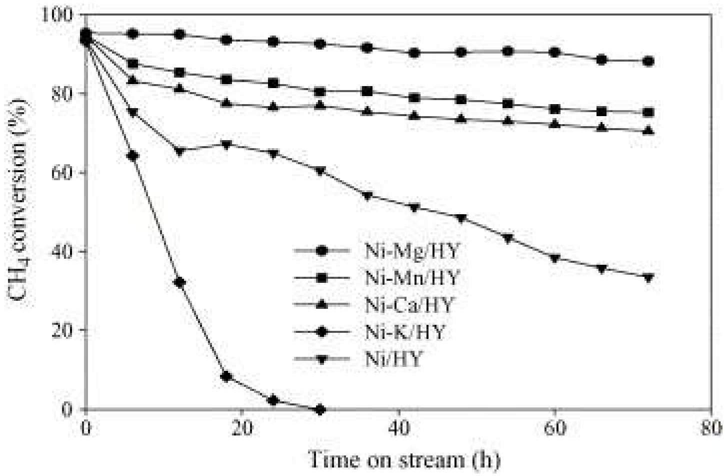

**Figure 12.** Effect of promoter on the performance of the Ni/HY catalyst at 700 °C (GHSV = 3500 $h^{-1}$) (Reproduced with permission from[171]).

Catalytic modifiers are used in small amounts, usually 0.01 to 10 wt.%, depending on the catalyst system concerned. The optimal amount of modifier differs according to the nature of the promoters, which have different abilities to modify the structure of the catalyst. Daza et al.,[172] for example, studied the behavior of Ni/Mg-Al modified by various weight-percentages of Ce (between 0 and 10 wt.%) and found that the weight percentage of the promoter is an important criterion to avoid carbon deposition. For example, the catalyst (Ni/Mg-Al) modified with 3 wt.% Ce showed a higher conversion of $CH_4$ (99%) and $CO_2$ (95%), with no decrease in stability, up to 100 h of the DRM reaction. For smaller amounts of modifier, the authors detected the presence of filamentous-type coke, which was absent for the catalyst promoted with 3 wt.% Ce. Ocsachoque et al.[173] reported that the presence of Ce in an $Al_2O_3$ support facilitates the activation of $CH_4$ and $CO_2$ and favors the suppression of carbon. Similarly, Akri et al.[136] introduced various amounts of Ce into illite-based Ni catalysts and observed that the addition of Ce both improves the porosity, which enhances the textural properties of the material and increases the resistance to agglomeration of Ni particles and deposition of carbon. They also reported that the mean size of the Ni nanoparticles decreases from 34.2 to 16.3 nm after addition of Ce. Compared to the Ni catalyst, the conversion of $CH_4$ and $CO_2$ increases to 82% and 72%, from 33% and 21%, respectively, due to the presence of Ce. As such, the introduction of Ce also improves the catalytic stability, which is attributed to the good redox properties and highly dispersed Ni nanoparticles (see **Figure 13**). Liu et al.,[174,175] in turn, used a Ni catalyst promoted by La and found that the catalyst containing 2 wt.% La was most active at 550 °C, while the catalyst containing 4 wt.% La was most active at 600 °C. The La content, therefore, affected the catalytic behavior. The authors attributed this improved effect to a high oxygen vacancy, greater Ni dispersion, greater $CO_2$ adsorption, and less carbon deposition due to amorphous carbon gasification caused by the presence of La. The effect of promoters from the lanthanide group on Co-Ni/$Al_2O_3$ catalysts was evaluated by Foo et al.,[176] who found an increase in the production of $H_2$ and CO and related this behavior to a higher oxidation of coke deposits on the surface. These authors also observed that coke deposition on the metal surface was drastically reduced, thus demonstrating a high resistance to coke formation following the order Ce > Pr > Sm. Debek et al.[177] used Ce, Zr and mixed CeZr promoters in Ni-Mg-Al catalysts with a hydrotalcite-like structure and noted that coking was reduced for all catalysts during the reaction. The catalysts promoted by Ce had a greater oxygen storage capacity, which could favor oxidation of the carbon deposits. For the Zr-promoted catalysts, these authors observed that Zr inhibited the direct decomposition of $CH_4$ and the WGS reaction. They also noticed that metal oxides based on Ni and $CeO_2$ have a higher oxygen-storage capacity and help to decompose $CO_2$. In a related study, Gandhi and Patel[178] used $Ni/Al_2O_3$ catalysts promoted by zirconia, ceria, and magnesia and analyzed the effects of these promoters on catalytic behavior, resistance of the catalysts to coking and pore structure and observed that 10% Ni/5% $ZrO_2$-$Al_2O_3$ provided the highest conversion and 10% Ni/5%$CeO_2$-$Al_2O_3$ was the most stable. The use of Ce, Ca and Zr as promoters in Ni/γ-$Al_2O_3$ showed that the Ce-modified catalyst exhibited improved activity compared to Ca and Zr, while a combination of Ce and Ca significantly increased catalytic activity and produced less carbon deposition (2.5 wt.%) compared to Ce alone (8.9 wt.%).[179] In another study, the effect of adding $ZrO_2$ to $Ni/Al_2O_3$ was investigated, with the authors finding a higher catalytic activity (71.3% $CH_4$ and 62.1% $CO_2$ conversion) compared to non-promoted $Ni/Al_2O_3$ (63.0% $CH_4$ and 57.0% $CO_2$ conversion).[180] The authors attributed this increase in catalytic activity to the ability of $ZrO_2$ to enhance $CO_2$ dissociation. Likewise, the $ZrO_2$-modified $Al_2O_3$ surface allows the Ni particles to interact better with the support and prevents the formation of $NiAl_2O_4$. This increased $CO_2$ dissociation leads to greater stability and reduced carbon deposition by increased gasification of dissociated oxygen and unsaturated intermediates.

Modification of the mesoporous supports with promoters also resulted in improved catalytic activities. Thus, various authors reported how a Ni/SBA-15 catalyst modified with MgO (3 wt.%) resulted in a conversion of 97.8% for $CH_4$ and 96.9% for $CO_2$, both of which are higher than for the non-promoted catalyst. (Ni/SBA-15) and the catalyst promoted with various wt.% of MgO (1, 5 and 7 wt.%).[181] The programmed temperature reduction analyzes (TPR-$H_2$) carried out in this study indicated that the addition of MgO markedly affects the reduction properties of the catalyst. Thus, the catalyst modified with 3 wt.% MgO is characterized by presenting better dispersed Ni particles than the rest of the catalysts, and has better basic properties upon adsorption of $CO_2$. A similar result was obtained for a Ni/Mo/SBA-15 catalyst modified with $CeO_2$ in comparison with its non-promoted counterpart.[182] Liu et al.[48] studied the effect of the presence of Ti, Mn and Zr in Ni/MCM-41 and reported a higher $CH_4$ conversion for the Ni-Zr-MCM-41 catalyst, as well as a lower carbon deposition. The higher conversion for Ni-Zr-MCM-41 could be related to a higher dispersion (5.6%) compared to those observed in Ni-Ti-MCM-41 and Ni Mn-MCM-41. Other researchers have studied the effect of the presence of $Y_2O_3$ as a promoter in NiO/SBA-15 and observed a significant effect on catalytic activity and carbon deposition.[183] Thus, a higher catalytic activity and stability up to 50 h were observed for the Y-NiO/SBA-15 catalyst. These results can be related to the smaller particle size, greater dispersion of NiO particles and high specific surface area.

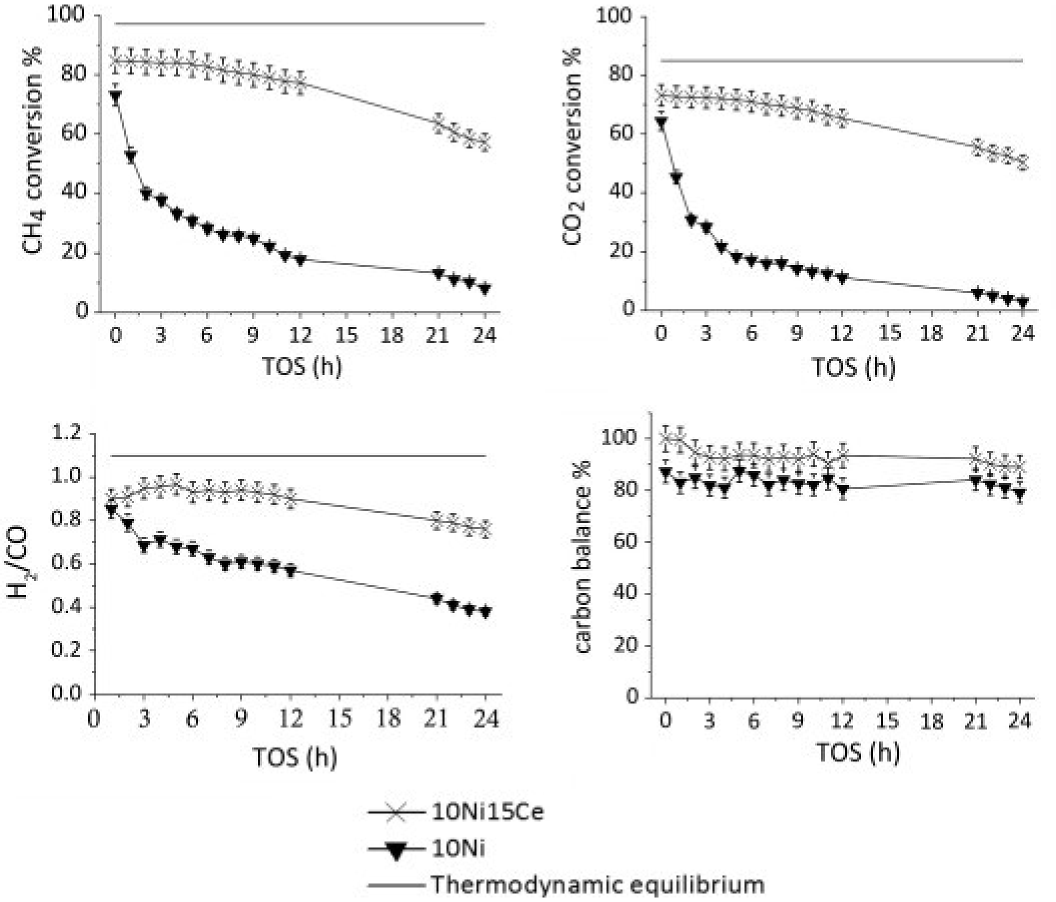

**Figure 13.** $CH_4$, $CO_2$ conversions, $H_2/CO$ ratio over 10Ni and 10Ni15Ce during reaction for 24 h; T = 800 °C, $CH_4/CO_2/O_2$ = 1/0.8/0.1, GHSV = 60,000 mL/h·g. (Reproduced with permission from[136]).

The acidic and basic centers on the catalyst surface also play a critical role in DRM. Thus, in the case of an acid catalyst, it had been proposed that these types of centers could stop the dissociative chemisorption of $CO_2$ on the catalyst surface due to the accumulation of dehydrogenated carbon, which undergoes graphitization and blocks the active sites responsible for $CO_2$ adsorption. As a consequence, the catalyst can be deactivated.[184] The presence of basic sites responsible for gasification of the deposited carbon could produce a positive effect on the inhibitory activity of coking via the Boudouard reaction.[185] In this regard, Ni et al.[186] studied modified Ni (5 wt.%) alumina catalysts with a $B_2O_3$ loading of between 0 and 10 wt.%. The formation of strong Lewis acid sites results in the deposition of a large amount of carbon on the catalyst, which causes a decrease in yield and stability. Weak Lewis acid sites and hydroxyl groups on the catalyst promote carbon removal, thereby increasing yield and stability. Quindimil et al.[187] studied the effect of the presence of La in Ni/zeolite catalysts (Y- and BETA). The presence of $La_2O_3$ allowed the generation of basic sites in the catalyst and promoted the dispersion of Ni, thus improving the yield and the conversion of $CH_4$. Abdullah et al.[39] proposed that the basic nature of the catalyst improves catalytic activity by reducing the activation energy of the reactants. $CH_4$, which is more stable, requires a higher activation energy than $CO_2$, therefore, the presence of basic sites on the catalyst allows the activation energy barrier to be overcome. The acid-base properties of the catalyst can also affect the reaction mechanism. Thus, the activation of $CH_4$ at the active metal and the activation of $CO_2$ on the acidic or basic support follow a bifunctional reaction pathway. When catalysts are based on inert materials such as $SiO_2$, $CH_4$ and $CO_2$ are activated at the active metal following the monofunctional route.[52]

### 4.3 Bimetallic catalysts

Several researchers have reported that the addition of noble metals to the Ni catalyst allows the catalytic activity to be improved by directly increasing the number of active Ni sites on the surface. It has been found that carbon deposition is inhibited when the size of the metal particle is reduced, and that this can also favor carbon gasification, especially for noble metals. Thermal sintering can also be reduced in these cases by increasing the dispersion and reducing metallic interactions with the support. Additionally, this makes it possible to increase the reducibility of the Ni catalyst, especially under the oxidizing atmospheres reported for the reforming of $CH_4$. When preparing modified metal catalysts containing much smaller amounts of another metal, close attention must be paid to the preparation method in order to obtain high catalytic yields for the modified catalysts. Co-impregnation is a widely used preparation method consisting in using an aqueous solution containing the two precursors. The two-step sequential impregnation method is another option for catalyst preparation.

The effect of the presence of noble metals (Ru, Pd) in Ni/$SiO_2$ catalysts prepared using the co-impregnation method on the catalytic behavior has been studied by Crisafulli et al.,[188] who reported that the catalytic behavior of Ni-Ru and Ni-Pd bimetallic catalysts depends on both the noble metal and the precursor used. Thus, in the case of bimetallic catalysts prepared using nitrate precursors of the noble metal, the presence of Ru strongly improved catalytic activity and stability. In catalysts prepared using chloride precursors, the presence of the noble metal (Ru or Pd) resulted in a moderate decrease in catalytic activity. The authors explained these different catalytic behaviors in terms of the degree of metal-metal interactions in each catalyst. Thus, the behavior of Ni-Ru catalysts was attributed to the formation of bimetallic Ni-Ru clusters with a surface covered mainly by Ni. This leads to an increase in the dispersion of metallic Ni and favors the formation of a more reactive intermediate carbonaceous species, thus inhibiting deactivation of the catalyst. In a later study,[189] the same authors extended their work by using zeolites (H-ZSM) as catalytic supports. The results obtained indicated that Ni-Ru/$SiO_2$ catalysts are much more active and stable than Ni-Ru/H-ZSM catalysts. Similarly, Jozwiak et al.[190] studied Ni/$SiO_2$ doped with Rh, Ru and Pd. A comparison of the catalytic results with those obtained using monometallic Ni catalysts showed that the bimetallic catalysts exhibited a lower deactivation rate and improved catalytic performance. A similar result was obtained for Rh-Ni/$\alpha$-$Al_2O_3$ catalysts prepared by co-impregnation. These catalysts showed higher catalytic performance and resistance to deactivation by carbon deposition than the corresponding monometallic catalysts.[191] Becerra et al.[192] reported that the addition of small amounts of Rh to a Ni/$\gamma$-$Al_2O_3$ catalyst using a sequential impregnation method resulted in an increase in the surface area of the metal, which in turn results in an increase in catalytic performance. Álvarez et al.[193,194] investigated Ni-Ru/MgO-$Al_2O_3$ catalysts and found that, although the bimetallic catalyst showed superior particle reducibility compared to the monometallic Ni and Ru catalysts, the strong interaction between Ni and Ru resulted in blocking of the active Ni centers by Ru atoms, thus inhibiting the activation of $CH_4$ and, therefore, a lower catalytic activity. These results were corroborated by Andraos et al.,[195] who also showed that these interactions caused suppression of the Boudouard reaction, an improvement in carbon gasification and, consequently, an increased stability for the catalyst. These authors suggested that the Ru in bimetallic Ni-Ru catalysts reduces the diffusion rate of carbon on the Ni surface, thus inhibiting the formation of carbon nanotubes. García-Dieguez et al.[196] and Mahoney et al.[197] also reported that the addition of noble metals can improve the dispersion of Ni species and decrease the formation of coke deposits. They added Pt to Ni/$CeZrO_2$ and Ni/$Al_2O_3$, which increased the reducibility of Ni. At lower temperatures, the bimetallic Pt-Ni catalyst showed a slightly higher activity for hydrogen production during the DRM reaction compared to the Ni-catalyst. In the case of the Rh-Ni system on nanofibrous alumina, García-Diéguez et al.[198] noted that, although the activity of the bimetallic catalyst was comparable to that of the monometallic ones, differences in $H_2$/CO selectivity were observed. Ma et al.[199] reported that bimetallic Pd-Ni exhibits a superior catalytic performance to the monometallic catalyst, which may be due to the synergistic effect between Pd and Ni, thus resulting in better structural characteristics and increased reducibility. Similarly, the greater dispersion of Ni and the production of additional active sites resulting from the addition of Pd improve the catalytic performance. Ozkara-Aydinoglu and Aksoylu[200] investigated bimetallic Pt-Ni catalysts and tried to find a correlation between catalytic activity and metal loading and their ratio. They concluded that the catalyst with the lowest Ni⁄Pt ratio showed the highest activity and stability. Meshkani et al.[201] studied Pt-Ni catalysts with different Pt contents (0.1-0.3 wt.%) supported on nanocrystalline magnesium oxide and found that the $CH_4$ and $CO_2$ conversions were higher than those obtained using monometallic catalysts and explained these findings by the increased Ni dispersion and resistance of the catalyst to carbon deposition. The excellent stability during operation for 50 h was attributed to the formation of a solid NiO-MgO solution and the high basicity of the catalysts. Pawelec et al.,[202,203] in turn, investigated the effect of preparation method and surface Ni content on the catalytic properties of Pt-Ni/ZSM-5 and Pd-Ni/MCM-41 catalysts. They noted that the catalyst prepared by sequential impregnation showed the best results in terms of activity and stability, possibly due to an increased dispersion of Ni metal caused by the intimate contact between Ni and Pt. In other words, the addition of Pt leads to the formation of small and easily reducible NiO particles. In the case of Pd catalysts, the catalytic performance is attributed to a synergistic effect between Ni and Pd, which leads to a high degree of reduction and a high metallic surface due to the increase in Ni dispersion.

Khani et al.[204] reported the effect of the presence of Pt and Ru in $Ni/ZnLaAlO_4$ catalysts. They observed that, although the Ni loading was three times that of Ru and Pt, $Ni/ZnLaAlO_4$-supported Pt and Ru catalysts exhibited much higher catalytic activity. Their TGA results also showed that carbon formation in the Pt- and Ru-containing catalysts was negligible, while the $Ni/ZnLaAlO_4$ catalyst exhibited a carbon formation of 7 wt.% at 700 $^oC$. $Ni/\gamma\text{-}Al_2O_3$ promoted by Y and its oxide ($Y_2O_3$) showed a higher conversion of reagents and exhibited traces of carbon deposition[205,206] (see **Figure 14**). The authors of these studies indicated that the higher catalytic activity of the Y-promoted catalyst was due to the improved metal-support interaction, the presence of smaller Ni particles, and, thus, a higher resistance to sintering. Steinhauer et al.[207] found that the catalytic performance of bimetallic Pd-Ni catalysts is significantly affected by the nature of the support in the order $TiO_2$ < $Al_2O_3$ < $SiO_2$ < $ZrO_2$ < $ZrO_2$-$La_2O_3$ ~ $La_2O_3$ and, in all cases, is higher than for the monometallic catalysts. These authors also observed that the optimal Ni/Pd ratio was 4:1 for a total metal loading of 7.5 wt.%, which gave the highest activity. Similarly, higher metal loads favor coke formation. The same authors investigated the effect of the calcination temperature of the metallic precursors and found that thermal treatment at 600 °C was the most suitable to obtain the highest catalytic performance. At lower temperatures, decomposition of the metal precursors is inhibited, while higher temperatures induce sintering of the metal centers. In conclusion, the presence of Rh, Pt and Pd in bimetallic catalysts increases the catalytic activity and stability against carbon and sulfur deposition compared to monometallic Ni catalysts.

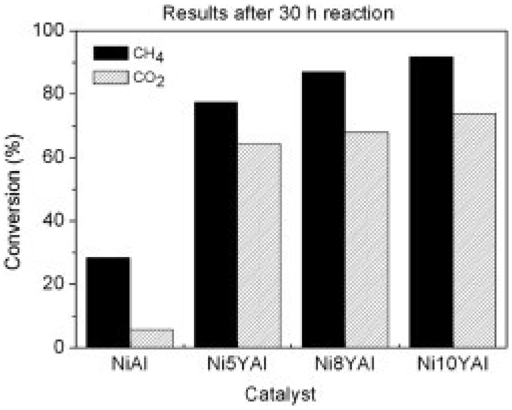

**Figure 14.** Effect of Y promotion on $CH_4$ and $CO_2$ conversion over a Ni/γ-$Al_2O_3$ catalyst (Reproduced with permission from[205]).

Other metals have also been studied in the formulation of bimetallic catalysts. Due to their similar electronic configuration, Co and Ni can easily form bimetallic alloy nanoparticles,[208] with a superior performance compared to monometallic catalysts being observed at low temperatures. Thus, San José-Alonso et al.[32] studied the catalytic behavior of Co-Ni/$Al_2O_3$ catalysts with different Co and Ni contents (9 wt.% total metal load) and found that the optimal activity and stability corresponded to the catalyst containing 8 wt.% Co, which they attributed to the improved activity of Co for the decomposition of $CH_4$, which is considered to be the rate-determining step in the DRM reaction.[209] This catalyst also exhibited good stability over time, which the authors attributed to the presence of large Co particles. In a similar study, Sengupta et al.[210,211] found that the most active catalyst at low temperature had the lowest Co content (Ni/Co = 3:1), which they attributed to the ability of this catalyst to simultaneously promote $CH_4$ decomposition and oxidation of the deposited coke. In an experiment to test stability, a bimetallic Ni-Co catalyst supported on $Al_2O_3$-MgO, which was prepared using the co-precipitation method, showed only low deactivation after use for 2000 h.[212] One of the key factors responsible for the excellent catalytic performance of this bimetallic catalyst is the preparation method. Thus, the high calcination temperature used during preparation of the catalyst results in the formation of strong interactions between the metal and the support, thus causing the catalyst to form stable spinel-like structures. In general, carbon formation is lower upon Ni-Co alloy formation during catalyst reduction than with individual Ni centers. Several catalyst synthesis methods have also been found to affect reaction performance. For example, the co-precipitation method tends to produce smaller metal particles than the wet impregnation method.

Zhang et al.[213] studied the behavior of monometallic Ni and Co supported on $Al_2O_3$, as well as their bimetallic homologues, in DRM at 700 $^{o}$C. The highest initial $CH_4$ conversion was observed for the 5 wt.% bimetallic Ni-Co/$Al_2O_3$ catalyst for each of the metals, with these systems containing the smallest metal oxide particles (13 nm). The higher initial activity is explained by the authors as being due to the presence of relatively small metal oxide particles. The metal oxide particle size for Co/$Al_2O_3$ is also larger than that for Ni/$Al_2O_3$, with a metal content of 10 wt.% in each case, which may explain the better performance of the Ni catalyst. The authors suggested an effect of the acidity of the catalysts on the catalytic behavior, in addition to an increase in the amount of carbon deposited on the surface. In a study on the promotion of Ni/MgO with Sn, Ce, Mn, and Co, the authors reported a higher catalytic activity and stability for the catalysts promoted by Co. Furthermore, these catalysts also showed a high resistance to carbon deposition. The higher catalytic performance of Co-promoted catalysts is attributed to their high affinity for oxygen species, which improves their ability to resist carbon deposition. In contrast, Ce- and Mn-promoted catalysts exhibited a worse catalytic performance as a consequence of the presence of larger NiO particles. In the case of the Mn-promoted catalyst, this can be explained by the agglomeration of metallic particles and, in the case of its Ce counterpart, by the segregation of Ce as $CeO_2$, and its immiscibility with MgO.[214] Ni-Co catalysts in which a spinel was used as support exhibited high activity and tolerance to the presence of sulfur, with this behavior depending on the Ni/Co ratio and the temperature used for spinel synthesis.[215] Of the catalysts investigated, $Ni_{0.375}Co_{0.375}Mg_{0.25}Al_2O_4$, which was synthesized at 1500 $^oC$, was found to be the most active and stable. The authors of this study proposed that the high catalytic activity is due to the presence of a large number of highly coordinated active metal centers at the edges and corners of the spinel particles, whereas the high resistance was attributed to the high oxygen-storage capacity of the spinel and the high population of active centers on the support surface suitable for $CO_2$ activation.

The Co-Ni catalysts prepared by Tsoukalou et al.[216] by reducing the perovskite $LaNi_{0.8}Co_{0.2}O_3$ showed high catalytic performance and stability due to the formation of $La_2O_2CO_3$, which is able to oxidize the carbon species deposited on the active centers.

Chen et al.[217] investigated the role of Cu as a promoter for a Ni catalyst supported on $SiO_2$ and indicated that the addition of Cu can stabilize the structure of the active center and prevent the Ni catalyst from being deactivated due to loss of Ni crystallites or sintering. The incorporation of Cu into the Ni catalyst resulted in the formation of Cu-Ni species that can modify the catalytic activity. These Cu-Ni species are responsible for balancing the removal of coke formed upon cracking $CO_2$ and $CH_4$ and hindering the accumulation of carbon on the Ni particles. However, even when the Cu-Ni species are trapped by carbon accumulation, they can still favor the main step in DRM, that is, the cleavage of C-H bonds to form CHx species.

Sharifi et al.[218,219] reported the synthesis of Cu-Ni/$Al_2O_3$-$ZrO_2$ catalysts using various methods, including sol-gel and two-stage impregnation. When using the sol-gel method, these authors obtained small, uniform, and compact particles that improved the conversions of $CO_2$ and $CH_4$ in comparison with the Ni/$Al_2O_3$-$ZrO_2$ catalyst. The impregnation method did not lead to the same results, probably due to sintering of the Cu particles, which tend to aggregate at high temperatures.

Ni-Cu/MgAlO-based catalysts with a hydrotalcite-like structure were investigated by Song et al.,[220] who found a strong dependence of catalytic activity and resistance to coke deposition on the Cu/Ni ratio. These authors reported that the optimal Cu/Ni ratios correspond to the interval between 0.25 and 0.5, with excessive carbon deposition being observed for the other ratios studied. They concluded that the Cu atoms in the Cu-Ni alloy particles provide centers for $CO_2$ dissociation, such that the oxygen species produced gasify the carbon, thus suppressing its graphitization (see **Figure 15**).

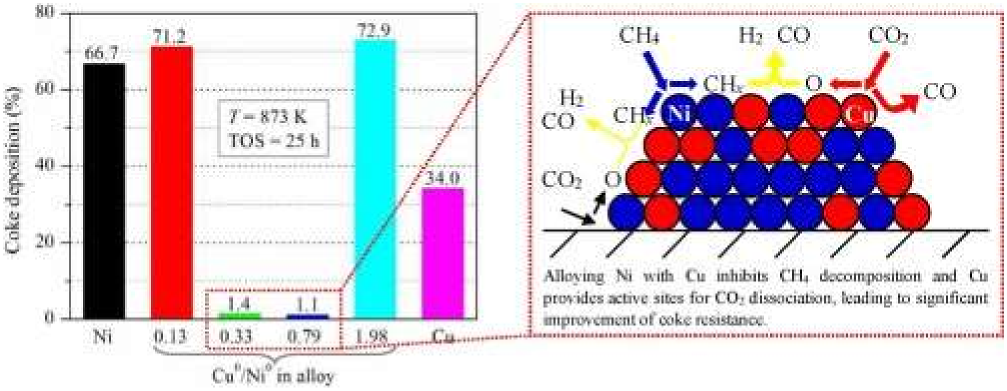

Alloying Ni with Cu inhibits $CH_4$ decomposition and Cu provides active sites for $CO_2$ dissociation, leading to significant improvement of coke resistance.

**Figure 15.** Optimal Cu/Ni ratio for Cu-Ni/MgAlO catalysts to minimize coke deposition (Reproduced with permission from[220]).

A Ni catalyst supported on $Al_2O_3$ and promoted by Sn was studied by Liu et al.,[221] who used two preparation methods, namely co-impregnation and a two-stage impregnation method. They observed that, after reduction, the Ni-Sn alloys formed changed the basic properties of Ni and increased the resistance to coke formation. Reina et al.[222,223] synthesized Sn-promoted Ni/$Al_2O_3$ and Ni/$Al_2O_3$-$CeO_2$ catalysts by subsequent impregnation using two Sn/Ni molar ratios: 0.02 and 0.04. The DRM reaction yield for the catalysts doped with small amounts of Sn was enhanced in terms of $CO_2$ and $CH_4$ conversions compared with monometallic catalysts. This enhancement was attributed to Sn atoms occupying carbon nucleation centers in the vicinity of Ni atoms, thus inhibiting coke-formation mechanisms. However, increasing the amount of Sn added to the Ni catalyst had a detrimental effect on the reaction yield. Seok et al.[224] and Quincoces et al.[225] used Ni/$Al_2O_3$ catalysts promoted by Mn and Mo and observed a higher resistance to carbon formation. They proposed that this was due to electronic effects of the Ni on the dissociation of carbon. Similarly, Theofanidis et al.[226,227] investigated the incorporation of Fe into Ni-based catalysts (Fe-Ni/$MgAl_2O_4$) and found that the active center is the Fe-Ni alloy, with Fe partially separating from the alloy to form FeOx during the DRM reaction. This process reduces carbon deposition on the surface, since the deposited coke will react with oxygen in the FeOx network and produce CO. Consequently, these Fe-Ni catalysts exhibited a high catalytic activity in the DRM reaction, as well as a high resistance to carbon deposition (see **Figure 16**). The active role of FeOx species in carbon removal was also reported by Song et al.[228] The research conducted by these authors showed that the structure of the $Ni_3Fe$ alloy facilitates the oxidation of metallic Fe to FeOx instead of the oxidation of Ni, thus favoring interaction of the FeOx species formed with the accumulated carbon and resulting in its gasification. Lima et al.[229] reported a similar catalytic behavior for $LaNi_xFe_{1-x}O_3$. Thus, the substitution of Ni by Fe enhanced the resistance to carbon formation, although with a tradeoff in terms of catalytic behavior, over 10 h at 650 °C. Recent studies using Fe-promoted Ni/MgO catalysts showed that the incorporation of Fe into the catalyst prevents carbon deposition and changes the nature of the carbon into a form that can be easily removed from the surface catalyst by $CO_2$ gasification.[230] These studies showed that both the decrease in the carbon deposition rate and the increase in the carbon gasification rate depend on the concentration of $CO_2$ in the gas stream, as well as on the Fe/(Fe + Ni) ratio. Kim et al.[231] used a $Mg_xAl_yO_z$ matrix derived from a hydrotalcite-like precursor as a catalytic support to obtain Fe-Ni/$Mg_xAl_yO_z$ catalysts. The optimized catalyst with a Ni/(Ni + Fe) ratio of 0.8 exhibited significantly higher activity and stability compared to the homologous monometallic Ni and Fe catalysts. These authors reached various conclusions: (i) deactivation of the monometallic Ni catalyst is due to the formation of graphitic carbon and whiskers; (ii) Fe is inactive in the DRM reaction, although it substantially improves the stability of Ni, the active metallic phase, in bimetallic formulations; (iii ) under the reaction conditions studied, the Fe in the Ni-Fe alloy particles is partially oxidized to FeOx, which leads to partial dealloying and therefore the formation of Ni-Fe richer in Ni-alloyed particles; (iv) Ni remains in the metallic state regardless of whether it is alloyed with Fe or not; and (v) the FeOx surface domains formed react with carbon deposits, thus reducing coke formation.

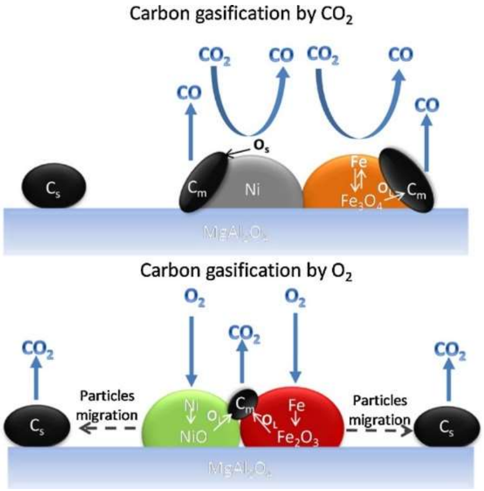

**Figure 16.** Proposed mechanisms of carbon gasification over Fe-Ni/$MgAl_2O_4$ (Reproduced with permission from[227]).

In addition to the incorporation of metals, some researchers have found that the addition of metal carbides to the catalyst improves the dispersion of the active metal, as well as the interaction between the active metal and the support. In that sense, Li et al.[232] discovered that the incorporation of molybdenum carbide increases Ni dispersion in a Ni-$ZrO_2$ catalyst. Their experimental results also showed that an appropriate amount of $Mo_2C$ loading results in a high surface content of Mo(II), which enhances the catalytic behavior, thus facilitating the DRM reaction. Along the same lines, Cheng and Huang[233] investigated the effect of incorporating Ni and Co into $Mo_2C$ catalysts and found a positive effect of the two metals on the $Mo_2C$ substrate that promoted the DRM reaction and enhanced stability. As a novel aspect, Zhang et al.[234] synthesized Ni-$Mo_2C$ catalysts using a method involving carburizing NiMoOx in the presence of $CH_4$ and $CO_2$, the reagents for the DRM reaction. These authors also reported a similar promoting effect on both activity and stability during the DRM reaction upon incorporating Ni into $Mo_2C$. Huang et al.[235] synthesized a series of SBA-15-supported bimetallic Mo-Ni catalysts by co-impregnation and observed that, although the bimetallic Mo-Ni catalysts showed a worse initial performance compared to the monometallic Ni catalyst, the former were more stable. They concluded that adjustment of the Mo/Ni atomic ratio allows the interaction between the metallic particle and the support, the metallic particle size and the basicity—all of which play a critical role in the catalytic activity—to be improved. Furthermore, the type and amount of carbon deposition, the resistance of the Ni particle to sintering, and the stability of the catalysts over time were also enhanced. In the case of Mo-Ni catalysts supported on $Al_2O_3$, Yao et al.[236] found a better catalytic performance in DRM compared to the monometallic Mo/$Al_2O_3$ catalyst but a worse performance than the monometallic Ni/$Al_2O_3$ catalyst. To explain the results, these authors considered a weaker interaction between the NiO species and the alumina support, a lower basicity, and the formation of a $MoNi_4$ phase in the bimetallic Mo-Ni/$Al_2O_3$ catalyst. They also observed that when the bimetallic catalyst was previously reduced at 700 $^oC$ instead of 900 $^oC$, its DRM performance was enhanced. This behavior was attributed to the formation of a separate phase, which does not interact with Mo, as well as to the basicity of the catalyst.

Mo-Ni metals as active catalytic phases supported on MgO and applied in the DRM reaction have been studied by Song et al.[237] In their study, these authors highlighted the urgent need for large-scale carbon fixation by recirculation of $CO_2$ and the economic importance of the DRM process for this purpose. The results obtained can be summarized as follows: (i) an absence of detectable coke deposits on the surfaces of the Mo-Ni particles even when operating under DRM conditions for more than 850 h, and (ii) stabilization during activation of the catalyst. The authors emphasized that their results open an industrially and economically viable path for carbon recovery, and propose a new approach to catalyst design, known as “Nanocatalysts on Single Crystal Edges” (NOSCE).

## 5. Challenges in the reaction systems

The characteristics of the DRM reaction have led researchers to focus mainly on developing highly active catalysts that are stable over time. However, other issues, such as irreversible deactivation, sintering of active metal phases, and carbon deposition complicate optimization of the catalyst formulation. As such, most efforts have focused on optimizing Ni-based catalysts as the active metal phase. However, a further line of research has focused on the DRM process to make the reaction conditions milder and favor the process at low temperatures. To that end, the DRM reaction assisted with plasma, light, and microwave activation has been studied.[238-250] These variants have significantly increased the efficiency of the DRM process, reduced catalyst deactivation to maximize pot life under mild reaction conditions, and could lead to commercialization of the DRM process.

Non-thermal plasma has been proposed, since it allows the thermodynamic limit to be exceeded in the DRM reaction, which is not possible with traditional thermal activation.[239]

The high-energy electrons generated in this type of reactor collide with the $CH_4$ and $CO_2$ molecules, thus causing non-selective bond cleavage and the formation of reactive ions and free radicals. Use of this technology reduces the reaction temperature markedly and deactivation of the active metal centers due to sintering [240]. Vaklili et al.[238] and Chung et al.[241] have applied this procedure with different types of catalysts. The studies conducted by these researchers indicate that the reaction conditions used for this technology are above the characteristics of the catalyst used. Catalysts with a perovskite-type structure, such as $NiTiO_3$, and low dielectric constant materials with a specific morphology and developed porous structure, such as MOF, seem more suitable for the plasma system due to their sensitivity to plasma. Kinetic studies and energy efficiency are the key aspects of this technique [242,247] (see **Figure 17**).

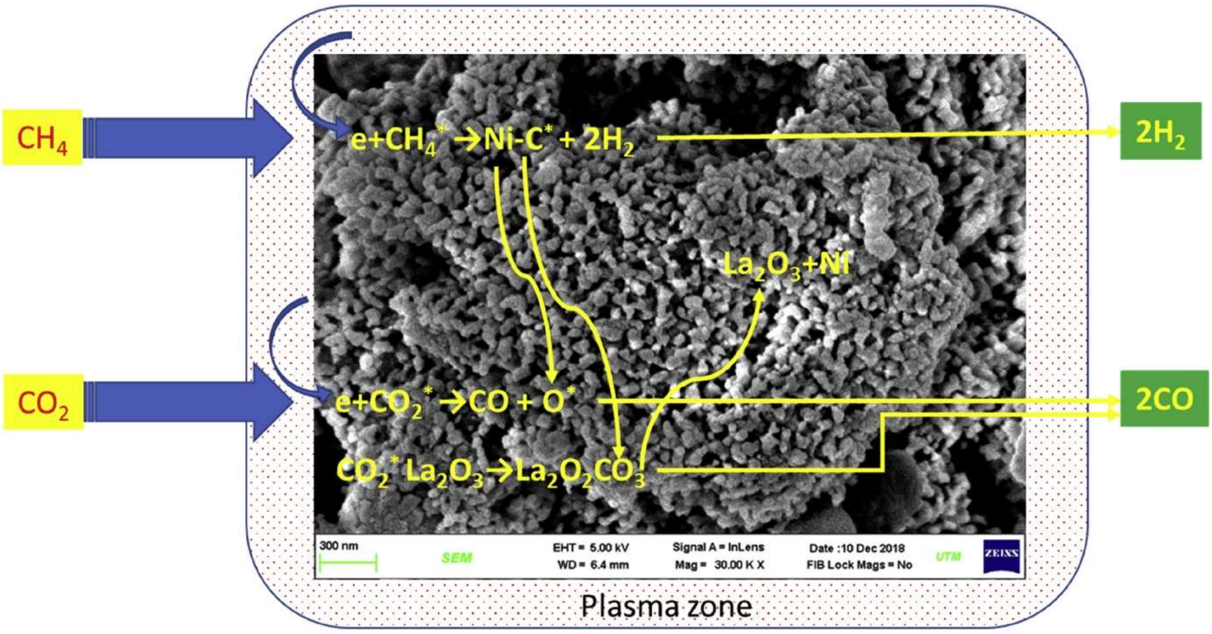

**Figure 17.** Proposed reaction mechanism for $La_2O_3$ co-supported $Ni/MgAl_2O_4$ plasma-catalyzed DRM (Reproduced with permission from[242]).

The photocatalytic DRM process could be a very interesting approach for the production of synthesis gas, since it could achieve a conversion higher than that predicted for the thermal system.[251] The studies carried out to date are preliminary and, in some cases, contradictory. Thus, for example, Cho et al.[252] proposed that photocatalytic supports should be sensitive to visible radiation and should be selected from metal oxides such as $ZnFe_2O_4$, $CaFe_2O_4$, and

$Cu_2O$. The same authors also proposed photocatalysts that are active under UV radiation. In both cases, the photoexcitation of pairs of electron holes promotes the DRM reaction in photoactive materials. In addition to gaining more information about the needs of the energy source, it will be necessary to reduce energy consumption and increase the efficiency of the process.

A more recent technology involves the use of microwaves in the DRM reaction. This technique has attracted attention due to the instantaneous nature of the heating, the decreased activation energy of the reagent molecules, and the increased catalytic stability due to the reduction of coke deposition.[248,249,251,252] Several researchers have indicated that the type of catalyst to be used in this process is also important, since this affects the heating mechanism, with such systems generally being based on carbonaceous materials.[248] The design of the reactor and control of the reaction variables are matters that have yet to be analyzed and clarified.

The chemical looping dry reforming of methane (CLDRM) is a new method of chemical looping combustion to perform DRM via the cyclic contact of catalysts and reagents[253] (see **Figure 18**). In this process, the active phase of the catalyst is reduced during the reaction and is subsequently reoxidized due to the presence of $CO_2$, thus regenerating the catalyst.[130,253-257] Various authors have indicated that the reaction occurring during the DRM and CLDRM processes is very similar in terms of the synthesis gas produced, with the same stoichiometric relationship. The difference between the two processes is that the main objective of CLDRM is to increase the yield of synthesis gas and optimize the activation of $CO_2$.[254] Moreover, RWGS and Boudouard reactions and carbon formation (see **Table 1**) are inhibited due to direct contact between $CH_4$, $CO_2$ and the catalyst. Some researchers have also reported that synthesis gas selectivity and production is higher in CLDRM as the RWGS reaction is inhibited because $H_2$ does not come into contact with $CO_2$, and carbon formation is suppressed as a result of oxidation in the regeneration cycle.[258] Ni catalysts have been used for CLDRM-type reactions. Thus, More et al.[259] have observed that Ni-Fe-type catalysts show good catalytic behavior and that, even with only small amounts of Ni, $CH_4$ activation is observed due to the cyclic reoxidation of Ni by $CO_2$.

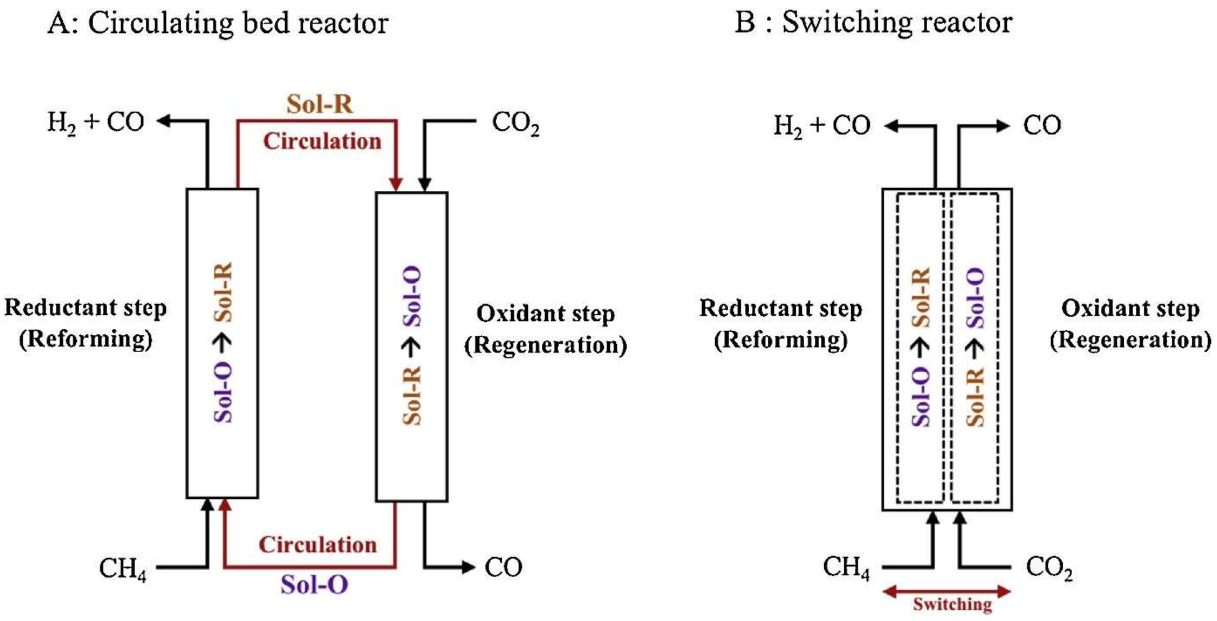

**Figure 18.** Schematic representation of the chemical looping dry reforming of methane (CLDRM) process using a circulating bed reactor (A) or switching feed reactor (B) (Reproduced with permission from[253]).

## Future perspectives and Conclusions

DRM is a promising and competitive pathway for converting two greenhouse gases ($CH_4$ and $CO_2$) into syngas for use as a valuable chemical feedstock, although this is not yet an industrially mature process. The studies conducted to date have allowed a good understanding of the reaction mechanism and the structure-activity relationship at an atomic level. As a result, it has been concluded that DRM is a reaction sensitive to the structure of the catalyst. The dehydrogenation of $CH_4$ and subsequent conversion of the carbonaceous species occurs at the active metal centers and coincides with the presence of $O_2$ on the surface of the catalyst and the dissociation of $CO_2$ at the basic centers. Given the endothermic character of the DRM reaction, research has focused on finding a suitable catalyst with superior activity, selectivity, and stability. This type of catalyst must necessarily have a high dispersion of the active metal phase and must be resistant to temperature and carbon deposition. The new materials and methods that have been incorporated into more traditional catalytic supports and preparation methods have significantly expanded the options for catalyst formulation.

In recent years, major efforts have also been made to improve traditional DRM, such as plasma, light, and microwave assistance instead of direct external heating, which allows the thermodynamic limitation to be overcome and lower reaction temperatures to be used. The combination of new catalysts with a more dispersed metallic phase and improved DRM systems seems to be the best option for optimizing and commercializing the process. Additionally, and in the search for a reactor that allows increased energy efficiency and separation of the final product, solar reactors and membrane reactors are promising options.

## Acknowledgements

The authors are grateful for financial support from the Spanish Ministry of Science and Innovation (MCIN/AEI/10.13039/501100011033) through project PID2020-112656RB-C21. JJTH thanks Universidad Pública de Navarra for a pre-doctoral grant. AG also thanks Santander Bank for funding via the Research Intensification Program.

## References

1. Z.Z. Noor, R.O. Yusuf, A.H. Abba, M.A.A. Hassan, M.F.M. Din, An overview for energy recovery from municipal solid wastes (MSW) in Malaysia scenario, Renew. Sustain. Energy Rev., 20, (2013), 378-384. https://doi.org/10.1016/j.rser.2012.11.050
2. V. Talyan, R.P. Dahiya, S. Anand, T.R. Sreekrishnan, Quantification of methane emission from municipal solid waste disposal in Delhi. Resour. Conserv. Recycl., 50, (2007), 240-259. https://doi.org/10.1016/j.resconrec.2006.06.002
3. D.J. Wuebbles, K. Hayhoe, Atmospheric methane and global change, Earth-Sci. Rev., 57, (2002), 177-210. http://dx.doi.org/10.1016/S0012-8252(01)00062-9.
4. O. Boucher, P. Friedlingstein, B. Collins, K.P. Shine, The indirect global warming potential and global temperature change potential due to methane oxidation, Environ. Res. Lett., 4, (2009), 044007.
5. R.O. Yusuf, Z.Z. Noor, A.H. Abba, M.A.A. Hassan, M.F.M. Din, Methane emission by sectors: a comprehensive review of emission sources and mitigation methods, Renew. Sustain. Energy Rev., 16, (2012), 5059-5070. http://dx.doi.org/ 10.1016/j.rser.2012.04.008
6. Agency, U.S.E.P., 2011. Inventory of U.S. Greenhouse Gas Emissions and Sinks: 1990
7. B. Raco, R. Battaglini, M. Lelli, Gas emission into the atmosphere from controlled landfills: an example from Legoli landfill (Tuscany, Italy), Environ. Sci. Pollut. Res., 17, (2010), 1197-1206. http://dx.doi.org/10.1007/s11356-010-0294-2
8. J.H. Lunsford, Catalytic conversion of methane to more useful chemicals and fuels: a challenge for the 21st century, Catal. Today, 63, (2000), 165-174. http://dx.doi.org/10.1016/S0920-5861(00)00456-9
9. C. Elvidge, D. Ziskin, K. Baugh, B. Tuttle, T. Ghosh, D. Pack, E. Erwin, M. Zhizhin, A fifteen year record of global natural gas flaring derived from satellite data, Energies, 2, (2009), 595-622. https://doi.org/10.3390/en20300595
10. N. Yang, R. Wang, Sustainable technologies for the reclamation of green- house gas $CO_2$, J. Clean. Prod., 103, (2015), 784-792. http://dx.doi.org/10.1016/j.jclepro.2014.10.025
11. F. Fayaz, H.T. Danh, C. Nguyen-Huy, K.B. Vu, B. Abdullah, D.-V.N. Vo, Pro- motional effect of Ce-dopant on $Al_2O_3$-supported Co catalysts for syngas pro- duction via $CO_2$ reforming of ethanol, Procedia Eng., 148, (2016), 646-653. http://dx.doi.org/10.1016/j.proeng.2016.06.530

12. M.B. Bahari, N.H.H. Phuc, B. Abdullah, F. Alenazey, D.-V.N. Vo, Ethanol dry reforming for syngas production over Ce-promoted Ni/$Al_2O_3$ catalyst, J. Environ. Chem. Eng., 4, (2016), 4830-4838. http://dx.doi.org/10.1016/j.jece.2016.01.038
13. I. Alirezaei, A. Hafizi, M.R. Rahimpour, S. Raeissi, Application of zirconium modified Cu-based oxygen carrier in chemical looping reforming, J. $CO_2$ Util. 14, (2016), 112-121. http://dx.doi.org/10.1016/j.jcou.2016.04.007
14. M.A. Peña, J.P. Gómez, J.L.G. Fierro, New catalytic routes for syngas and hydrogen production, Appl. Catal. A: General, 144, (1996), 7-57. http://dx.doi.org/ 10.1016/0926-860X(96)00108-1
15. Y.J.O. Asencios, E.M. Assaf, Combination of dry reforming and partial oxidation of methane on NiO-MgO-$ZrO_2$ catalyst: effect of nickel content, Fuel Process. Technol., 106, (2013), 247-252. http://dx.doi.org/10.1016/j.fuproc.2012.08.004
16. V. Palma, A. Ricca, E. Meloni, M. Martino, M. Miccio, P. Ciambelli, Experimental and numerical investigations on structured catalysts for methane steam reforming intensification, J. Clean. Prod., 111 (Part A), (2016), 217-230. http://dx.doi.org/ 10.1016/j.jclepro.2015.09.004
17. J. Fan, L. Zhu, P. Jiang, L. Li, H. Liu, Comparative exergy analysis of chemical looping combustion thermally coupled and conventional steam methane reforming for hydrogen production, J. Clean. Prod., 131, (2016), 247-258. http://dx.doi.org/10.1016/j.jclepro.2016.05.040
18. A.M. Ranjekar, G.D. Yadav, Steam reforming of methanol for hydrogen production: a critical analysis of catalysis, processes and scope, Ind. Eng. Chem. Res., 60, (2021), 89-113. https://doi.org/10.1021/acs.iecr.0c05041
19. A.D. Shejale, G.D. Yadav, Cu promoted Ni-Co/hydrotalcite catalyst for improved hydrogen production in comparison with several modifed Ni-based catalysts via steam reforming of ethanol, Int. J. Hydrogen Energy, 42, (2017), 11321-11332. https://doi.org/10.1016/j.ijhydene.2017.03.052
20. Y. Li, L. Zhang, Z. Zhang, Q. Liu, S. Zhang, Q. Liu, G. Hu, Y. Wang, X. Hu, Steam reforming of the alcohols with varied structures: Impacts of acidic sites of Ni catalysts on coking, Appl. Catal. A: General, 584, (2019), 117162. https://doi.org/10.1016/j.apcata.2019.117162

21. A.D. Shejale, G.D. Yadav, Noble metal promoted Ni-Cu/$La_2O_3$-MgO catalyst for renewable and enhanced hydrogen production via steam reforming of bio-based n-butanol: effect of promotion with Pt, Ru and Pd on catalytic activity and selectivity, Clean Technol. Environ. Policy, 21, (2019), 1323-1339. https://doi.org/10.1007/s10098-019-01708-X
22. A.D. Shejale, G.D. Yadav, Sustainable and selective hydrogen production by steam reforming of bio-based ethylene glycol: Design and development of Ni-Cu/mixed metal oxides using M ($CeO_2$, $La_2O_3$, $ZrO_2$)-MgO mixed oxides, Int. J. Hydrogen Energy, 46, (2021), 4808-4826. https://doi.org/10.1016/j.ijhydene.2019.11.031
23. A.D. Shejale, G.D. Yadav, Ni-Cu and Ni-Co supported on La-Mg based metal oxides prepared by coprecipitation and impregnation for superior hydrogen production via steam reforming of glycerol, Ind. Eng. Chem. Res., 57, (2018), 4785-4797. https://doi.org/10.1021/acs.iecr.7b05150
24. S.D. Davidson, H. Zhang, J. Sun, Y. Wang, Supported metal catalysts for alcohol/ sugar alcohol steam reforming, Dalton Trans., 43, (2014), 11782-11802. https://doi.org/10.1039/C4DT00521J
25. P. Gangadharan, K.C. Kanchi, H.H. Lou, Evaluation of the economic and environmental impact of combining dry reforming with steam reforming of methane, Chem. Eng. Res. Des., 90, (2012), 1956-1968. http://dx.doi.org/10.1016/j.cherd.2012.04.008
26. S.T. Oyama, P. Hacarlioglu, Y. Gu, D. Lee, Dry reforming of methane has no future for hydrogen production: comparison with steam reforming at high pressure in standard and membrane reactors, Int. J. Hydrog. Energy, 37, (2012), 10444-10450. http://dx.doi.org/10.1016/j.ijhydene.2011.09.149
27. M.A. Nieva, M.M. Villaverde, A. Monzón, T.F. Garetto, A.J. Marchi, Steam-methane reforming at low temperature on nickel-based catalysts, Chem. Eng. J., 235, (2014), 158-166. http://dx.doi.org/10.1016/j.cej.2013.09.030
28. L.S. Carvalho, A.R. Martins, P. Reyes, M. Oportus, A. Albonoz, V. Vicentini, M.d.C. Rangel, Preparation and characterization of Ru/MgO-$Al_2O_3$ catalysts for methane steam reforming, Catal. Today, 142, (2009), 52-60. http://dx.doi.org/10.1016/j.cattod.2009.01.010

29. A. S. Larimi, S.M. Alavi, Ceria-Zirconia supported Ni catalysts for partial oxidation of methane to synthesis gas, Fuel, 102, (2012), 366-371. http://dx.doi.org/10.1016/j.fuel.2012.06.050
30. E. Ruckenstein, Y.H. Hu, Methane partial oxidation over NiO/MgO solid solution catalysts, Appl. Catal. A: General, 183, (1999), 85-92. http://dx.doi.org/10.1016/S0926-860X(99)00047-2
31. K. Selvarajah, N.H.H. Phuc, B. Abdullah, F. Alenazey, D.-V.N. Vo, Syngas production from methane dry reforming over Ni/$Al_2O_3$ catalyst, Res. Chem. Intermed., 42, (2016), 269-288. http://dx.doi.org/10.1007/s11164-015-2395-5
32. D. San José-Alonso, J. Juan-Juan, M.J. Illán-Gómez, M.C. Román-Martínez, Ni, Co and bimetallic Ni-Co catalysts for the dry reforming of methane, Appl. Catal. A: General, 371, (2009), 54-59. http://dx.doi.org/10.1016/j.apcata.2009.09.026
33. T. Wurzel, S. Malcus, L. Mleczko, Reaction engineering investigations of $CO_2$ reforming in a fluidized-bed reactor, Chem. Eng. Sci., 55, (2000), 3955-3966. http://dx.doi.org/10.1016/S0009-2509(99)00444-3
34. J. Xu, W. Zhou, Z. Li, J. Wang, J. Ma, Biogas reforming for hydrogen production over nickel and cobalt bimetallic catalysts, Int. J. Hydrog. Energ., 34, (2009), 6646-6654. http://dx.doi.org/10.1016/j.ijhydene.2009.06.038
35. D. Fraenkel, R. Levitan, M. Levy, A solar thermochemical pipe based on the $CO_2$-$CH_4$ (1:1) system, Int. J. Hydrog. Energ., 11, (1986), 267-277. http://dx.doi.org/10.1016/0360-3199(86)90187-4
36. D. Li, Y. Nakagawa, K. Tomishige, Methane reforming to synthesis gas over Ni catalysts modified with noble metals, Appl. Catal. A-General, 408, (2011), 1-24. https://doi.org/10.1016/j.apcata.2011.09.018
37. M Usman, W.M.A. Wan Daud, H.F. Abbas, Dry reforming of methane: influence of process parameters-A review, Renew. Sustain. Energy Rev., 45, (2015), 710-744. https://doi.org/10.1016/j.rser.2015.02.026
38. Z. Bian, S. Das, M.H. Wai, P. Hongmanorom, S. Kawi, A review on bimetallic nickel-based catalysts for $CO_2$ reforming of methane, ChemPhysChem 18, (2017), 3117-3134. https://doi.org/10.1002/cphc.201700529

39. B. Abdullah, N.A. Abd Ghani, D.-V.N. Vo, Recent advances in dry reforming of methane over Ni-based catalysts, J. Clean. Prod., 162, (2017), 170-185. https://doi.org/10.1016/j.jclepro.2017.05.176
40. G. Zhang, J. Liu, Y. Xu, Y. Sun, A review of $CH_4$-$CO_2$ reforming to synthesis gas over Ni-based catalysts in recent years (2010-2017), Int. J. Hydrogen Energy, 43, (2018), 15030-15054. https://doi.org/10.1016/j.ijhydene.2018.06.091
41. N.A.K. Aramouni, J.G. Touma, B.A. Tarboush, J. Zeaiter, M.N. Ahmad, Catalyst design for dry reforming of methane: Analysis review, Renew. Sustain. Energy Rev., 82, (2018), 2570-2585. https://doi.org/10.1016/j.rser.2017.09.076
42. A. Abdulrasheed, A.A. Jalil, Y. Gambo, M. Ibrahim, H.U. Hambali, M.Y.S. Hamid, A review on catalyst development for dry reforming of methane to syngas: recent advances, Renew. Sustain. Energy Rev., 108, (2019), 175-193. https://doi.org/10.1016/j.rser.2019.03.054
43. A.M. Ranjekar, G.D. Yadav, Dry reforming of methane for syngas production: A review and assessment of catalyst development and efficacy, J. Indian Chem. Soc., 98, (2021), 100002. https://doi.org/10.1016/j.jics.2021.100002
44. C. Wang, Y. Wang, M. Chen, D. Liang, Z. Yang, W. Cheng, Z. Tang, J. Wang, H. Zhang, Recent advances during $CH_4$ dry reforming for syngas production: A mini review, Intern. J. Hydrogen Energy, 46, (2021), 5852-5874. https://doi.org/10.1016/j.ijhydene.2020.10.240
45. M.C.J. Bradford, M.A. Vannice, $CO_2$ reforming of $CH_4$. Catal. Rev. Sci. Eng., 41, (1999), 1-42. https://doi.org/10.1081/CR-100101948
46. P.M. Mortensen, Ib Dybkjær, Industrial scale experience on steam reforming of $CO_2$-rich gas, Appl. Catal. A: General, 495, (2015), 141-151. https://doi.org/10.1016/j.apcata.2015.02.022
47. J.-M. Lavoie, Review on dry reforming of methane, a potentially more environmentally-friendly approach to the increasing natural gas exploitation, Front. Chem. 2, (2014). http://dx.doi.org/10.3389/fchem.2014.00081
48. D. Liu, X.-Y. Quek, H.H.A. Wah, G. Zeng, Y. Li, Y. Yang, Carbon dioxide reforming of methane over nickel-grafted SBA-15 and MCM-41 catalysts, Catal. Today, 148, (2009), 243-250. http://dx.doi.org/10.1016/j.cattod.2009.08.014

49. S. Wang, G.Q. Lu, G.J. Millar, Carbon dioxide reforming of methane to produce synthesis gas over metal-supported catalysts: State of the art, Energy & Fuels, 10, (1996), 896-904. http://dx.doi.org/10.1021/ef950227t

50. A. J. Brungs, A.P.E. York, J.B. Claridge, C. Márquez-Alvarez, M.L.H. Green, Dry reforming of methane to synthesis gas over supported molybdenum carbide catalysts, Catal. Lett., 70, (2000), 117-122. https://doi.org/10.1023/A:1018829116093

51. M.K. Nikoo, N.A.S. Amin, Thermodynamic analysis of carbon dioxide reforming of methane in view of solid carbon formation, Fuel Process. Technol., 92, (2011), 678-691. http://dx.doi.org/10.1016/j.fuproc.2010.11.027

52. D. Pakhare, J. Spivey, A review of dry ($CO_2$) reforming of methane over noble metal catalysts, Chem. Soc. Rev., 43, (2014), 7813-7837. http://dx.doi.org/10.1039/C3CS60395D

53. J.R. Rostrup-Nielsen, Industrial relevance of coking, Catal. Today, 37, (1997), 225-232. http://dx.doi.org/10.1016/S0920-5861(97)00016-3

54. J.M. Ginsburg, J. Piñaa, T. El Solh, H.I. de Lasa, Coke Formation over a nickel catalyst under methane dry reforming conditions: thermodynamic and kinetic models, Ind. Eng. Chem. Res., 44, (2005), 4846-4854. http://dx.doi.org/10.1021/ie0496333

55. C.H. Bartholomew, Carbon deposition in steam reforming and methanation, Catal. Rev. Sci. Eng., 24, (1984), 67-112. https://doi.org/10.1080/03602458208079650

56. J. Sehested, Four challenges for nickel steam-reforming catalysts, Catal. Today, 111, (2006), 103-110. http://dx.doi.org/10.1016/j.cattod.2005.10.002

57. A.M. Gadalla, B. Bower, Carbon dioxide reforming of methane on nickel catalysts, Chem. Eng. Sci., 44, (1989), 2825-2829. https://doi.org/10.1016/0009-2509(89)85092-4

58. H.Y. Wang, A.C. Lua, Deactivation and kinetic studies of unsupported Ni and Ni-Co-Cu alloy catalysts used for hydrogen production by methane decomposition, Chem. Eng. J., 243, (2014), 79-91. http://dx.doi.org/10.1016/j.cej.2013.12.100

59. D.L. Hoang, S.H. Chan, O.L. Ding, Kinetic and modelling study of methane steam reforming over sulfide nickel catalyst on a gamma alumina support, Chem. Eng. J., 112, (2005), 1-11. http://dx.doi.org/10.1016/j.cej.2005.06.004

60. P.A.U. Aldana, F. Ocampo, K. Kobl, B. Louis, F. Thibault-Starzyk, M. Daturi, P. Bazin, S. Thomas, A.C. Roger, Catalytic $CO_2$ valorization into $CH_4$ on Ni-based ceria-zirconia.

Reaction mechanism by *operando* IR spectroscopy, Catal. Today, 215, (2013), 201-207. http://dx.doi.org/10.1016/j.cattod.2013.02.019

61. Q. Pan, J. Peng, T. Sun, S. Wang, S. Wang, Insight into the reaction route of $CO_2$ methanation: promotion effect of medium basic sites, Catal. Commun., 45, (2014), 74-78. http://dx.doi.org/10.1016/j.catcom.2013.10.034
62. S. Zhang, C. Shi, B. Chen, Y. Zhang, Y. Zhu, J. Qiu, C. Au, Catalytic role of $\beta$-$Mo_2C$ in DRM catalysts that contain Ni and Mo, Catal. Today, 258, (2015), 676-683. https://doi.org/10.1016/j.cattod.2015.01.014
63. X.Y. Li, D. Li, H. Tian, L. Zeng, Z.J. Zhao, J.L. Gong, Dry reforming of methane over Ni/$La_2O_3$ nanorod catalysts with stabilized Ni nanoparticles, Appl. Catal. B: Environmental, 202, (2017), 683-694. https://doi.org/10.1016/j.apcatb.2016.09.071
64. L. Qian, Z. Ma, Y. Ren, H. Shi, B. Yue, S. Feng, J. Shen, S. Xie, Investigation of La promotion mechanism on Ni/SBA-15 catalysts in $CH_4$ reforming with $CO_2$, Fuel, 122, (2014), 47-53. https://doi.org/10.1016/j.fuel.2013.12.062
65. B. Bachiller-Baeza, C. Mateos-Pedrero, M.A. Soria, A. Guerrero-Ruiz, U. Rodemerck, I. Rodríguez-Ramos, Transient studies of low-temperature dry reforming of methane over Ni-CaO/$ZrO_2$-$La_2O_3$, Appl. Catal. B: Environmenal, 129, (2013), 450-459. https://doi.org/10.1016/j.apcatb.2012.09.052
66. M. Steib, Y. Lou, A. Jentys, J.A. Lercher, Enhanced activity in methane dry reforming by carbon dioxide induced metal-oxide interface restructuring of nickel-zirconia, ChemCatChem, 9, (2017), 3809-3813. https://doi.org/10.1002/cctc.201700686
67. Y. Cao, M. Lu, J. Fang, L. Shi, D. Zhang, Hexagonal boron nitride supported meso$SiO_2$-confined Ni catalysts for dry reforming of methane, Chem. Commun., 53, (2017), 7549-7552. https://doi.org/10.1039/C7CC02007D
68. K. Nagaoka, K. Seshan, J. Lercher, K.-I. Aika, Activation mechanism of methane-derived coke (CHx) by $CO_2$ during dry reforming of methane e comparison for Pt/$Al_2O_3$ and Pt/$ZrO_2$, Catal. Lett., 70, (2000), 109-116. http://dx.doi.org/10.1023/A:1018877032022
69. Y. Kathiraser, U. Oemar, E.T. Saw, Z. Li, S. Kawi, Kinetic and mechanistic aspects for $CO_2$ reforming of methane over Ni based catalysts, Chem. Eng. J., 278, (2015), 62-78. http://dx.doi.org/10.1016/j.cej.2014.11.143
70. Y. Cui, H. Zhang, H. Xu, W. Li, Kinetic study of the catalytic reforming of $CH_4$ with $CO_2$ to syngas over Ni/$\alpha$-$Al_2O_3$ catalyst: the effect of temperature on the reforming mechanism,

Appl. Catal. A: General, 318, (2007), 79-88. http://dx.doi.org/10.1016/j.apcata.2006.10.044

71. E. Akpan, Y. Sun, P. Kumar, H. Ibrahim, A. Aboudheir, R. Idem, Kinetics, experimental and reactor modeling studies of the carbon dioxide reforming of methane (CDRM) over a new e catalyst in a packed bed tubular reactor, Chem. Eng. Sci., 62, (2007), 4012-4024. http://dx.doi.org/10.1016/j.ces.2007.04.044
72. X.E. Verykios, Catalytic dry reforming of natural gas for the production of chemicals and hydrogen, Intern. J. Hydrogen Energy, 28, (2003), 1045-1063. http://dx.doi.org/10.1016/S0360-3199(02)00215-X
73. Z. Zhang, X.E. Verykios, Carbon dioxide reforming of methane to synthesis gas over Ni/$La_2O_3$ catalysts, Appl. Catal. A: General, 138, (1996), 109-133. http://dx.doi.org/10.1016/0926-860X(95)00238-3
74. V.A. Tsipouriari, X.E. Verykios, Carbon and oxygen reaction pathways of $CO_2$ reforming of methane over Ni/$La_2O_3$ and Ni/$Al_2O_3$ catalysts studied by isotopic tracing techniques, J. Catal., 187, (1999), 85-94. http://dx.doi.org/10.1006/jcat.1999.2565
75. V.A. Tsipouriari, X.E. Verykios, Kinetic study of the catalytic reforming of methane with carbon dioxide to synthesis gas over Ni/$La_2O_3$ catalyst, Catal. Today, 64, (2001), 83-90. http://dx.doi.org/10.1016/S0920-5861(00)00511-3
76. M.M.B. Quiroga, A.E.C. Luna, Kinetic analysis of rate data for dry reforming of methane, Ind. Eng. Chem. Res., 46, (2007), 5265-5270. http://dx.doi.org/10.1021/ie061645w
77. A. Topalidis, D.E. Petrakis, A. Ladavos, L. Loukatzikou, P.J. Pomonis, A kinetic study of methane and carbon dioxide interconversion over 0.5%Pt/$SrTiO_3$ catalysts, Catal. Today, 127, (2007), 238-245. http://dx.doi.org/10.1016/j.cattod.2007.04.015
78. G. Xu, K. Shi, Y. Gao, H. Xu, Y. Wei, Studies of reforming natural gas with carbon dioxide to produce synthesis gas: X. The role of $CeO_2$ and MgO promoters, J. Mol. Catal. A: Chem., 147, (1999), 47-54. http://dx.doi.org/10.1016/S1381-1169(99)00127-2
79. J.F. Múnera, S. Irusta, L.M. Cornaglia, E.A. Lombardo, D. Vargas Cesar, M. Schmal, Kinetics and reaction pathway of the $CO_2$ reforming of methane on Rh supported on lanthanum-based solid, J. Catal., 245, (2007), 25-34. http://dx.doi.org/10.1016/j.jcat.2006.09.008

80. M.S. Fan, A.Z. Abdullah, S. Bhatia, Utilization of greenhouse gases through dry reforming: screening of nickel-based bimetallic catalysts and kinetic studies, ChemSusChem, 4, (2011), 1643-1653. http://dx.doi.org/10.1002/cssc.201100113

81. S.Y. Foo, C.K. Cheng, T.H. Nguyen, A.A. Adesina, Kinetic study of methane $CO_2$ reforming on Co-Ni/$Al_2O_3$ and Ce-Co-Ni/$Al_2O_3$ catalysts, Catal. Today, 164, (2011), 221-226. https://doi.org/10.1016/j.cattod.2010.10.092

82. C. Wang, N. Sun, M. Kang, X. Wen, N. Zhao, F. Xiao, W. Wei, T. Zhao, Y. Sun, The bifunctional mechanism of $CH_4$ dry reforming over a Ni-CaO-$ZrO_2$ catalyst: further evidence via the identification of the active sites and kinetic studies, Catal. Sci. Technol., 3, (2013), 2435-2443. https://doi.org/10.1039/C3CY00153A

83. J. Zhang, H. Wang, A.K. Dalai, Effects of metal content on activity and stability of Ni-Co bimetallic catalysts for $CO_2$ reforming of $CH_4$, Appl. Catal. A: General, 339, (2008), 121-129. http://dx.doi.org/10.1016/j.apcata.2008.01.027

84. F. Pompeo, N.N. Nichio, M.M.V.M. Souza, D.V. Cesar, O.A. Ferretti, M. Schmal, Study of Ni and Pt catalysts supported on α-$Al_2O_3$ and $ZrO_2$ applied in methane reforming with $CO_2$, Appl. Catal. A: General, 316, (2007), 175-183. http://dx.doi.org/10.1016/j.apcata.2006.09.007

85. X. Zhao, H. Li, J. Zhang, L. Shi, D. Zhang, Design and synthesis of NiCe@m-$SiO_2$ yolk-shell framework catalysts with improved coke- and sintering-resistance in dry reforming of methane, Int. J. Hydrogen Energy, 41, (2016), 2447-2456. http://dx.doi.org/10.1016/j.ijhydene.2015.10.111

86. J.-S. Chang, S.-E. Park, K.-W. Lee, M.J. Choi, Catalytic reforming of methane with carbon dioxide over pentasil zeolite-supported nickel catalyst, Stud. Surf. Sci. Catal, 84, (1994), 1587-1594. https://doi.org/10.1016/S0167-2991(08)63707-6

87. F. Menegazzo, M. Signoretto, F. Pinna, P. Canton, N. Pernicone, Optimization of bimetallic dry reforming catalysts by temperature programmed reaction, Appl. Catal. A: General, 439-440, (2012), 80-87. https://doi.org/10.1016/j.apcata.2012.06.041

88. A. Albarazi, M.E. Gálvez, P. Da Costa, Synthesis strategies of ceria-zirconia doped Ni/SBA-15 catalysts for methane dry reforming, Catal. Commun., 59, (2015), 108-112. https://doi.org/10.1016/j.catcom.2014.09.050

89. H.R. Gurav, S. Dama, V. Samuel, S. Chilukuri, Influence of preparation method on activity and stability of Ni catalysts supported on Gd doped ceria in dry reforming of methane, J. $CO_2$ Util., 20, (2017), 357-367. https://doi.org/10.1016/j.jcou.2017.06.014

90. J. Niu, X. Du, J. Ran, R. Wang, Dry ($CO_2$) reforming of methane over Pt catalysts studied by DFT and kinetic modeling, Appl. Surf. Sci., 376, (2016), 79-90. http://dx.doi.org/10.1016/j.apsusc.2016.01.212

91. J. Kehres, J.G. Jakobsen, J.W. Andreasen, J.B. Wagner, H. Liu, A. Molenbroek, J. Sehested, I. Chorkendoff, T. Vegge, Dynamical properties of a Ru/$MgAl_2O_4$ catalyst during reduction and dry methane reforming, J. Phys. Chem. C, 116, (2012), 21407-21415. http://dx.doi.org/10.1021/jp3069656

92. M.M. Nair, S. Kaliaguine, Structured catalysts for dry reforming of methane, New J. Chem., 40, (2016), 4049-4060. http://dx.doi.org/10.1039/C5NJ03268G

93. M.A. Goula, N.D. Charisiou, K.N. Papageridis, A. Delimitis, E. Pachatouridou, E.F. Iliopoulou, Nickel on alumina catalysts for the production of hydrogen rich miXtures via the biogas dry reforming reaction: influence of the synthesis method, Int. J. Hydrogen Energy, 40, (2015), 9183-9200. https://doi.org/10.1016/j.ijhydene.2015.05.129

94. S.J.H. Rad, M. Haghighi, A.A. Eslami, F. Rahmani, N. Rahemi, Sol-gel vs. impregnation preparation of MgO and $CeO_2$ doped Ni/$Al_2O_3$ nanocatalysts used in dry reforming of methane: effect of process conditions, synthesis method and support composition, Int. J. Hydrogen Energy, 41, (2016), 5335-5350. http://dx.doi.org/10.1016/j.ijhydene.2016.02.002

95. Q. Zhang, J. Wang, P. Ning, T. Zhang, M. Wang, K. Long, J. Huang, Dry reforming of methane over Ni/SBA-15 catalysts prepared by homogeneous precipitation method, Korean J. Chem. Eng., 34, (2017), 2823-2831. http://dx.doi.org/10.1007/s11814-017-0182-2

96. Z. Hao, Q. Zhu, Z. Jiang, B. Hou, H. Li, Characterization of aerogel Ni/$Al_2O_3$ catalysts and investigation on their stability for $CH_4$-$CO_2$ reforming in a fluidized bed, Fuel Process. Technol., 90, (2009), 113-121. https://doi.org/10.1016/j.fuproc.2008.08.004

97. Z. Shang, S. Li, L. Li, G. Liu, X. Liang, Highly active and stable alumina supported nickel nanoparticle catalysts for dry reforming of methane, Appl. Catal. B: Environmental, 201, (2017), 302-309. https://doi.org/10.1016/j.apcatb.2016.08.019

98. L. Yao, Y. Wang, J. Shi, H. Xu, W. Shen, C. Hu, The influence of reduction temperature on the performance of ZrOx/Ni-MnOx/$SiO_2$ catalyst for low-temperature $CO_2$ reforming of methane, Catal. Today, 281, (2017), 259-267. https://doi.org/10.1016/j.cattod.2016.05.031

99. M.S. Aw, M. Zorko, P. Djinovic´, A. Pintar, Insights into durable NiCo catalysts on β-SiC/$CeZrO_2$ and γ-$Al_2O_3$/$CeZrO_2$ advanced supports prepared from facile methods for $CH_4$-$CO_2$ dry reforming, Appl. Catal. B: Environmental, 164, (2015), 100-112. https://doi.org/10.1016/j.apcatb.2014.09.012

100. I. Luisetto, S. Tuti, C. Battocchio, S. Lo Mastro, A. Sodo, Ni/$CeO_2$-$Al_2O_3$ catalysts for the dry reforming of methane: the effect of $CeAlO_3$ content and nickel crystallite size on catalytic activity and coke resistance, Appl. Catal. A: General, 500, (2015), 12-22. https://doi.org/10.1016/j.apcata.2015.05.004

101. J. Chen, Q. Wu, J. Zhang, J. Zhang, Effect of preparation methods on structure and performance of Ni/$Ce_{0.75}Zr_{0.25}O_2$ catalysts for $CH_4$-$CO_2$ reforming, Fuel, 87, (2008), 2901-2907. https://doi.org/10.1016/j.fuel.2008.04.015

102. N. Rahemi, M. Haghighi, A.A. Babaluo, M.F. Jafari, P. Estifaee, Synthesis and physicochemical characterizations of Ni/$Al_2O_3$-$ZrO_2$ nanocatalyst prepared *via* impregnation method and treated with non-thermal plasma for $CO_2$ reforming of $CH_4$, J. Ind. Eng. Chem., 19, (2013), 1566-1576. https://doi.org/10.1016/j.jiec.2013.01.024

103. T. Odedairo, J. Chen, Z. Zhu, Metal-support interface of a novel Ni-$CeO_2$ catalyst for dry reforming of methane, Catal. Commun. 31, (2013), 25-31. https://doi.org/10.1016/j.catcom.2012.11.008

104. H.O. Seo, J.K. Sim, K.-D. Kim, Y.D. Kim, D.C. Lim, S.H. Kim, Carbon dioxide reforming of methane to synthesis gas over a $TiO_2$-Ni inverse catalyst, Appl. Catal. A: General, 451, (2013), 43-49. https://doi.org/10.1016/j.apcata.2012.10.037

105. X. Chen, K. Honda, Z.-G. Zhang, A comprehensive comparison of $CH_4$-$CO_2$ reforming activities of NiO/$Al_2O_3$ catalysts under fixed- and fluidized-bed operations, Appl. Catal. A: General, 288, (2005), 86-97. https://doi.org/10.1016/j.apcata.2005.04.037

106. K.-M. Kang, H.-W. Kim, I.-W. Shim, H.-Y. Kwak, Catalytic test of supported Ni catalysts with core/shell structure for dry reforming of methane, Fuel Process. Technol., 92, (2011), 1236-1243. https://doi.org/10.1016/j.fuproc.2011.02.007

107. J. Liu, S.Z. Qiao, J.S. Chen, X.W. Lou, X. Xing, G.Q. Lu, Yolk/shell nanoparticles: new platforms for nanoreactors, drug delivery and lithium-ion batteries, Chem. Commun., 47, (2011), 12578-12591. https://doi.org/10.1039/C1CC13658E

108. Y. Lu, D. Guo, Y. Ruan, Y. Zhao, S. Wang, X. Ma, Facile one-pot synthesis of Ni@HSS as a novel yolk-shell structure catalyst for dry reforming of methane, J $CO_2$ Util., 24, (2018), 190-199. https://doi.org/10.1016/j.jcou.2018.01.003

109. Z. Li, B. Jiang, Z. Wang, S. Kawi, High carbon resistant Ni@Ni phyllosilicate@$SiO_2$ core shell hollow sphere catalysts for low temperature $CH_4$ dry reforming, J. $CO_2$ Util., 27, (2018), 238-246. https://doi.org/10.1016/j.jcou.2018.07.017

110. W. Liu, L. Li, X. Zhang, Z. Wang, X. Wang, H. Peng, Design of Ni-$ZrO_2$@$SiO_2$ catalyst with ultra-high sintering and coking resistance for dry reforming of methane to prepare syngas, J. $CO_2$ Util. 27, (2018), 297-307. https://doi.org/10.1016/j.jcou.2018.08.003

111. G. Gunduz Meric, H. Arbag, L. Degirmenci, Coke minimization via SiC formation in dry reforming of methane conducted in the presence of Ni-based core-shell microsphere catalysts, Int. J. Hydrogen Energy, 42, (2017), 16579-16588. https://doi.org/10.1016/j.ijhydene.2017.05.121

112. K. Jabbour, P. Massiani, A. Davidson, S. Casale, N. El Hassan, Ordered mesoporous "one-pot" synthesized Ni-Mg(Ca)-$Al_2O_3$ as effective and remarkably stable catalysts for combined steam and dry reforming of methane (CSDRM), Appl. Catal. B: Environmental, 201, (2017), 527-542. https://doi.org/10.1016/j.apcatb.2016.08.009

113. S. Das, J. Ashok, Z. Bian, N. Dewangan, M.H. Wai, Y. Du, A. Borgna, K. Hidajat, S. Kawi, Silica-ceria sandwiched Ni core-shell catalyst for low temperature dry reforming of biogas: coke resistance and mechanistic insights, Appl. Catal. B: Environmental, 230, (2018), 220-236. https://doi.org/10.1016/j.apcatb.2018.02.041

114. M. Wang, Q. Zhang, T. Zhang, Y. Wang, J. Wang, K. Long, Z. Song, X. Liu, P. Ning, Facile one-pot synthesis of highly dispersed Ni nanoparticles embedded in HMS for dry reforming of methane, Chem. Eng. J., 313, (2017), 1370-1381. https://doi.org/10.1016/j.cej.2016.11.055

115. N.H. Elsayed, N.R.M. Roberts, B. Joseph, J.N. Kuhn, Low temperature dry reforming of methane over Pt-Ni-Mg/ceria-zirconia catalysts, Appl. Catal. B: Environmental, 179, (2015), 213-219. https://doi.org/10.1016/j.apcatb.2015.05.021

116. K. Jabbour, N. El Hassan, A. Davidson, S. Casale, P. Massiani, Factors affecting the long-term stability of mesoporous nickel-based catalysts in combined steam and dry reforming of methane, Catal. Sci. Technol., 6, (2016), 4616-4631. https://doi.org/10.1039/C6CY00032K
117. M.A. Goula, N.D. Charisiou, G. Siakavelas, L. Tzounis, I. Tsiaoussis, P. Panagiotopoulou, G. Goula, I.V. Yentekakis, Syngas production via the biogas dry reforming reaction over Ni supported on zirconia modified with $CeO_2$ or $La_2O_3$ catalysts, Int. J. Hydrogen Energy, 42, (2017), 13724-13740. https://doi.org/10.1016/j.ijhydene.2016.11.196
118. L.P. Teh, H.D. Setiabudi, S.N. Timmiati, M.A.A. Aziz, N.H.R. Annuar, N.N. Ruslan, Recent progress in ceria-based catalysts for the dry reforming of methane: A review, Chem. Eng. Sci., 239, (2021), 116606. https://doi.org/10.1016/j.ces.2021.116606
119. S. Sokolov, E.V. Kondratenko, M.-M. Pohl, A. Barkschat, U. Rodemerck, Stable low-temperature dry reforming of methane over mesoporous $La_2O_3$-$ZrO_2$ supported Ni catalyst, Appl. Catal. B: Environmental, 113-114, (2012), 19-30. http://dx.doi.org/10.1016/j.apcatb.2011.09.035
120. J.W. Han, J.S. Park, M.S. Choi, H. Lee, Uncoupling the size and support effects of Ni catalysts for dry reforming of methane, Appl. Catal. B: Environmental, 203, (2017), 625-632. https://doi.org/10.1016/j.apcatb.2016.10.069
121. R. Zhang, G. Xia, M. Li, Y. Wu, H. Nie, D. Li, Effect of support on the performance of Ni-based catalyst in methane dry reforming, J. Fuel Chem. Technol., 43, (2015), 1359-1365. https://doi.org/10.1016/S1872-5813(15)30040-2
122. S.S. Kim, S.M. Lee, J.M. Won, H.J. Yang, S.C. Hong, Effect of Ce/Ti ratio on the catalytic activity and stability of Ni/$CeO_2$-$TiO_2$ catalyst for dry reforming of methane, Chem. Eng. J., 280, (2015), 433-440. https://doi.org/10.1016/j.cej.2015.06.027
123. M. Usman, W.M.A.W. Daud, An investigation on the influence of catalyst composition, calcination and reduction temperatures on Ni/MgO catalyst for dry reforming of methane, RSC Adv. 6, (2016), 91603-91616. https://doi.org/10.1039/C6RA15256B
124. R. Zanganeh, M. Rezaei, A. Zamaniyan, Dry reforming of methane to synthesis gas on NiO-MgO nanocrystalline solid solution catalysts, Int J Hydrogen Energy, 38, (2013), 3012-3018. https://doi.org/10.1016/j.ijhydene.2012.12.089

125. J. Guo, H. Lou, H. Zhao, D. Chai, X. Zheng, Dry reforming of methane over nickel catalysts supported on magnesium aluminate spinels, Appl. Catal. A: General, 273, (2004), 75-82. http://dx.doi.org/10.1016/j.apcata.2004.06.014
126. X. Zhang, Q. Zhang, N. Tsubaki, Y. Tan, Y. Han, Carbon dioxide reforming of methane over Ni nanoparticles incorporated into mesoporous amorphous $ZrO_2$ matrix, Fuel, 147, (20159, 243-252. http://dx.doi.org/10.1016/j.fuel.2015.01.076
127. W. Tao, H. Cheng, W. Yao, X. Lu, Q. Zhu, G. Li, Z. Zhou, Syngas production by $CO_2$ reforming of coke oven gas over Ni/$La_2O_3$-$ZrO_2$ catalysts, Int J Hydrogen Energy, 39, (2014), 18650-18658. https://doi.org/10.1016/j.ijhydene.2014.02.029
128. D. Dong, X. Shao, Z. Wang, C. Lievens, J. Yao, H. Wang, C.-Z. Li, Fibrous NiO/$CeO_2$ nanocatalysts for the partial oxidation of methane at microsecond contact times, RSC Adv. 3, (2013), 1341-1345. https://doi.org/10.1039/C2RA21229C
129. Z. Wang, X. Shao, A. Larcher, K. Xie, D. Dong, C.-Z. Li, A study on carbon formation over fibrous NiO/$CeO_2$ nanocatalysts during dry reforming of methane, Catal. Today, 216, (2013), 44-49. https://doi.org/10.1016/j.cattod.2013.05.023
130. A. Löfberg, J. Guerrero-Caballero, T. Kane, A. Rubbens, L. Jalowiecki-Duhamel, Ni/$CeO_2$ based catalysts as oxygen vectors for the chemical looping dry reforming of methane for syngas production, Appl. Catal. B: Environmental, 212, (2017), 159-174. https://doi.org/10.1016/j.apcatb.2017.04.048
131. M.M. Makri, M.A. Vasiliades, K.C. Petallidou, Effect of support composition on the origin and reactivity of carbon formed during dry reforming of methane over 5 wt% Ni/$Ce_{1-x}M_xO_{2-\delta}$ (M = $Zr^{4+}$, $Pr^{3+}$) catalysts, Catal. Today, 259, (2016), 150-164. https://doi.org/10.1016/j.cattod.2015.06.010
132. L. Xu, H. Song, L. Chou, Carbon dioxide reforming of methane over ordered mesoporous NiO-MgO-$Al_2O_3$ composite oxides, Appl. Catal. B: Environmental, 108-109, (2011), 177-190. http://dx.doi.org/10.1016/j.apcatb.2011.08.028
133. H. Drobná, M. Kout, A. Soltysek, V.M. González-Delacruz, A. Caballero, L. Capek, Analysis of Ni species formed on zeolites, mesoporous silica and alumina supports and their catalytic behavior in the dry reforming of methane, React. Kinet. Mech. Catal., 121, (2017), 255-274. https://doi.org/10.1007/s11144-017-1149-3

134. S.M. Sidik, A.A. Jalil, S. Triwahyono, T.A.T. Abdullah, A. Ripin, $CO_2$ reforming of $CH_4$ over Ni/mesostructured silica nanoparticles (Ni/MSN), RSC Adv., 5, (2015), 37405-37414. https://doi.org/10.1039/c5ra04320d
135. W. Donphai, K. Faungnawakij, M. Chareonpanich, J. Limtrakul, Effect of Ni-CNTs/mesocellular silica composite catalysts on carbon dioxide reforming of methane, Appl. Catal. A: General, 475, (2014), 16-26. https://doi.org/10.1016/j.apcata.2014.01.014
136. M. Akri, T. Chafik, P. Granger, P. Ayrault, C. Batiot-Dupeyrat, Novel nickel promoted illite clay based catalyst for autothermal dry reforming of methane, Fuel, 178, (2016), 139-147. https://doi.org/10.1016/j.fuel.2016.03.018
137. H. Liu, L. Yao, H.B. Hadj Taief, M. Benzina, P. Da Costa, M.E. Gálvez, Natural clay-based Ni-catalysts for dry reforming of methane at moderate temperatures, Catal. Today, 306, (2018), 51-57. https://doi.org/10.1016/j.cattod.2016.12.017
138. H.G. Liu, H.B. Hadjltaiel, M. Benzina, M.E. Galvez, P. Da Costa, Natural clay based nickel catalysts for dry reforming of methane: on the effect of support promotion (La, al, Mn), Int. J. Hydrogen Energy, 44, (2019), 246-255. https://doi.org/10.1016/j.ijhydene.2018.03.004
139. Y. Chen, T.H. Chen, H.B. Liu, P. Zhang, C. Wang, S.W. Dong, D. Chen, J. Xie, X. Zou, S.L. Suib, C. Li, High catalytic performance of the Al-promoted Ni/Palygorskite catalysts for dry reforming of methane, Appl. Clay Sci., 188, (2020), 105498. https://doi.org/10.1016/j.clay.2020.105498
140. X. Lin, R. Li, M. Lu, C. Chen, D. Li, Y. Zhan, L. Jiang, Carbon dioxide reforming of methane over Ni catalysts prepared from Ni-Mg-Al layered double hydroxides: Influence of Ni loadings, Fuel, 162, (2015), 271-280. https://doi.org/10.1016/j.fuel.2015.09.021
141. X.D. Feng, J. Feng, W.Y. Li, $CO_2$ reforming of $CH_4$ over a highly active and stable Ni- Mg-Al catalyst, Int. J. Hydrogen Energy, 42, (2017), 3036-3042. https://doi.org/10.1016/j.ijhydene.2016.09.205
142. R. García, G. Soto, N. Escalona, C. Sepúlveda, M.J. Orellana, N. Morales, L.R. Radovic, R. Buitrago-Sierra, F. Rodriguez-Reinoso, A. Sepúlveda-Escribano, Methane dry reforming over Ni supported on pine sawdust activated carbon: effects of support surface properties and metal loading, Quim. Nova, 38, (2015), 506-509. https://doi.org/10.5935/0100-4042.20150058

143. I. Izhab, N.A.S. Amin, M. Asmadi, Dry reforming of methane over oil palm shell activated carbon and ZSM-5 supported cobalt catalysts, Int. J. Green Energy, 14, (2017), 831-838. https://doi.org/10.1080/15435075.2017.1334659

144. F. Martinez-Ortega, C. Batiot-Dupeyrat, G. Valderrama, J.M. Tatibouët, Methane catalytic combustion on La-based perovskite catalysts, Comptes Rendus de l'Académie des Sciences - Series IIC - Chemistry, 4, (2001), 49-55. https://doi.org/10.1016/S1387-1609(00)01202-0

145. C. Batiot-Dupeyrat, G. Valderrama, A. Meneses, F. Martinez, J. Barrault, J.M. Tatibouët, Pulse study of $CO_2$ reforming of methane over $LaNiO_3$, Appl. Catal. A: General, 248, (2003), 143-151. https://doi.org/10.1016/S0926-860X(03)00155-8

146. C. Batiot-Dupeyrat, G.A.S. Gallego, F. Mondragon, J. Barrault, J.M. Tatibouët, $CO_2$ reforming of methane over $LaNiO_3$ as precursor material, Catal. Today, 107-108, (2005), 474-480. https://doi.org/10.1016/j.cattod.2005.07.014

147. T. Odedairo, J. Ma, J. Chen, Z. Zhu, Cr-doped La-Ni-O catalysts derived from perovskite precursors for $CH_4$-$CO_2$ reforming under microwave irradiation, Chem. Eng. Technol., 39, (2016), 1551-1560. https://doi.org/10.1002/ceat.201500702

148. G. Valderrama, A. Kiennemann, M.R. Goldwasser, Dry reforming of $CH_4$ over solid solutions of $LaNi_{1-X}Co_XO_3$, Catal. Today, 133-135, (2008), 142-148. https://doi.org/10.1016/j.cattod.2007.12.069

149. G. Valderrama, A. Kiennemann, M.R. Goldwasser, La-Sr-Ni-Co-O based perovskite-type solid solutions as catalyst precursors in the $CO_2$ reforming of methane, J. Power Sources, 195, (2010), 1765-1771. https://doi.org/10.1016/j.jpowsour.2009.10.004

150. G. Valderrama, C. Urbina De Navarro, M.R. Goldwasser, $CO_2$ reforming of $CH_4$ over Co-La-based perovskite-type catalyst precursors, J. Power Sources, 234, (2013), 31-37. https://doi.org/10.1016/j.jpowsour.2013.01.142

151. S.M. Lima, J.M. Assaf, M.A. Peña, J.L.G. Fierro, Structural features of $La_{1-X}Ce_XNiO_3$ miXed oxides and performance for the dry reforming of methane, Appl. Catal. A: General, 311, (2006), 94-104. https://doi.org/10.1016/j.apcata.2006.06.010

152. H.Y. Wang, E. Ruckenstein, Carbon dioxide reforming of methane to synthesis gas over supported rhodium catalysts: the effect of support, Appl. Catal. A: General, 204, (2000), 143-152. https://doi.org/10.1016/S0926-860X(00)00547-0

153. E. Ruckenstein, Y.H. Hu, Carbon dioxide reforming of methane over nickel/alkaline earth metal oxide catalysts, Appl. Catal. A: General, 133, (1995), 149-161. https://doi.org/10.1016/0926-860X(95)00201-4

154. E. Ruckenstein, Y.H. Hu, Role of support in $CO_2$ reforming of $CH_4$ to syngas over Ni catalysts, J. Catal., 162, (1996), 230-238. https://doi.org/10.1006/jcat.1996.0280

155. Y.H. Hu, E. Ruckenstein, The characterization of a highly effective NiO/MgO solid solution catalyst in the $CO_2$ reforming of $CH_4$, Catal. Lett., 43, (1997), 71-77. https://doi.org/10.1023/A:1018982304573

156. E. Ruckenstein, Y.H. Hu, The effect of precursor and preparation conditions of MgO on the $CO_2$ reforming of $CH_4$ over NiO/MgO catalysts, Appl. Catal. A: General, 154, (1997), 185-205. https://doi.org/10.1016/S0926-860X(96)00372-9

157. E. Ruckenstein, Y.H. Hu, Role of lattice oxygen during $CO_2$ reforming of methane over NiO/MgO solid solutions, Catal. Lett., 51, (1998), 183-185. https://doi.org/10.1023/A:1019030311127

158. Y.H. Hu, E. Ruckenstein, Binary MgO-based solid solution catalysts for methane conversion to syngas, Catal. Rev.-Sci. Eng., 44, (2002), 423-453. https://doi.org/10.1081/CR-120005742

159. N. Sahli, C. Petit, A.C. Roger, A. Kiennemann, S. Libs, M.M. Bettahar, Ni catalysts from $NiAl_2O_4$ spinel for $CO_2$ reforming of methane, Catal. Today, 113, (2006), 187-193. https://doi.org/10.1016/j.cattod.2005.11.065

160. Y. Beltrán, C. Fernández, G. Pecchi, R. Jiménez, Dry reforming of methane on grafted-supported Rh catalysts: Effect of the metal-support interaction on the reaction rate, React. Kinet. Mech. Catal., 120, (2017), 459-475. https://doi.org/10.1007/s11144-016-1110-X

161. K. Li, C. Pei, X. Li, S. Chen, X. Zhang, R. Liu, J. Gong, Dry reforming of methane over $La_2O_2CO_3$-modified $Ni/Al_2O_3$ catalysts with moderate metal support interaction, Appl. Catal. B: Environmental, 264, (2020), 118448. https://doi.org/10.1016/j.apcatb.2019.118448

162. P.K. Chaudhary, N. Koshta, G. Deo, Effect of $O_2$ and temperature on the catalytic performance of $Ni/Al_2O_3$ and $Ni/MgAl_2O_4$ for the dry reforming of methane (DRM), Int. J. Hydrogen Energy, 45, (2020), 4490-4500. https://doi.org/10.1016/j.ijhydene.2019.12.053

163. A. Valentini, E.R. Leite, R.F. Gonçalvez, L.E.B. Soledade, Y. Maniette, E. Longo, D. Probst, Improved activity and stability of Ce-Promoted Ni/γ-$Al_2O_3$ catalysts for carbon dioxide reforming of methane, Lat. Am. Appl. Res., 34, (2004), 165-172.

164. J.A.C Dias, J.M. Assaf, Influence of calcium content in Ni/CaO/γ-$Al_2O_3$ catalysts for $CO_2$-reforming of methane, Catal. Today, 85, (2003), 59-68. http://dx.doi.org/10.1016/S0920-5861(03)00194-9

165. R. Lanza, J.A. Velasco, S.G. Järas, Recent developments and achievements in partial oxidation of methane with and without addition of stream, in: Catalysis; Spivey, J.J., Dooley, K.M., Eds, The Royal Society of Chemistry: Cambridge, 2011, Col. 23, pp.50-95.

166. V.R. Choudhary, B.S. Uphade, A.S. Mamman, Large enhancement in methane-to- syngas conversion activity of supported Ni catalysts due to precoating of catalyst supports with MgO, CaO or rare-earth oxide, Catal. Lett., 32, (1995), 387-390. https://doi.org/10.1007/BF00813233

167. V.R. Choudhary, A.M. Rajput, Simultaneous carbon dioxide and steam reforming of methane to syngas over NiO-CaO catalyst, Ind. Eng. Chem. Res., 35, (1996), 3934-3939. https://doi.org/10.1021/ie960002l

168. Z. Alipour, M. Rezaei, F. Meshkani, Effect of alkaline earth promoters (MgO, CaO, and BaO) on the activity and coke formation of Ni catalysts supported on nanocrystalline $Al_2O_3$ in dry reforming of methane, J. Ind. Eng. Chem., 20, (2014), 2858-2863. https://doi.org/10.1016/j.jiec.2013.11.018

169. A.E. Castro Luna, M.E. Iriarte, Carbon dioxide reforming of methane over a metal modified Ni-$Al_2O_3$ catalyst, Appl. Catal. A: General, 343, (2008), 10-15. http://dx.doi.org/10.1016/j.apcata.2007.11.041

170. B.M. Nagaraja, D.A. Bulushev, S. Beloshapkin, J.R. Ross, The effect of potassium on the activity and stability of Ni-MgO-$ZrO_2$ catalysts for the dry reforming of methane to give synthesis gas, Catal. Today, 178, (2011), 132-136. https://doi.org/10.1016/j.cattod.2011.08.040

171. H. Jeong, K.I. Kim, D. Kim, I.K. Song, Effect of promoters in the methane reforming with carbon dioxide to synthesis gas over Ni/HY catalysts, J. Mol. Catal. A: Chemical, 246, (2006), 43-48. https://doi.org/10.1016/j.molcata.2005.10.013

172. C.E. Daza, J. Gallego, F. Mondragón, S. Moreno, R. Molina, High stability of Ce-promoted Ni/Mg-Al catalysts derived from hydrotalcites in dry reforming of methane, Fuel, 89, (2010), 592-603. http://dx.doi.org/10.1016/j.fuel.2009.10.010

173. M. Ocsachoque, F. Pompeo, G. Gonzalez, Rh-Ni/$CeO_2$-$Al_2O_3$ catalysts for methane dry reforming, Catal. Today, 172, (2011), 226-231. https://doi.org/10.1016/j.cattod.2011.02.057

174. Z.W. Liu, H.S. Roh, K.W. Jun, Carbon dioxide reforming of methane over Ni/$La_2O_3$/$Al_2O_3$, J. Ind. Eng. Chem., 9, (2003), 267-274.

175. H. Liu, D. Wierzbicki, R. Debek, M. Motak, T. Grzybek, P. Da Costa, M.E. Gálvez, La-promoted Ni-hydrotalcite-derived catalysts for dry reforming of methane at low temperatures, Fuel, 182, (2016), 8-16. https://doi.org/10.1016/j.fuel.2016.05.073

176. S.Y. Foo, C.K. Cheng, T.H. Nguyen, A.A. Adesina, Evaluation of lanthanide-group promoters on Co-Ni/$Al_2O_3$ catalysts for $CH_4$ dry reforming, J. Mol. Catal. A: Chemical, 344, (2011), 28-36. https://doi.org/10.1016/j.molcata.2011.04.018

177. R. Dębek, M.E. Galvez, F. Launay, M. Motak, T. Grzybek, P. Da Costa, Low temperature dry methane reforming over Ce, Zr and CeZr promoted Ni-Mg-Al hydrotalcite-derived catalysts, Int. J. Hydrogen Energy, 41, (2016), 11616-11623. https://doi.org/10.1016/j.ijhydene.2016.02.074

178. S. P. Gandhi, S. Patel, Dry reforming of methane over supported nickel catalysts promoted by zirconia, ceria and magnesia, Int. J. Adv. Res. Eng. Technol., 6, (2015), 131-146.

179. A. S. Al-Fatesh, A. H. Fakeeha, A.E. Abasaeed, Effects of selected promoters on Ni/Y-$Al_2O_3$ catalyst performance in methane dry reforming, Chin. J. Catal., 32, (2011), 1604-1609. https://doi.org/10.1016/S1872-2067(10)60267-7

180. S. Therdthianwong, C. Siangchin, A. Therdthianwong, Improvement of coke resistance of Ni/$Al_2O_3$ catalyst in $CH_4$/$CO_2$ reforming by $ZrO_2$ addition, Fuel Process. Technol., 89, (2008), 160-168. https://doi.org/10.1016/j.fuproc.2007.09.003

181. B. Huang, X. Li, S. Ji, B. Lang, F. Habimana, C. Li, Effect of MgO promoter on Ni-based SBA-15 catalysts for combined steam and carbon dioxide reforming of methane, J. Nat. Gas Chem., 17, (2008), 225-231. https://doi.org/10.1016/S1003-9953(08)60055-9

182. J. Huang, R. Ma, Z. Gao, C. Shen, W. Huang, Characterization and catalytic activity of $CeO_2$-Ni/Mo/SBA-15 catalysts for carbon dioxide reforming of methane, Chin. J. Catal., 33, (2012), 637-644. https://doi.org/10.1016/S1872-2067(11)60347-1

183. J.F. Li, C. Xia, C.T. Au, B.S. Liu, $Y_2O_3$-promoted NiO/SBA-15 catalysts highly active for $CO_2/CH_4$ reforming, Int. J. Hydrogen Energy, 39, (2014), 10927-10940. https://doi.org/10.1016/j.ijhydene.2014.05.021

184. T.S. Phan, A.R. Sane, B. Rêgo de Vasconcelos, A. Nzihou, P. Sharrock, D. Grouset, D.P. Minh, Hydroxyapatite supported bimetallic cobalt and nickel catalysts for syngas production from dry reforming of methane, Appl. Catal. B: Environmental, 224, (2018), 310-321. https://doi.org/10.1016/j.apcatb.2017.10.063

185. A. W. Budiman, S.H. Song, T.S. Chang, C.H. Shin, M.J. Choi, Dry reforming of methane over cobalt catalysts: a literature review of catalyst development, Catal. Surv. Asia, 16, (2012), 183-197. https://doi.org/10.1007/s10563-012-9143-2

186. J. Ni, L. Chen, J. Lin, S. Kawi, Carbon deposition on borated alumina supported nano-sized Ni catalysts for dry reforming of $CH_4$, Nano Energy, 1, (2012), 674-686. https://doi.org/10.1016/j.nanoen.2012.07.011

187. A. Quindimil, U. De-La-Torre, B. Pereda-Ayo, J.A. González-Marcos, J.R. González-Velasco, Ni catalysts with La as promoter supported over Y- and BETA-zeolites for $CO_2$ methanation, Appl. Catal. B: Environmental, 238, (2018), 393-403. https://doi.org/10.1016/j.apcatb.2018.07.034

188. C. Crisafulli, S. Scirè, R. Maggiore, S. Minicò, S. Galvagno, $CO_2$ reforming of methane over Ni-Ru and Ni-Pd bimetallic catalysts, Catal. Lett., 59, (1999), 21-26. https://doi.org/10.1023/A:1019031412713

189. C. Crisafulli, S. Scirè, S. Minicò, L. Solarino, Ni-Ru bimetallic catalysts for the $CO_2$ reforming of methane, Appl. Catal. A: General, 225, (2002), 1-9. https://doi.org/10.1016/S0926-860X(01)00585-3

190. W.K. Jozwiak, M. Nowosielska, J. Rynkowski, Reforming of methane with carbon dioxide over supported bimetallic catalysts containing Ni and noble metal: I. Characterization and activity of $SiO_2$ supported Ni-Rh catalysts, Appl. Catal. A: General, 280, (2005), 233-244. https://doi.org/10.1016/j.apcata.2004.11.003

191. Z.Y. Hou, T. Yashima, Small amounts of Rh-promoted Ni catalysts for methane reforming with $CO_2$, Catal. Lett., 89, (2003), 193-197. https://doi.org/10.1023/A:1025746211314

192. A. Becerra, M.E. Iriarte, M. Dimitrjewits, A. Castro-Luna, Promoting effects of rhodium on supported nickel catalysts in the dry reforming of methane, Bol. Soc. Chil. Quim., 47, (2002), 385-392. http://dx.doi.org/10.4067/S0366-16442002000400010

193. A. Álvarez M., L.F. Bobadilla, V. Garcilaso, M.A. Centeno, J.A. Odriozola, $CO_2$ reforming of methane over Ni-Ru supported catalysts: on the nature of active sites by operando DRIFTS study, J. $CO_2$ Util., 24, (2018), 509-515, https://doi.org/10.1016/j.jcou.2018.01.027

194. A. Álvarez M., M.A. Centeno, J.A. Odriozola, Ru-Ni catalyst in the combined dry steam reforming of methane: the importance in the metal order addition, Top. Catal., 59, (2016), 303-313. https://doi.org/10.1007/s11244-015-0426-5

195. S. Andraos, R. Abbas-Ghaleb, D. Chlala, A. Vita, C. Italiano, M. Laganà, L. Pino, M. Nakhl, S. Specchia, Production of hydrogen by methane dry reforming over ruthenium-nickel based catalysts deposited on $Al_2O_3$, $MgAl_2O_4$, and YSZ, Int. J. Hydrogen Energy, 44 (2019), 25706-25716. https://doi.org/10.1016/j.ijhydene.2019.08.081

196. M. García-Diéguez, E. Finocchio, M.A. Larrubia, L.J. Alemany, G. Busca, Characterization of alumina-supported Pt, Ni and PtNi alloy catalysts for the dry reforming of methane, J Catal., 274, (2010), 11-20. https://doi.org/10.1016/j.jcat.2010.05.020

197. E.G. Mahoney, J.M. Pusel, S.M. Stagg-Williams, S. Faraji, The effects of Pt addition to supported Ni catalysts on dry ($CO_2$) reforming of methane to syngas, J $CO_2$ Util., 6, (2014), 40-44. https://doi.org/10.1016/j.jcou.2014.01.003

198. M. García-Diéguez, I.S. Pieta, M.C. Herrera, M.A. Larrubia, L.J. Alemany, RhNi nanocatalysts for the $CO_2$ and $CO_2$+$H_2O$ reforming of methane, Catal. Today, 172, (2011), 136-142. https://doi.org/10.1016/j.cattod.2011.02.012

199. Q. Ma, J. Sun, X. Gao, J. Zhang, T. Zhao, Y. Yoneyama, N. Tsubaki, Ordered mesoporous alumina-supported bimetallic Pd-Ni catalysts for methane dry reforming reaction, Catal. Sci. Technol., 6, (2016), 6542-6550. https://doi.org/10.1039/C6CY00841K

200. S. Ozkara-Aydnolu, A.E. Aksoylu, $CO_2$ reforming of methane over Pt-Ni/$Al_2O_3$ catalysts: Effects of catalyst composition, and water and oxygen addition to the feed, Int. J. Hydrogen Energy, 36, (2011), 2950-2959. https://doi.org/10.1016/j.ijhydene.2010.11.080

201. F. Meshkani, M. Rezaei, Nanocrystalline MgO supported nickel-based bimetallic catalysts for carbon dioxide reforming of methane, Int. J. Hydrogen Energy, 35, (2010), 10295-10301. https://doi.org/10.1016/j.ijhydene.2010.07.138
202. B. Pawelec, S. Damyanova, K. Arishtirova, J.L.G. Fierro, L. Petrov, Structural and surface features of PtNi catalysts for reforming of methane with $CO_2$, Appl. Catal. A: General, 323, (2007), 188-201. https://doi.org/10.1016/j.apcata.2007.02.017
203. S. Damyanova, B. Pawelec, K. Arishtirova, J.L.G. Fierro, C. Sener, T. Dogu, MCM-41 supported PdNi catalysts for dry reforming of methane, Appl. Catal. B: Environmental, 92, (2009), 250-261. https://doi.org/10.1016/j.apcatb.2009.07.032
204. Y. Khani, Z. Shariatinia, F. Bahadoran, High catalytic activity and stability of $ZnLaAlO_4$ supported Ni, Pt and Ru nanocatalysts applied in the dry, steam and combined dry-steam reforming of methane, Chem. Eng. J., 299, (2016), 353-366. https://doi.org/10.1016/j.cej.2016.04.108
205. L. Sun, Y. Tan, Q. Zhang, H. Xie, F. Song, Y. Han, Effects of $Y_2O_3$-modification to Ni/$\gamma$-$Al_2O_3$ catalysts on autothermal reforming of methane with $CO_2$ to syngas, Int J Hydrogen Energy, 38, (2013), 1892-1900. https://doi.org/10.1016/j.ijhydene.2012.11.114
206. C. Shi, P. Zhang, Effect of a second metal (Y, K, Ca, Mn or Cu) addition on the carbon dioxide reforming of methane over nanostructured palladium catalysts, Appl. Catal. B: Environmental, 115-116, (2012), 190-200. https://doi.org/10.1016/j.apcatb.2011.12.002
207. B. Steinhauer, M.R. Kasireddy, J. Radnik, A. Martin, Development of Ni-Pd bimetallic catalysts for the utilization of carbon dioxide and methane by dry reforming, Appl. Catal. A: General, 366, (2009), 333-341. https://doi.org/10.1016/j.apcata.2009.07.021
208. Z. Wu, B. Yang, S. Miao, W. Liu, J. Xie, S. Lee, M.J. Pellin, D. Xiao, D. Su, D. Ma, Lattice strained Ni-Co alloy as a high-performance catalyst for catalytic dry reforming of methane, ACS Catal., 9, (2019), 2693-2700. https://doi.org/10.1021/acscatal.8b02821
209. J. Estephane, S. Aouad, S. Hany, B. El Khoury, C. Gennequin, H. El Zakhem, J. El Nakat, A. Aboukaïs, E. Abi Aad, $CO_2$ reforming of methane over Ni-Co/ZSM5 catalysts. Aging and carbon deposition study, Int. J. Hydrogen Energy, 40, (2015), 9201-9208,. https://doi.org/10.1016/j.ijhydene.2015.05.147

210. S. Sengupta, K. Ray, G. Deo, Effects of modifying Ni/$Al_2O_3$ catalyst with cobalt on the reforming of $CH_4$ with $CO_2$ and cracking of $CH_4$ reactions, Int. J. Hydrogen Energy, 39, (2014), 11462–11472. https://doi.org/10.1016/j.ijhydene.2014.05.058

211. R. Kumari, S. Sengupta, Catalytic $CO_2$ reforming of $CH_4$ over $MgAl_2O_4$ supported Ni-Co catalysts for the syngas production, Int. J. Hydrogen Energy, 45, (2020), 22775-22787. https://doi.org/10.1016/j.ijhydene.2020.06.150

212. J. Zhang, H. Wang, A.K. Dalai, Development of stable bimetallic catalysts for carbon dioxide reforming of methane, J. Catal., 249, (2007), 300-310. http://dx.doi.org/10.1016/j.jcat.2007.05.004

213. X. Zhang, Z. Vajglova, P. Mäki-Arvela, M. Peurla, H. Palonen, D.Yu. Murzin, S.A. Tungatarova, T.S. Baizhumanova, Y.A. Aubakirov, Mono- and bimetallic Ni-Co catalysts in dry reforming of methane, ChemistrySelect, 6, (2021), 3424-3434. https://doi.org/10.1002/slct.202100686

214. M. Yu, K. Zhu, Z. Liu, H. Xiao, W. Deng, X. Zhou, Carbon dioxide reforming of methane over promoted Nix/$Mg_{1-x}O$ (111) platelet catalyst derived from solvothermal synthesis, Appl. Catal. B: Environmental, 148-149, (2014), 177-190. https://doi.org/10.1016/j.apcatb.2013.10.046

215. S.T. Misture, K.M. McDevitt, K.C. Glass, D.D. Edwards, J.Y. Howe, K.D. Rector, H. He, S.C. Vogel, Sulfur-resistant and regenerable Ni/Co spinel-based catalysts for methane dry reforming, Catal. Sci. Technol., 5, (2015), 4565-4574. https://doi.org/10.1039/C5CY00800J

216. A. Tsoukalou, Q. Imtiaz, S.M. Kim, P.M. Abdala, S. Yoon, C.R. Müller, Dry reforming of methane over bimetallic Ni-M/$La_2O_3$ (M=Co, Fe): the effect of the rate of $La_2O_2CO_3$ formation and phase stability on the catalytic activity and stability, J. Catal., 343, (2016), 208-214. https://doi.org/10.1016/j.jcat.2016.03.018

217. H.-W. Chen, C.-Y. Wang, C.-H. Yu, L.-T. Tseng, P.-H. Liao, Carbon dioxide reforming of methane reaction catalyzed by stable nickel copper catalysts, Catal. Today, 97, (2004), 173-180. http://dx.doi.org/10.1016/j.cattod.2004.03.067

218. M. Sharifi, M. Haghighi, F. Rahmani, S. Karimipour, Syngas production via dry reforming of $CH_4$ over Co- and Cu-promoted Ni/$Al_2O_3$-$ZrO_2$ nanocatalysts synthesized via sequential impregnation and sol-gel methods, J. Nat. Gas Sci. Eng., 21, (2014), 993-1004. https://doi.org/10.1016/j.jngse.2014.10.030

219. M. Sharifi, M. Haghighi, F. Rahmani, N. Rahemi, Reforming of biogas over Co and Cu-Promoted Ni/$Al_2O_3$-$ZrO_2$ nanocatalyst synthesized via sequential impregnation method, J. Renew. Energy Environ., 1, (2014), 53-63. https://doi.org/10.30501/JREE.2014.70056

220. K. Song, M. Lu, S. Xu, C. Chen, Y. Zhan, D. Li, C. Au, L. Jiang, K. Tomishige, Effect of alloy composition on catalytic performance and coke-resistance property of Ni-Cu/Mg(Al)O catalysts for dry reforming of methane, Appl. Catal. B: Environmental, 239, (2018), 324-333. https://doi.org/10.1016/j.apcatb.2018.08.023

221. J. Liu, H. Peng, W. Liu, X. Xu, X. Wang, C. Li, W. Zhou, P. Yuan, X. Chen, W. Zhang, H. Zhan, Tin modification on Ni/$Al_2O_3$: designing potent coke-resistant catalysts for the dry reforming of methane, ChemCatChem, 6, (2014), 2095-2104. https://doi.org/10.1002/cctc.201402091

222. T. Stroud, T.J. Smith, E. Le Saché, J.L. Santos, M.A. Centeno, H. Arellano-Garcia, J.A. Odriozola, T.R. Reina, Chemical $CO_2$ recycling via dry and bi reforming of methane using Ni-Sn/$Al_2O_3$ and Ni-Sn/$CeO_2$-$Al_2O_3$ catalysts, Appl. Catal. B: Environmental, 224, (2018), 125-135. https://doi.org/10.1016/j.apcatb.2017.10.047

223. E. Le Saché, S. Johnson, L. Pastor-Perez, B.A. Horri, T.R. Reina, Biogas upgrading via dry reforming over a Ni-Sn/$CeO_2$-$Al_2O_3$ catalyst: influence of the biogas source, Energies, 12, (2019), 1007. https://doi.org/10.3390/en12061007

224. S.H. Seok, S.H. Han, J.S. Lee, The role of MnO in Ni/MnO-$Al_2O_3$ catalysts for carbon dioxide reforming of methane, Appl. Catal. A: General, 215, (2001), 31-38. https://doi.org/10.1016/S0926-860X(01)00528-2

225. C.E. Quincoces, S.P. de Vargas, P. Grange, M.G. González, Role of Mo in $CO_2$ reforming of $CH_4$ over Mo promoted Ni/$Al_2O_3$ catalysts, Mater. Lett., 56, (2002), 698-704. https://doi.org/10.1016/S0167-577X(02)00598-0

226. S.A. Theofanidis, V.V. Galvita, H. Poelman, G.B. Marin, Enhanced carbon-resistant dry reforming Fe-Ni catalyst: role of Fe, ACS Catal., 5, (2015), 3028-3039. https://doi.org/10.1021/acscatal.5b00357

227. S.A. Theofanidis, R. Batchu, V.V. Galvita, H. Poelman, G.B. Marin, Carbon gasification from Fe-Ni catalysts after methane dry reforming, Appl. Catal. B: Environmental, 185, (2016), 42-55. https://doi.org/10.1016/j.apcatb.2015.12.006

228. Z. Song, Q. Wang, C. Guo, S. Li, W. Yan, W. Jiao, L. Qiu, X. Yan, R. Li, Improved effect of Fe on the stable NiFe/$Al_2O_3$ catalyst in low-temperature dry reforming of methane, Ind. Eng. Chem. Res., 59, (2020), 17250-17258. https://doi.org/10.1021/acs.iecr.0c01204
229. S.M. de Lima, J.M. Assaf, Ni-Fe catalysts based on perovskite-type oxides for dry reforming of methane to syngas, Catal. Lett., 108, (2006), 63-70. https://doi.org/10.1007/s10562-006-0026-x
230. T. Zhang, Z. Liu, Y.-A. Zhu, Z. Liu, Z. Sui, K. Zhu, X. Zhou, Dry reforming of methane on Ni-Fe-MgO catalysts: influence of Fe on carbon-resistant property and kinetics, Appl. Catal. B: Environmental, 264, (2020), 118497. https://doi.org/10.1016/j.apcatb.2019.118497
231. S.M. Kim, P.M. Abdala, T. Margossian, D. Hosseini, L. Foppa, A. Armutlulu, W. van Beek, A. Comas-Vives, C. Copéret, C. Müller, Cooperativity and dynamics increase the performance of NiFe dry reforming catalysts, J. Am. Chem. Soc., 139, (2017), 1937-1949. https://doi.org/10.1021/jacs.6b11487
232. W. Li, Z. Zhao, P. Ren, G. Wang, Effect of molybdenum carbide concentration on the Ni/$ZrO_2$ catalysts for steam-$CO_2$ bi-reforming of methane, RSC Adv., 5, (2015), 100865-100872. https://doi.org/10.1039/C5RA22237K
233. J.M. Cheng, W. Huang, Effect of cobalt (nickel) content on the catalytic performance of molybdenum carbides in dry-methane reforming, Fuel Process. Technol., 91, (2010), 185-193. https://doi.org/10.1016/j.fuproc.2009.09.011
234. A.J. Zhang, A.M. Zhu, B.B. Chen, S.H. Zhang, C.T. Au, C.A. Shi, In-situ synthesis of nickel modified molybdenum carbide catalyst for dry reforming of methane, Catal. Commun., 12, (2011), 803-807. https://doi.org/10.1016/j.catcom.2011.01.019
235. T. Huang, W. Huang, J. Huang, P. Ji, Methane reforming reaction with carbon dioxide over SBA-15 supported Ni-Mo bimetallic catalysts, Fuel Process. Technol., 92, (2011), 1868-1875. https://doi.org/10.1016/j.fuproc.2011.05.002
236. L. Yao, M.E. Galvez, C.W. Hu, P. Da Costa, Mo-promoted Ni/$Al_2O_3$ catalyst for dry reforming of methane, Int. J. Hydrogen Energy, 42, (2017), 23500-23507, https://doi.org/10.1016/j.ijhydene.2017.03.208
237. Y. Song, E. Ozdemir, S. Ramesh, A. Adishev, S. Subramanian, A. Harale, M. Albuali, B.A. Fadhel, A. Jamal, D. Moon, S.H. Choi, C.T. Yavuz, Dry reforming of methane by stable Ni-Mo nanocatalysts on single-crystalline MgO, Science, 367, (2020), 777-781. https://science.sciencemag.org/content/367/6479/777/tab-pdf

238. R. Vakili, R. Gholami, C.E. Stere, S. Chansai, H.H. Chen, S.M. Holmes, Y. Jiao, C. Hardacre, X. Fan, Plasma-assisted catalytic dry reforming of methane (DRM) over metal organic frameworks (MOFs)-based catalysts, Appl. Catal. B: Environmenal, 260, (2020), 118195. https://doi.org/10.1016/j.apcatb.2019.118195

239. A.H. Khoja, M. Tahir, N.A. Saidina Amin, Recent developments in non-thermal catalytic DBD plasma reactor for dry reforming of methane, Energy Convers. Manag., 183, (2019), 529-560. https://doi.org/10.1016/j.enconman.2018.12.112

240. X. Tu, J.C. Whitehead, Plasma dry reforming of methane in an atmospheric pressure AC gliding arc discharge: Cogeneration of syngas and carbon nanomaterials, Int. J. Hydrogen Energy, 39, (2014), 9658-9669. https://doi.org/10.1016/j.ijhydene.2014.04.073

241. W.-C. Chung, I.Y. Tsao, M.-B. Chang, Novel plasma photocatalysis process for syngas generation via dry reforming of methane, Energy Convers. Manag., 164, (2018), 417-428. https://doi.org/10.1016/j.enconman.2018.03.024

242. A. H. Khoja, M. Tahir, N.A.S. Amin, A. Javed, M.T. Mehran, Kinetic study of dry reforming of methane using hybrid DBD plasma reactor over $La_2O_3$ co-supported $Ni/MgAl_2O_4$ catalyst, Int. J. Hydrogen Energy, 45, (2020), 12256-12271. https://doi.org/10.1016/j.ijhydene.2020.02.200

243. X. Tao, C. Yang, L. Huang, D. Xu, DBD plasma combined with catalysts derived from NiMgAlCe hydrotalcite for $CO_2$ reforming of $CH_4$, Mater. Chem. Phys., 250, (2020), 123118. https://doi.org/10.1016/j.matchemphys.2020.123118

244. D. Ray, P.M.K. Reddy, C. Subrahmanyam, Ni-Mn/$\gamma$-$Al_2O_3$ assisted plasma dry reforming of methane, Catal. Today, 309, (2018), 212-218. https://doi.org/10.1016/j.cattod.2017.07.003

245. H. Wang, J. Han, B. Zhao, L. Qin, Y. Wang, F. Yu, Non-thermal plasma enhanced dry reforming of $CH_4$ with $CO_2$ over activated carbon supported Ni catalysts, Mol. Catal. 475, (2019), 110486. https://doi.org/10.1016/j.mcat.2019.110486

246. H. Wang, B. Zhao, L. Qin, Y. Wang, F. Yu, J. Han, Non-thermal plasma-enhanced dry reforming of methane and $CO_2$ over Ce-promoted Ni/C catalysts, Mol. Catal., 485, (2020), 110821. https://doi.org/10.1016/j.mcat.2020.110821

247. J.T. Sun, Q. Chen, Y.W. Guo, Z.L. Zhou, Y. Song, Quantitative behavior of vibrational excitation in AC plasma assisted dry reforming of methane, J. Energy Chem., 46, (2020), 133-143. https://doi.org/10.1016/j.jechem.2019.11.002

248. H.M. Nguyen, J. Sunarso, C. Li, G.H. Pham, C. Phan, S.M. Liu, Microwave-assisted catalytic methane reforming: a review, Appl. Catal. A: General, 599, (2020), 117620. https://doi.org/10.1016/j.apcata.2020.117620

249. I.D. García, A. Stankiewicz, H. Nigar, Syngas production via microwave-assisted dry reforming of methane, Catal. Today, 362, (2020), 72-80. https://doi.org/10.1016/j.cattod.2020.04.045

250. T. Kulandaivalu, A.R. Mohamed, K.A. Ali, M. Mohammadi, Photocatalytic carbon dioxide reforming of methane as an alternative approach for solar fuel production-a review, Renew. Sustain. Energy Rev., 134, (2020), 110363. https://doi.org/10.1016/j.rser.2020.110363

251. F. Pan, X. Xiang, W. Deng, H. Zhao, X. Feng, Y. Li, A novel photo-thermo-chemical approach for enhanced carbon dioxide reforming of methane, ChemCatChem, 10, (2018), 940-945. https://doi.org/10.1002/cctc.201701565

252. Y. Cho, S. Shoji, A. Yamaguchi, T. Hoshina, T. Fujita, H. Abe, M. Miyauchi, Visible-light-driven dry reforming of methane using semiconductor-supported catalyst, Chem. Comm., 56, (2020), 4611-4514. https://doi.org/10.1039/D0CC00729C

253. J. Guerrero-Caballero, T. Kane, N. Haidar, L. Jalowiecki-Duhamel, A. Löfberg, Ni, Co, Fe supported on Ceria and Zr doped Ceria as oxygen carriers for chemical looping dry reforming of methane, Catal. Today, 333, (2019), 251-258. https://doi.org/10.1016/j.cattod.2018.11.064

254. Z. Huang, H. Jiang, F. He, D. Chen, D. Wei, K. Zhao, A. Zheng, Y. Feng, Z. Zhao, H. Li, Evaluation of multi-cycle performance of chemical looping dry reforming using $CO_2$ as an oxidant with Fe-Ni bimetallic oxides, J. Energy Chem., 25, (2016), 62-70. https://doi.org/10.1016/j.jechem.2015.10.008

255. Z. Huang, F. He, D. Chen, K. Zhao, G. Wei, A. Zheng, Z. Zhao, H. Li, Investigation on reactivity of iron nickel oxides in chemical looping dry reforming, Energy, 116, (2016), 53-63. https://doi.org/10.1016/j.energy.2016.09.101

256. L. Protasova, F. Snijkers, Recent developments in oxygen carrier materials for hydrogen production via chemical looping processes, Fuel, 181, (2016), 75-93. https://doi.org/10.1016/j.fuel.2016.04.110

257. M. Luo, Y. Yi, S. Wang, Z. Wang, M. Du, J. Pan, Q. Wang, Review of hydrogen production using chemical-looping technology, Renew. Sustain. Energy Rev., 81, (2018), 3186-3214. https://doi.org/10.1016/j.rser.2017.07.007

258. A. Löfberg, T. Kane, J. Guerrero-Caballero, L. Jalowiecki-Duhamel, Chemical looping dry reforming of methane: toward shale-gas and biogas valorization, Chem. Eng. Process Process Intensif., 122, (2017), 523-5299. https://doi.org/10.1016/j.cep.2017.05.003

## Captions

**Table 1.** Main reactions in the dry reforming of methane (DRM).

**Table 2.** Reaction mechanisms for the dry reforming of methane (DRM) proposed by several authors.

**Figure 1**. TEM images of pyrolytic carbon on a $MgAl_2O_4$ carrier (A), encapsulating carbon (B), and whisker carbon (C) on $Ni/MgAl_2O_4$ catalysts (Reproduced with permission from[39]).

**Figure 2.** Thermodynamic prediction of quantities and conversions at equilibrium calculated as a function of temperature. 1 atm and 2 moles of feed ($CO_2/CH_4$ = 1).

**Figure 3.** Reaction mechanism proposed on a Ni-CeZr sol-gel sample for: (a) $CO_2$ methanation and (b) CO formation. (Reproduced with permission from[60]).

**Figure 4.** Effect of synthesis method (impregnation (I) and sol-gel (SG)) on $H_2/CO$ molar ratio in the product at various temperatures: (a) $Ni/Al_2O_3$-MgO (NAM) and (b) $Ni/Al_2O_3$-$CeO_2$ (NAC) (Reproduced with permission from[94]).

**Figure 5.** Schematic representation of the atomic layer deposition method for the synthesis of a Ni catalyst (Reproduced with permission from[97]).

**Figure 6.** $H_2$-TPR profiles for catalysts calcined at 100 °C: citric acid method (CA) (a); sol-gel method (SG) (b); wet impregnation method (WI) (c); co-precipitation method (CP) (d) (Reproduced with permission from[100]).

**Figure 7.** Schematic representation of the synthesis of Ni-$SiO_2$ and Ni-$SiO_2$@$CeO_2$ catalysts. (Reproduced with permission from[113]).

**Figure 8.** Schematic representation of the main chemical reaction steps in the $CH_4$ and $CO_2$ activation routes on 5 wt.% $Ni/Ce_{0.8}Pr_{0.2}O_{2-\delta}$ catalyst (Reproduced with permission from[131]).

**Figure 9.** Performances of catalysts with and without carbon nanotube (CNT) composites on mesoporous silica (MS) with time on-stream during the dry reforming reaction at 650 °C for 24 h. (a) $CH_4$ conversion, (b) $CO_2$ conversion, (c) $H_2/CO$ molar ratio. (○) 5Ni/MS, (□) 10 Ni/MS, (●) 5Ni-CNT/MS, (■) 10Ni-CNT/MS (Reproduced with permission from[135]).

**Figure 10.** Schematic representation of the effect of air or $CO_2$ on Ni dispersion in the $Ni/La_2O_3$ catalyst (Reproduced with permission from[161]).

**Figure 11.** $CH_4$ conversion vs. time on-stream at 250 °C over the Ni/MgO-$ZrO_2$ catalyst (NM5Z2) with various K loadings (Reproduced with permission from[170]). (Reaction conditions:

catalyst weight: 20 mg, reduction conditions: 250 °C/2h; $CH_4/CO_2/Ar$ ratio: 1:1:8; total flow rate: 50 ml/min.).

**Figure 12.** Effect of promoter on the performance of the Ni/HY catalyst at 700 °C (GHSV = 3500 $h^{-1}$) (Reproduced with permission from[171]).

**Figure 13.** $CH_4$, $CO_2$ conversions, $H_2/CO$ ratio over 10Ni and 10Ni15Ce during reaction for 24 h; T = 800 °C, $CH_4/CO_2/O_2$ = 1/0.8/0.1, GHSV = 60,000 mL/h·g. (Reproduced with permission from[136]).

**Figure 14.** Effect of Y promotion on $CH_4$ and $CO_2$ conversion over a Ni/γ-$Al_2O_3$ catalyst (Reproduced with permission from[205]).

**Figure 15.** Optimal Cu/Ni ratio for Cu-Ni/MgAlO catalysts to minimize coke deposition (Reproduced with permission from[220]).

**Figure 16.** Proposed mechanisms of carbon gasification over Fe-Ni/$MgAl_2O_4$ (Reproduced with permission from[227]).

**Figure 17.** Proposed reaction mechanism for $La_2O_3$ co-supported Ni/$MgAl_2O_4$ plasma-catalyzed DRM (Reproduced with permission from[242]).

**Figure 18.** Schematic representation of the chemical looping dry reforming of methane (CLDRM) process using a circulating bed reactor (A) or switching feed reactor (B) (Reproduced with permission from[253]).